OPERA

Model representation of radionuclide diffusion in Boom Clay

OPERA-PU-NRG6131

Radioactive substances and ionizing radiation are used in medicine, industry, agriculture, research, education and electricity production. This generates radioactive waste. In the Netherlands, this waste is collected, treated and stored by COVRA (Centrale Organisatie Voor Radioactief Afval). After interim storage for a period of at least 100 years radioactive waste is intended for disposal. There is a world-wide scientific and technical consensus that geological disposal represents the safest long-term option for radioactive waste.

Geological disposal is emplacement of radioactive waste in deep underground formations. The goal of geological disposal is long-term isolation of radioactive waste from our living environment in order to avoid exposure of future generations to ionising radiation from the waste. OPERA (OnderzoeksProgramma Eindberging Radioactief Afval) is the Dutch research programme on geological disposal of radioactive waste.

Within OPERA, researchers of different organisations in different areas of expertise will cooperate on the initial, conditional Safety Cases for the host rocks Boom Clay and Zechstein rock salt. As the radioactive waste disposal process in the Netherlands is at an early, conceptual phase and the previous research programme has ended more than a decade ago, in OPERA a first preliminary or initial safety case will be developed to structure the research necessary for the eventual development of a repository in the Netherlands. The safety case is conditional since only the long-term safety of a generic repository will be assessed. OPERA is financed by the Dutch Ministry of Economic Affairs and the public limited liability company Electriciteits-Produktiemaatschappij Zuid-Nederland (EPZ) and coordinated by COVRA. Further details on OPERA and its outcomes can be accessed at www.covra.nl.

This report concerns a study conducted in the framework of OPERA. The conclusions and viewpoints presented in the report are those of the author(s). COVRA may draw modified conclusions, based on additional literature sources and expert opinions. A .pdf version of this document can be downloaded from www.covra.nl.

OPERA-PU-NRG6131
Title: Model representation of radionuclide diffusion in Boom Clay
Authors: J.C.L. Meeussen (NRG), E. Rosca-Bocancea (NRG), T.J. Schröder (NRG), M. Koenen (TNO), F. Valega Mackenzie (TNO), N. Maes (SCK), C. Bruggeman (SCK)
Date of publication: 7 February 2017
Keywords: radionuclide diffusion, Boom Clay, modelling, anion diffusion, clay charge, molecular dynamics

Content

Summary

The migration of radionuclides through the host rock plays an important role for the long-term safety of disposal concepts in clay. Due to the slow transport of radionuclides in the host rock, most radionuclides will be decayed before they can enter the surrounding aquifers. For the generic OPERA disposal concept in Boom Clay, the delayed transport of radionuclides through the host rock can be assumed as the most important safety function on the long-term. It is therefore important to understand the basic processes behind the migration of radionuclides in the host rock sufficiently well to be able to make a credible quantitative assessment of the effects of long-term underground disposal of radioactive waste.

Overall nuclide migration rates in Boom Clay are determined by a combination of chemical and physical processes. This report focuses on the physical aspects of nuclide migration, on a model approach and required model parameters. An important source of information for these parameters are the results of the Belgian research programme as part of which radionuclide behaviour in Boom Clay has been studied for over 30 years. Since the Boom Clay conditions in the Netherlands are expected to be slightly different from the Belgian situation, an assessment was carried out of the transferability of the data obtained on Belgian samples for predicting/describing radionuclide transport in the Netherlands. The results show that although expected higher salinity, higher pressures, and higher temperatures in the Dutch situation are likely to have some effect on diffusion coefficients, the order of magnitude of these effects limited.

The resulting estimated set of transport parameters for the Dutch situation was summarized into a database that together with the set of retardation factors resulting from Task 6.1.2 forms the complete set input data for modelling migration of radionuclides through the Boom Clay.

Samenvatting

De migratie van radionucliden door het gastgesteente speelt een belangrijke rol voor de langtermijn veiligheid van eindbergingsconcepten in klei. Vanwege de zeer trage diffusie van stoffen in het gastgesteente zullen de meeste radionucliden vervallen zijn, voordat deze de klei kunnen verlaten. Het zeer trage transport van radionucliden speelt een essentiële rol voor de veiligheid van het generieke OPERA bergingsconcept in Boomse Klei. Om tot een betrouwbare uitspraak over de lange-termijn veiligheid te kunnen komen, is het daarom belangrijk om de processen achter dit transportgedrag goed te begrijpen en in kaart te brengen.

Het transportgedrag van radionucliden in Boomse Klei wordt bepaald door een combinatie van fysische en chemische processen. Dit rapport richt zich op de fysische aspecten, een modelbenadering en de benodigde modelparameters. Een belangrijke bron van informatie over deze parameters is het Belgische eindbergingsonderzoek in het kader waarvan het migratiegedrag van radionucliden in Boomse Klei al ca. 30 jaar wordt bestudeerd. Omdat de fysisch chemische condities van Boomse Klei in Nederland iets anders zijn dan in België is ook gekeken naar de overdraagbaarheid van deze parameters naar de Nederlandse situatie. De resultaten hiervan laten zien dat alhoewel de hogere druk, hogere temperatuur en hogere zoutconcentraties de diffusiesnelheden enigszins zullen beïnvloeden, de verwachtte grootte van deze invloed beperkt zal zijn.

De resulterende set fysische transport parameters voor de Nederlandse situatie is samengevat in een database M6.1.3.2. Samen met de retardatiefactoren bepaald in Task

6.1.2 vormt dit een complete set invoerdata voor het modelleren van radionuclidemigratie door Boomse Klei.

1. Introduction

1.1. *Background*

The five-year research programme for the geological disposal of radioactive waste – OPERA- started on 7 July 2011 with an open invitation for research proposals. In these proposals, research was proposed for the tasks described in the OPERA Research Plan.

1.2. *Objectives*

The main objective of WP6.1 *Radionuclide migration* is to provide a consistent approach for the modelling of radionuclide migration by diffusion in the undisturbed part of the host rock (Boom Clay) for the purpose of the safety assessments as part of the OPERA Safety Case.

This report describes the execution and results of the research proposed for task *6.1.3* in the Research Plan denoted as *Modelling of diffusion processes*. In this task the role of diffusion in the complex and heterogeneous Boom Clay is analysed.

In the present work a reference database will be compiled with diffusion parameters required to calculate the migration of different radionuclides through the Boom Clay. The diffusion parameters in combination with sorption parameters provided within Task 6.1.2 on the modelling approach for sorption processes [Schröder et al., 2016a, Schröder et al., 2016b] and information resulting from OPERA Task 6.1.4 on the presence and mobility of colloidal particles in the Boom Clay [Durce et al., 2016] will serve as input for the performance assessment calculations carried out in WP7 *Scenario and performance assessment*. The interaction between the OPERA Tasks 6.1.2, 6.1.3, 6.1.4 and WP7 is given in the figure below.

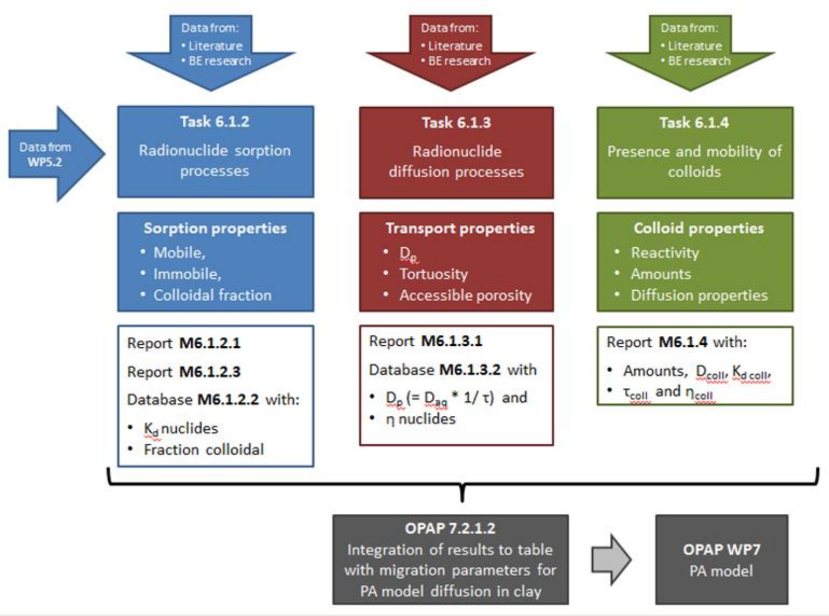

Figure 1-1 Schematic overview of relationship between OPERA WP6.1 tasks and WP7

1.3. *Realization*

The literature study, analyses and calculations presented in this report are performed by NRG, SCK·CEN and TNO. Because in practice sorption and diffusion processes cannot be studied independently from each other, this task was performed in close cooperation with Task 6.1.2 *Modelling approach for sorption processes* and Task 6.1.4 *Mobility and presence of Colloidal particles.*

1.4. Explanation contents

The current understanding of diffusion and the fundamental features and modelling approaches of diffusion processes in porous media are summarized in Chapter 2. An overview of the modelling approach for diffusion currently followed in the Belgian programme on geological waste disposal is given in Chapter 3.

The application and benefits of molecular modelling for the purpose of gaining improved insight into the interactions between charged clay surfaces on the diffusion of radionuclides is assessed in Chapter 4.

Chapter 5 summarizes the general considerations regarding the modelling approach for OPERA, and Chapter 6 describes the mathematical model, the implementation of that model and the derivation of the related migration parameters. The conclusions and recommendations are summarized in Chapter 7.

2. Current understanding and modelling of diffusion processes

This chapter provides an overview of the fundamental features of diffusion processes in general (Section 2.1) and diffusion in aqueous solutions in particular (Section 2.2). The current understanding and modelling approaches of radionuclide diffusion in porous media are summarized in Section 2.3. Phenomena such as anion exclusion and surface diffusion of cations are included.

2.1. Fundamental features of diffusion processes

The concept of diffusion is widely used in many disciplines. There are two ways to define the notion of *diffusion*:

- the phenomenological or thermodynamic approach based on Fick's laws of diffusion and their mathematical consequences, or
- the physical and atomistic one also known as statistical approach, that considers the random (statistical) walk of the diffusing particles.

In the phenomenological approach diffusion is defined as the movement of a particle from a region of high concentration to a region of low concentration without bulk solution motion. According to Fick's laws, the diffusion flux is proportional to the negative gradient of concentrations. Various formulations of Fick's laws were developed in the frame of thermodynamics.

From a statistical point of view, diffusion is considered to be a result of the random walk of the diffusing particles, the moving molecules being self-propelled by thermal energy.

There are four different types of diffusion [Shackelford & Daniel, 1991]:

- *self-diffusion* (essentially Brownian motion representing the spontaneous (random) movement (diffusion) of molecules in the absence of concentration (or chemical) potential gradient, the motion of these molecules cannot be traced),
- *tracer diffusion* (diffusion of one chemical species at low chemical concentrations into another, it is identical to self-diffusion but uses small amounts of isotopic species (tracer), the presence of the isotopic species causes small concentration gradients, because of their small concentrations, the movement of the tracers is not tied to the movement of the ions of opposite signs),
- *salt diffusion* or chemical diffusion (occurs in a presence of concentration (or chemical potential) gradient and results in net transport of mass),
- *counter diffusion or interdiffusion* (process whereby different ions are diffusing against (in opposite direction to) each other, concentration gradients are established in opposite directions).

The case of salt diffusion is representative for the cases involving containment of waste by geological barriers [Shackelford & Daniel, 1991].

2.2. Diffusion in aqueous solutions

2.2.1. Fick's first law for aqueous solutions

Diffusion is a process by which solute molecules move from areas of higher concentration to areas of lower concentration by random Brownian movement. The mass flux is proportional to the concentration gradient and it is described by the Fick's first law which in one dimension is [Atkins, p.848], [NEA/OECD, 1996, p.66]:

$$J = -D_0 \frac{\partial C}{\partial x} \qquad (1)$$

where:

J - diffusive mass flux [mol/m^{2}s],
D_0 - diffusion coefficient or diffusivity of the solute in free water or 'free-solution' diffusion coefficient (in absence of porous medium) [m^2/s],
C - aqueous phase concentration of the solute [mol/m^3],
x - distance in the direction of transport [m].

The rate of transport is determined by the diffusivity and the concentration gradient. The diffusivity or diffusion coefficient (*D*) is a proportionality constant between the diffusion flux and the concentration gradient of the diffusing species. The value of the diffusion coefficient depends on the viscosity, the temperature and some other properties of the medium and of the diffusing particles as well.

The relation between the diffusion coefficient of an ion in water and its ionic mobility u is given by the Einstein relation [Atkins 1996, p.849]

$$D_0 = \frac{uRT}{zF} \qquad (2)$$

with:
u - absolute mobility of the particle [m^2 s^{-1} V^{-1}],
R - universal gas constant [J K^{-1} mol^{-1}],
T - absolute temperature [K],
z - absolute value of ionic valence [-],
F - Faraday constant [C mol^{-1}],

The Stokes-Einstein equation describes the relation between the diffusion coefficient and the viscosity of the medium [Atkins 1996, p.850]:

$$D_0 = \frac{kT}{6\pi\eta a} \qquad (3)$$

with :
k - Boltzmann constant [J K^{-1}],
T - absolute temperature [K],
π - Pi constant [-],
η - absolute (dynamic) viscosity of the diffusion medium (water) [kg m^{-1} s^{-1}],
a - hydrodynamic radius of a (spherical) particle [m].

The temperature-dependency of the viscosity of water can be represented by an Arrhenius-type equation [Atkins, 1996, p.833]:

$$\eta \sim \exp(\frac{+E_A}{RT}) \qquad (4)$$

E_A is the apparent activation energy [J mol^{-1}].

2.2.2. Fick’s second law for aqueous solutions

Fick’s first law applies to steady state systems, where the concentration remains constant. Diffusion in case of concentrations changing in time is described by Fick’s second law of diffusion. The corresponding diffusion equation that gives the change of the concentration (C) in space (x) and time (t) is:

$$\frac{\partial C(x,t)}{\partial t} = D_0 \frac{\partial^2 C(x,t)}{\partial x^2} \qquad (5)$$

In case of first-order decay of the solute equation (5) is extended with a decay term and becomes:

$$\frac{\partial C(x,t)}{\partial t} = D_0 \frac{\partial^2 C(x,t)}{\partial x^2} - \lambda C \qquad (6)$$

where λ is the decay constant [s^{-1}].

2.3. Diffusion in porous media

The conventional diffusion equations based on Fick’s laws are not always adequate to describe the diffusive mass transport in complex environments such as for example the natural porous media on larger scale (i.e. larger than the pore scale). In some situations the diffusion was found to be characterized by a slower propagation of the concentration front on larger scale than expected on basis of the diffusion behaviour observed in pure solutions. In other situations the particles manifested a higher diffusion rate and pass the specified distance faster than in the classical case. The mathematical models to describe diffusive transport in porous media on larger scale were adapted to cover the properties of the porous media.

2.3.1. Fick’s first law for diffusion in porous media

In case of diffusion in the fluid phase of a saturated porous medium, Fick’s first law becomes:

$$J = -D_{eff} \frac{\partial C}{\partial x} \qquad (7)$$

with D_{eff} - effective (also known as intrinsic or non-retarded) diffusion coefficient [m^2/s] that can be related to the diffusion coefficient in free water (D_o) by:

$$D_{eff} = \eta D_{pore} = \eta \frac{\delta}{\theta^2} D_0 \qquad (8)$$

with:

D_{pore} - pore water coefficient (or bulk diffusion coefficient) accounting for the effects of tortuosity [m^2/s],
D_0 - diffusion coefficient in free water [m^2/s],
θ^2 - tortuosity factor [-],
δ - constrictivity factor [-],
η - total porosity [-],

The tortuosity factor (θ^2) is equal to $(L_a/L)^2$ where L_a is the (longer) path around the solid grains the molecules have to pass and L is the strait-line distance[a]. The constrictivity expresses the effect of the widening or narrowing of the pores on the diffusivity and is a function of pore diameter and the size of the diffusing particles.

It is, however, difficult (or impossible) to distinguish these two factors and therefore they often are combined in a geometrical factor:

$$\frac{\delta}{\theta^2} = \frac{1}{G} \tag{9}$$

with:

G - geometrical factor [-].

In soils, in the case of transport only by diffusion, only a part of the total porosity, called *effective porosity* (η_{eff}) or *diffusion accessible porosity* is available for mass transport. The effective porosity is always equal to or less than the total porosity ($\eta_{eff}<\eta$) excluding the fraction of pores that are not interconnected and thus not-available for mass transport. The effective accessible porosity in porous media is considerable lower than the total porosity, which makes it appropriate to use the effective accessible porosity (η_{eff}) instead the total porosity:

$$J = -\eta_{eff} D_{pore} \frac{\partial C}{\partial x} \tag{10}$$

The relationship between the effective and bulk solution diffusion coefficients can be also expressed through electrical conductivities of the bulk fluid phase (K_f) and the saturated porous medium (K_m) [NEA/OECD, 1996, p.71]:

$$D_{eff} = \left(\frac{K_m}{K_f}\right) D_w = \frac{D_w}{f} \tag{11}$$

K_m - electrical conductivity of the bulk fluid phase [S m^{-1}],
K_f - electrical conductivity of the saturated porous medium [S m^{-1}],
f - formation factor [-].

A general expression for the calculation of the formation factor f is:

$$f = \eta^{-m} \tag{12}$$

with:

m - cementation factor depending on porosity and pore water composition [-],
η - porosity [-].

The simplest way of describing diffusive transport through sorptive media is by coupling a diffusion model to a linear adsorption coefficient (K_d) or the retardation factor (R) in a combined diffusion/adsorption model (see also [Schröder et al., 2016a] on the modelling of sorption processes in Boom Clay).

---

[a] Note that in some studies the ‘inverse’ definition for tortuosity $(L/L_a)^2$ is used, e.g. [Shackelford & Moore, 2013, p. 135].

The diffusion coefficient for retarded diffusive species is known as the *apparent diffusion coefficient* D_{app} [NEA/OECD, 1996, p.70]:

$$D_{app} = \frac{D_{eff}}{\eta R} = \frac{D_{pore}}{R} = \left(\frac{\delta}{\theta^2}\right)\frac{D_0}{R} \qquad (13)$$

with R - retardation factor, applicable under the assumptions of fast, reversible, equilibrium reactions which can be expressed as linear sorption isotherm.

The distribution coefficient K_d can be used to estimate the retardation factor:

$$R = 1 + \frac{\rho_b \cdot K_d}{\eta} \qquad (14)$$

with:
ρ_b - bulk density of the solid phase [kg m^{-3}],
K_d - distribution coefficient $K_d = C_s/C$ [m^3 kg^{-1}],
C_s - solid-phase (or sorbed) concentration of the diffusing particle [kg/kg],
C - aqueous-phase (or dissolved) concentration of the diffusing particle [kg m^{-3}],
η - porosity [-].

The equation 13 becomes in this case:

$$D_{app} = \left(\frac{\delta}{\theta^2}\right) D_0 \frac{\eta}{\eta + \rho_b \cdot K_d} \qquad (15)$$

2.3.2. Fick’s second law for diffusion in porous media

The replacement of D_0 by D_{app} allows applying Fick’s second law for transient diffusion of non-decaying species to porous media:

$$\frac{\partial C(x,t)}{\partial t} = D_{app} \frac{\partial^2 C(x,t)}{\partial x^2} \qquad (16)$$

For solid properties and adsorption coefficient constant in time and space, this equation takes the form [Bourg et al, 2003]:

$$(\eta + \rho_b \cdot K_d)\frac{\partial C}{\partial t} = \frac{\eta D_0}{\theta^2}\frac{\partial^2 C(x,t)}{\partial x^2} \qquad (17)$$

This equation can be extended with radioactive decay, for first order decay leading to:

$$(\eta + \rho_b \cdot K_d)\frac{\partial C}{\partial t} = \frac{\eta D_0}{\theta^2}\frac{\partial^2 C(x,t)}{\partial x^2} - \lambda C \qquad (18)$$

where λ is the first order decay coefficient [s^{-1}].

The modelling approaches based on Fick’s laws can be completed with semi-empirical constants (e.g. anion accessible porosity, surface diffusion coefficient) to consider the effects of electrochemical processes such as anion exclusion or surface diffusion as will be discussed in the next section.

To address the heterogeneity of natural clay depositions, some authors take the inner structure of the porous medium (see Figure 2-1) into consideration using several porosity types and by dividing the total porosity into sub-volumes [Bourg, 2003; Tournassat et al., 2011; Appelo, 2007, 2008 & 2010].

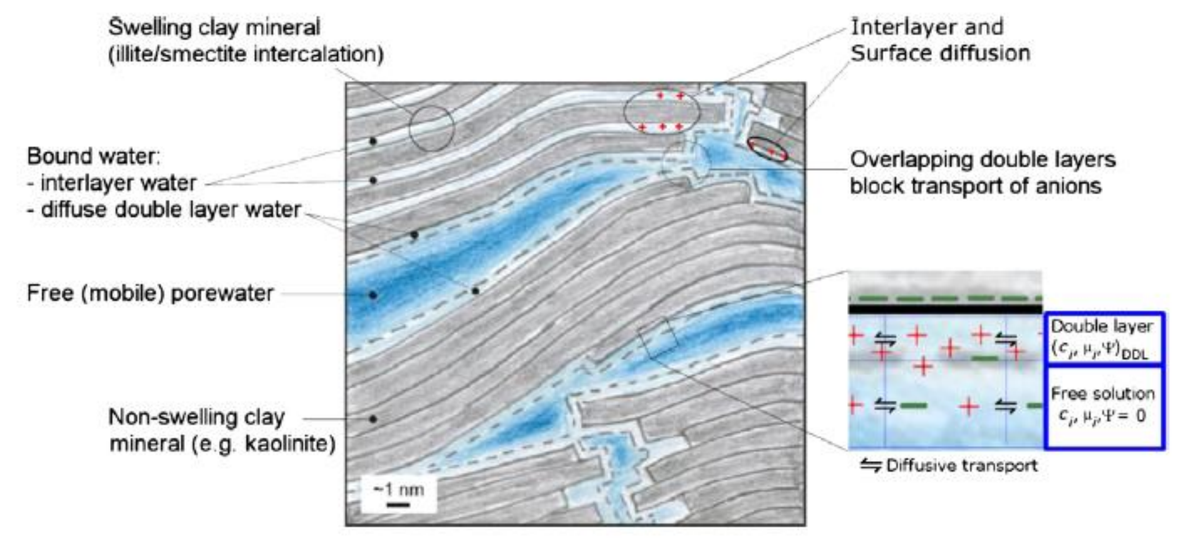

Figure 2-1 A diagram of the pore space in Opalinus Clay showing three water-types with associated diffusion domains [Appelo et al.; 2010, p.5].

Two types of pores (porosities) are usually used when modelling diffusion and adsorption in compacted bentonite [Bourg, 2003; Tournassat et al., 2011; Appelo, 2007, 2008 & 2010] and clay containing rocks:

- large pores (interparticle space) where diffusion is not relevantly affected by the surface and
- interlayer pores (also named ‘diffuse-layer’ porosity) which are very thin and where the diffusion is considerable affected by the surface induced phenomena such as anion exclusion and cation diffusion along the surface.

Since the pore space has non-uniform electrochemical properties, three different diffusion domains (*sub-volumes* or *pore spaces*) are considered in some modelling approaches (e.g. [Tournassat et al., 2011; Appelo, 2007, 2008 & 2010]):

- interlayer water (water and cations between the montmorilonite layers, devoid of anions),
- electrostatic double layer (EDL) or diffuse double layer (DDL) water (water, an excess of cations and a deficit of anions),
- bulk or free pore water (charged balanced aqueous solution of cations and anions).

The distribution of the pore water of these three types depend on a number of factors such as the clay content of the clay containing rock, the compaction of the rock, the ionic strength and composition of the pore water as well as the nature of cations present in the pore water.

[Tournassat & Appelo, 2011] propose a three step approach to establish the proportions of different water types in bentonite. As a first step the impurities are extracted from the solid part. Secondly, the amount of interlayer water is established and finally the remaining porosity is subdivided into a charged fraction (DDL) and free pore water.

The assessment of interlayer diffusion coefficients is problematic because the interlayer solution is very different from pure liquid water [Bourg et al., 2003].

The term 'speciation' describes the distribution of an element over different chemical bindings or forms. E.g. soluble uranium can – dependent on the chemical circumstances - be present as charged soluble ion UO_2^{2+}, as uncharged soluble $UO_2(OH)_2$, or, most likely, a mixture of these (and other) species. The speciation determines the charge and size of an ion, which can affect the diffusion by e.g. anion exclusion. It is thus important to know the speciation of a radionuclide in order to be able to understand its migration behaviour (e.g. UO_2^{2+} will have different migration behaviour then the uncharged $UO_2(OH)_2^0(aq)$). The speciation of a component is influenced by the pH, the redox potential and the presence of ligands. An important mathematical tool to evaluate the speciation is 'chemical equilibrium modelling' or 'geochemical modelling' (e.g. [Appelo, 2005; Lindsay, 1999]), that makes use of the assumption that all species are in thermodynamic equilibrium. For more information on the modelling of speciation as part of the OPERA assessment of radionuclide migration in Boom Clay, see [Schröder et al., 2016a, Schröder et al., 2016b].

In [Appelo et al., 2007, 2010] an approach for modelling multicomponent diffusion is described. Different from many other numerical models that assume the same diffusion coefficients, accessible porosity and tortuosity factor for all solutes, in this approach each solute is given its own tracer diffusion coefficient [Appelo et al., 2007, Table 1].

2.4. *Electrostatic effects on (ion) diffusion*

The bulk media, e.g. clay particles in Boom Clay, generally have a charged surface. This can result in perceptible gradients of the distribution of species close to a (charged) surface and further away in the bulk solution. The areas near a surface where differing concentrations of ions can be found than in the bulk solution are often denoted as 'electrostatic double layer' or 'diffuse double layer' (DDL). The general features of the electrostatic layers are usually addressed by the Gouy-Chapman and Stern model [Atkins, 1996, p.1008*f*]. Several macroscopic models exist to describe the complex behaviour of ion binding in these layers (e.g. [Kinniburgh et al. 1999; Hiemstra et al., 1996], see also [Schröder et al., 2016a]). The electrostatic properties of argillaceous host rock are relevant for diffusion because the DDL can strongly influence the distribution of ions in pore space, with the extent of the DDL depending on the ionic strength of the pore water. Furthermore, adsorption of ions to the surface of a charged particle modifies the surface charge distribution, and influences the extent and composition of the DDL. In the next two subsections, the effects of '*anion exclusion*' and '*surface diffusion*' and their model representation are summarized.

2.4.1. Anion exclusion and semipermeable membrane behaviour

In porous media with negatively charged particles, such as clays and sediments, often, lower diffusivities (D_{eff}) are observed for anions [Garcia-Gutierez et al., 2004], [Bruggeman et al., 2010a], [Kozaki et al., 1998], [Kozaki et al., 2001], [Van Loon et al., 2007]. Lower diffusivities and respectively higher tortuosities for anions could be explained by:

- Donnan effect excluding anions from accessing narrow interlayer pores in clays,
- Size exclusion and dead end pores,
- Anion exclusion from diffusion layers by the negative charge of the solid.

Electrostatic **anion exclusion** from the DDL by the negative charge of the solid, also called negative absorption of anions, can be accounted for by using a so-called '*anion accessible porosity*' coefficient [Tournassat et al., 2011] or '*effective porosity*' (η_{eff}) [Bourg et al, 2003]. In that case anions are excluded from part of the pore space because of electrostatic repulsion, and effectively can only enter part of the total pore space or porosity. The equations 15 and 16/17 become:

$$D_{app} = \left(\frac{\delta}{\theta^2}\right) D_0 \frac{\eta_{an}}{\eta_{an} + \rho_b \cdot K_d} \qquad (19)$$

$$(\eta_{an} + \rho_b K_d)\frac{\partial C}{\partial t} = \frac{\eta_{an} D_0}{\theta^2}\frac{\partial^2 C(x,t)}{\partial x^2} \qquad (20)$$

This coefficient (η_{an}) considers the fraction of porosity that does not participate in the diffusive transport of anions. Modelling approaches capable to predict the value of η_{an} in compacted Na-bentonite have been proposed and tested in [Tournasset et al., 2011]. Although this study focuses on bentonite properties it is expected that those models could be also applicable for natural clay formations with similar diffusion properties as the bentonite and significant contents in swelling clay minerals.

The models for anion exclusion can be divided in two groups [Tournassat et al., 2011]:

- Donnan type pore space models and
- Anion free interlayer models.

In the Donnan pore space models the entire pore space is taken as the Donnan volume and assigned the full charge of montmorillonite.

The anion-free interlayer models assume that the interlayer porosity is devoid of anions and subdivide the external volume into a Donnan volume and a free fraction.

The electrochemical interactions are usually considered by incorporation of a diffuse double layer (DDL) in the mathematical models.

The incorporation of a DDL in [Appelo et al, 2007] has been carried out by splitting a pore in two parts: one is a charge free solution, the other a diffuse double layer (see Figure 2-2).

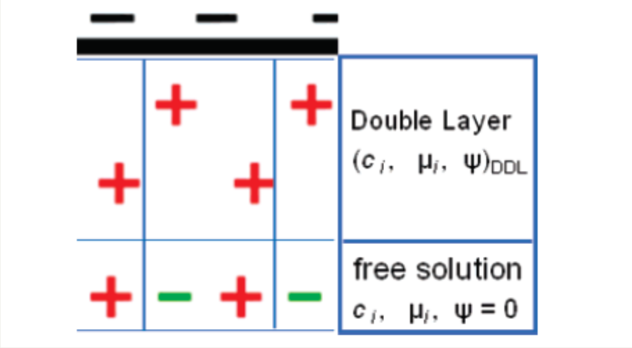

Figure 2-2 Discretization of a pore with a charge-free solution and a diffuse double layer that forms the basis for the multicomponent diffusion model in PHREEQC (from [Appelo et al, 2007]).

The diffusive transport is calculated separately for free pore water and the DDL and then summed up for the interfaces between two cells.

In [Appelo et al., 2007, 2010] the diffusive flux is calculated based on the electrochemical potential rather than on concentration, leading to following expression that is valid even when the solution is not electrically neutral:

$$J_i = -D_{0,i}\left(\frac{\partial \ln(\gamma_i)}{\partial \ln(c_i)} + 1\right)\frac{\partial c_i}{\partial x} + D_{0,i} z_i c_i \frac{\sum_{j=1}^{n} D_{0,j} z_j \left(\frac{\partial \ln(\gamma_j)}{\partial \ln(c_j)} + 1\right)\frac{\partial c_j}{\partial x}}{\sum_{j=1}^{n} D_{0,j} z_j^2 c_j} \qquad (21)$$

With:

i - subscript introduced for species,
j - subscript introduced for species to show that they origin from the potential term,
$D_{0,i}$ - tracer diffusion coefficient in water [m^2/s],
z_i - charge number [-],
γ_i - activity coefficient [-],
c_i - concentration [mol/m^3].

The concentration in the DDL is calculated by the Donnan approximation which assumes a single potential for the DDL as an entity (eq. 22) and optimizes the potential to achieve charge neutrality (eq. 23):

$$c_{i,DDL} = c_i \exp\left(\frac{-z_i F \Psi_{DDL}}{RT}\right) \qquad (22)$$

$$\sum z_i c_{i,DDL} + \sigma_{DDL} = 0 \qquad (23)$$

with:

$c_{i,DDL}$ - concentration of species i in Donnan volume [mol/m^3],
c_i - concentration of species i in free solution [mol/m^3],
F - Faraday constant [$C\ mol^{-1}$-],
Ψ_{DDL} - averaged electrical potential in the DDL [V],
σ_{DDL} - compensating charge to achieve charge neutrality [C],
R - universal gas constant [$J\ K^{-1}\ mol^{-1}$],
T - absolute temperature [K].

The Donnan Equilibrium is assumed in many studies in the diffuse layer calculations [Wersin et al.,2004], [Appelo et al.,2007 and 2008].

2.4.2. Surface diffusion of cations and interlayer diffusion

In some experiments with clays, cations appear to exhibit higher diffusion coefficients (D_{eff}) than neutral species ([Gimmi&Kosakowski, 2011], [Glaus et al., 2007], [Melkior et al., 2005], [Muurinen, 1994], [Van Loon et al., 2004 and 2005]).

This increased diffusion for cations can be explained by:

- Interlayer or surface diffusion of sorbed cations (e.g. [Bourg, 2004], [Bourg et al., 2007]) or
- Diffusion of cations in the diffuse double layer formed at the interface between negatively charged clay surfaces and surrounding water containing an excess of cations [Appelo&Wersin; 2007].

The '*surface diffusion*', '*diffusion along the surface*' or '*diffusion of adsorbed species along the solid surface*' can be accounted for by a semi-empirical 'surface diffusion' coefficient D_{surf} representing the diffusion coefficient in the interfacial region.

To account for the surface diffusion of the sorbed cations, a surface diffusion coefficient was introduced, $D_{surf.}$ The laws of Fick in this case are described as follows [Muurinen, 1994]:

$$J = -\eta D_{pore}\frac{\partial C}{\partial x} - \rho_b D_{surf} K_d \frac{\partial C}{\partial x} = -(D_{eff} + \rho_b D_{surf} K_d)\frac{\partial C}{\partial x} = D^*_{eff}\frac{\partial C}{\partial x} \tag{24}$$

$$\frac{\partial C}{\partial t} = \frac{D^*_{eff}}{(\eta + \rho_b K_d)}\frac{\partial^2 C}{\partial x^2} = D^*_{app}\frac{\partial^2 C}{\partial x^2} \tag{25}$$

with $D^*_{eff}=D_{eff}+\eta_b D_{surf} K_d$ and $D^*_{app}=(\eta D_{pore}+\rho_b D_{surf} K_d)/(\eta+\rho_b K_d)$ being lumped as effective and apparent diffusion coefficients interpreting the experiments. The parameter K_{surf} is used for fitting the apparent diffusion versus K_d.

In this approach the diffusion of cations has two separate contributions, one associated with the movement through the free pore water and other associated with the movement along the interface between the solid and liquid phases.

A similar approach is used in [Muurinen & Lehikonen, 1995], [Soudek et al., 1983]:

$$(\eta + \rho_b \cdot K_d)\frac{\partial C}{\partial t} = \frac{\partial}{\partial x}\left[\frac{\eta D_0}{\theta^2}\frac{\partial C(x,t)}{\partial x} + \frac{D_{surf}\rho_b K_d}{\theta^2_{surf}}\frac{\partial C(x,t)}{\partial x}\right] \tag{26}$$

where:

D_0	- cation diffusion coefficient for free water,
D_{surf}	- cation surface diffusion coefficient,
ρ_b	- bulk density of the porous material,
K_d	- distribution coefficient,
θ^2_{surf}	- tortuosity of the surface path.

For equal tortuosity of the pores and surface paths, this equation takes the form:

$$(\eta + \rho_b \cdot K_d)\frac{\partial C}{\partial t} = \frac{\partial}{\partial x}\left[\frac{(\eta D_0 + D_{surf}\rho_b K_d)}{\theta^2}\frac{\partial C(x,t)}{\partial x}\right] = \frac{\partial}{\partial x}\left[(D_{eff} + D_{eff,surf})\frac{\partial C(x,t)}{\partial x}\right] \tag{27}$$

with:

D_{eff}	- effective diffusion coefficient,
$D_{eff,\ surf}$	- effective surface diffusion coefficient [Zheng et al., 2011, p.3]

In [Molera & Eriksen, 2002], [Molera, 2002] a different approach is proposed that assumes a time average fraction of the sorbed cations (f) to be mobile. For a constant tortuosity within the pore space the flux and concentration equations become:

$$J = -\eta D_{pore}\frac{\partial C}{\partial x} - f\rho_b D_{pore} K_d \frac{\partial C}{\partial x} = -(D_{eff} + f\rho_b D_{pore} K_d)\frac{\partial C}{\partial x} = D^*_{eff}\frac{\partial C}{\partial x} \tag{28}$$

$$\frac{\partial C}{\partial t} = \frac{D_{eff}^{*}}{(\eta + \rho_b K_d)} \frac{\partial^2 C}{\partial x^2} = D_{app}^{*} \frac{\partial^2 C}{\partial x^2} \tag{29}$$

with $D^{*}_{eff}=D_{eff}+f\eta_b D_{pore}K_d$ and $D^{*}_{app}=(\eta D_{pore}+f\rho_b D_{pore}K_d)/(\eta+\rho_b K_d)$ being lumped as effective and apparent diffusion coefficients interpreting the experiments.

These approaches make no distinction between different adsorption mechanisms (specific and diffuse layer adsorption) and have no predictive power.

An integrated sorption-diffusion model was implemented in [Ochs et al., 1998, 2001], [Sato & Yoshikawa, 1995], [Kato et al., 1995]. In this approach a new parameter was introduced: the electrostatic constrictivity, δ_{el}, representing the ratio between the average concentration of the diffusing ion in the DDL and its concentration in the bulk water. This parameter was fitted to a set of diffusion data on compacted bentonites.

$$J = -\eta D_{pore} \delta_{el} \frac{\partial C}{\partial x} = -D_{eff} \delta_{el} \frac{\partial C}{\partial x} = D_{eff}^{*} \frac{\partial C}{\partial x} \tag{30}$$

$$\frac{\partial C}{\partial t} = \frac{D_{eff}^{*}}{(\eta + \rho_b K_d)} \frac{\partial^2 C}{\partial x^2} = D_{app}^{*} \frac{\partial^2 C}{\partial x^2} \tag{31}$$

with:

$$\delta_{el} = \frac{1}{C_b d} \int_0^d C(x) dx$$

where d is the pore width and C(x) is the local concentration of the ion in the DDL as function of x.

In [Appelo et al., 2010] the pore water is subdivided in three sub-volumes or pore spaces (see Section 2.3.2) and the total flux is represented as the sum of the fluxes in these three sub-domains.

$$J_{free} = -f_{free} \eta D_0 \frac{\delta}{\theta^2} \frac{\partial C}{\partial x} = -f_{free} \eta D_{pore} \frac{\partial C}{\partial x} \tag{32}$$

$$J_{DDL} = -f_{IL} \eta D_0 (\frac{\delta}{\theta^2})_{IL} \frac{C_{IL}}{\beta} \frac{\partial \beta}{\partial x} = -f_{DDL} \eta D_{pore} \frac{C_{DDL}}{C} \frac{\partial C}{\partial x} \tag{33}$$

$$J_{IL} = -f_{DDL} \eta D_0 \frac{\delta}{\theta^2} \frac{C_{DDL}}{C} \frac{\partial C}{\partial x} \tag{34}$$

with f_{free}, f_{DDL} and f_{IL} - fractions of free, diffuse double layer and interlayer water; ß- molar or equivalent fraction of surface complexed or ion-exchanged cations, $(\delta/\theta^2)_{IL}$ - tortuosity and constrictivity specific to interlayer region.

$$J = -\eta D_0 \frac{\delta}{\theta^2} \left(f_{free} + f_{DDL} \frac{C_{DDL}}{C} \right) - \frac{\partial C}{\partial x} \tag{35}$$

3. Overview of the SCK·CEN approach to describe radionuclides migration

This chapter provides an overview of the approach that is currently followed in the Belgian programme on geological waste disposal to study and parameterise migration of Radionuclides in Boom Clay.

In Belgium, since 1974 major studies have been executed to assess the long-term safety of disposal of high-level waste and spent fuel in a clay formation. In particular, Boom Clay has been studied as a potential host formation for a repository.

Clay sedimentary formations have to provide both a physical (limited or negligible water flow) and a chemical (retention) barrier for radionuclide transport. Therefore, one of the key questions for a repository's safety assessment concerns the predominant radionuclide-transport mechanism.

In order to describe diffusion-driven transport for solutes, performance assessment calculations in Belgium are based on the following parameters:

- solubility of the solute C_{sol} (mol/l),
- retardation factor R (dimensionless),
- pore diffusion coefficient D_{pore} (m^2/s), and
- diffusion accessible porosity η (dimensionless).

Values for these parameters as well as a sound understanding of the underlying processes need to be provided for all radionuclides that are considered for the safety assessment. The collection of extensive databases for all those radionuclides is however not an easy task, since the diffusion behaviour of radionuclides in porous media is a complex process affected by many parameters, such as:

- the properties of the diffusing species,
- the properties of the medium itself (pore structure, degree of compaction, adsorption properties, dry density),
- the geochemistry of the system (pore water chemistry) and
- the temperature.

3.1. Strategy – Sorting the radionuclides in phenomenological groups

Ideally, a thermodynamic database should be constructed containing all intrinsic thermodynamic quantities related to the geochemical processes that occur. In reality, however, this is hard to achieve. Moreover, the objective when providing radionuclide transport parameters for PA is not only to deliver the necessary data, but also to build confidence in those data. Confidence building relies upon the drafting of scientifically defensible phenomenological models for each radionuclide under consideration. Those models should describe all major processes and mechanisms which control the transport of each radionuclide under the far field conditions of interest for geological disposal in Boom clay. For the following reasons such a rigorous approach is unfeasible for all radionuclides at the present time:

(1) The current scientific insight into the roles and importance of different phases (minerals, solid organic matter, humic colloids) and their interrelationships is limited.

(2) Thermodynamic (sorption/interaction) models are only available for sufficiently pure solids and simple solid-fluid systems.

(3) An experimental programme for all radionuclides present in the waste would require a very time-consuming and costly research and development effort.

(4) Uncertainties with respect to several processes limit the interpretation of data and not all processes are sufficiently understood (e.g. eigencolloid formation, functional group composition of humic substances, etc.).

(5) Thermodynamics alone are unsuitable for describing kinetic processes such as colloidal behaviour.

Because of these issues it was decided on a strategic approach to deduce these migration parameters from all available information and data sources (thermodynamic data, experiments on the Boom Clay, literature data) in a consistent way.

In brief, this strategic approach consists of:

(1) Subdividing all radionuclides considered into radionuclide groups exhibiting chemically analogous characteristics;

(2) Drafting phenomenological models that fit all radionuclides in a particular group;

(3) Assigning consistent parameter ranges for all radionuclides that belong to a particular group.

The cornerstone of this methodology involves the drafting of so-called “phenomenological models”. Phenomenological models are geochemically consistent models that are able to describe, both in a qualitative and quantitative way, how radionuclides migrate under the specific far-field conditions of a disposal site.

These models are based on the combined insights gained from:

- general scientific insights/knowledge concerning their general chemical/ thermodynamic characteristics, and
- experimental observations of the geochemical behaviour of the various considered radionuclides.

Phenomenological models are also general enough to allow the different radionuclides to be considered by the PA, to be divided into groups.

A group encompasses all radionuclides that have sufficient similarities with respect to the processes to which they are subjected during transport. Therefore, groups are selected based on similarities in speciation, sorption and migration behaviour. These characteristics are crucial to understand and predict retention/migration of all radionuclides within the group.

For each group, a phenomenological model is built, in which the shared characteristics play a dominant role. That model fulfils multiple purposes:

(1) It allows to draw parallels between the retention/migration behaviours of all radionuclides within a specific group;

(2) It is used to select parameter values that are then delivered as input to the safety assessment.

(3) It is used to assess changes in these parameter values that are caused by physico-chemical perturbations or by the spatial heterogeneity of the Boom Clay formation.

By grouping radionuclides, SCK·CEN aims at providing scientifically justifiable retention/migration parameters for all individual radionuclides, even if not all data are available to be able to determine them specifically.

The grouping of chemical elements and the choices of distinctions between groups is based on a number of arguments:

(1) thermodynamic considerations – similarities in inorganic speciation in Boom Clay pore water, calculated using the MOLDATA database ([Wang et al., 2011], [Salah & Wang, 2012]);
(2) experimental observations – similarities in sorption, solubility in the presence of organics, migration behaviour under conditions relevant for the Boom Clay; and
(3) scientific literature – general similarities in environmental conditions (not limited to the Boom Clay).

As the next step, at least one “representative radionuclide” is selected for each group. Selection of that radionuclide is based on the amount of experimental and literature data available to support understanding, description and prediction of its retention/migration behaviour under Boom Clay conditions. For each representative radionuclide, a “Topical Report” is provided in which all these data are presented, and parameter values are delivered as input to the safety assessment, together with justifications for their selection. The main processes and mechanisms to which the radionuclide is subjected under Boom Clay conditions are highlighted. The main geochemical parameters that influence the behaviour of the radionuclide are discussed, preferably in a quantitative way. Possible uncertainties or knowledge gaps are pinpointed and their influence is assessed. As such, these Topical Reports describe the scientific basis for the final parameter selection.

3.2. Choices and overview of groups and reference elements

The use of group-specific phenomenological models has several advantages:

- They aim at providing a thorough scientific basis (both qualitatively and quantitatively) for the migration parameter data sets that are delivered to PA. Additionally, they provide a realistic framework that enables assessment of parameter uncertainties and deviations of data ranges related to perturbations, spatial variability, etc.
- They enable selection of realistic parameter ranges for radionuclides for which no, or only limited batch and/or migration data are available. They allow comparison of different radionuclides within the same conceptual framework: this will clarify the parameter value choices for different radionuclides. Chemical consistency is maintained throughout the parameter selection.
- They also allow pinpointing more precisely where more data is needed, for which an experimental programme should be set up as part of future scientific research studies.

The disadvantages are:

- Placing the radionuclides in a correct group/assign a correct phenomenological model to each nuclide is not always straightforward. For some nuclides no data are available and the choice relies on expert judgement.
- Phenomenological models must be sufficiently elaborate and scientifically sound to enable the selection of realistic migration parameter values. Model uncertainty is propagated to all radionuclides selected for that particular group.

For each phenomenological model at least one detailed Topical Report (TR) has been prepared to explain in detail all the data and knowledge that culminates in the model. Up to now, the reference elements are HTO [Bruggeman et al., 2013], iodine (I), caesium (Cs) [Maes et al., 2011b], strontium (Sr) [Maes et al., 2012], technetium (Tc) [Bruggeman et al., 2010d], americium (Am)/europium (Eu) [Bruggeman et al., 2012b], and uranium (U) [Salah et al., 2015]. Apart from these, a substantial report is also available on selenium (Se) [Canniere et al., 2010], HCO_3^- [Aertsens et al., 2008b] and Natural Organic Matter (NOM) [Bruggeman & Craen, 2012a]. It is argued that these elements sufficiently cover all the different possible phenomena that potentially influence every safety-relevant radionuclide under the geochemical conditions of the Boom Clay.

The groups (and respective phenomenological models) that are considered and the assignment of the radionuclides to the various groups are outlined below (see also Table 3-1):

1. The first group comprises the reference conservative tracer HTO. HTO is very frequently used both in lab-scale migration experiments and in meter-scale *in situ* experiments, to obtain reference transport parameters for the Boom Clay.
2. A second group is made up by the anions, containing mostly non-metal elements from groups IVA to VIIA in Mendeleev's table (with the exception of Mo). The reference element for this group is iodine (as iodide, I^-). Se is also part of this group, both as the oxyanion selenate (SeO_4^{2-}) and as the biselenide anion (HSe^-). Other elements belonging to this group are carbon (C, as bicarbonate, HCO_3^-), molybdenum (as molybdate, MoO_4^{2-}) and chlorine (as chloride, Cl^-). The anion group is characterised by limited or no sorption/retardation and due to the anion-exclusion phenomenon, the diffusion accessible porosity is reduced compared to HTO.
3. The third group consists of alkali and alkaline earth metals that are not hydrolysed under Boom Clay conditions (thus, excluding Be). These metals are predominantly adsorbed through ion exchange and their transport is influenced by surface diffusion processes. Two different subgroups are distinguished . The first subgroup contains monovalent cations with small hydrolysed radius that are preferably bound to illite ion exchange sites. These cations also do not have a solubility limit. The second subgroup contains divalent cations that may form aqueous complexes with CO_3^{2-} and that are solubility-limited due to the formation of carbonate phases. They preferably bind to the interlayer ion exchange sites of smectite minerals.
4. The fourth and largest group consists of elements that exhibit transport behaviour determined mostly by their affinity for dissolved organic matter (DOM) colloids naturally present in the pore water of the Boom Clay. This affinity in practice means that a large part of the nuclide speciation in the Boom Clay pore water consists of humic-associated species (either as true complexes or as colloidal associations). Since these species are generally less well sorbed/retained, they will travel faster than their dissolved/inorganic counterparts. This large group is again subdivided. DOM itself is considered as a reference tracer and it is assumed that humic colloid-associated species have the same transport properties as DOM. Furthermore, the heavy metals, the trivalent lanthanides/actinides and the tetravalent lanthanides/actinides are distinguished (the latter group also contains the pentavalent Pa). The differences between these subgroups are not very significant, and other subdivisions are equally possible (e.g. a subgroup combining both the tetravalent Ln/Ac as well as the tetravalent heavy metals). The main difference between the trivalent Ln/Ac and the others is the importance of carbonate complexes in their inorganic speciation. The main difference between tetravalent Ln/Ac and the others is their well-documented eigencolloid behaviour (although several heavy metals such as Tc, Zr, Sn may also form eigencolloids).

Table 3-1 Assignment of the radionuclides to different groups based on the considered phenomenological model describing their behaviour in Boom Clay

Element	Eq. Species	Group
HTO	HTO	
I	I(-)	Anion
Cl	Cl(-)	Anion
Se (1)	HSe(-)	Anion
Nb	$Nb(OH)_6(-)$	Anion
Se (2)	$SeO_4(2-)$	Anion
Mo	$MoO_4(2-)$	Anion
C	$HCO_3(-)$	Anion
Cs	Cs(+)	IEX cation
Rb	Rb(+)	IEX cation
Sr	$Sr(2+)/SrCO_3(aq)$	IEX cation
Ca	$Ca(2+)/CaCO_3(aq)$	IEX cation
Ra	$Ra(2+)/RaCO_3(aq)$	IEX cation
NOM	NOM	
Tc	$TcO(OH)_2(aq)$	Transition metal + NOM
Ag	AgHS(aq)	
Be	$BeO_2(2-)$	
Ni	$Ni(CO_3)_2(2-)$	
Pd	$Pd(OH)_2(aq)$	
Zr	$Zr(OH)_4(aq)$	
Sn	$Sn(OH)_5(-)$	
Am	$Am(CO_3)_2(-)$	Trivalent Ln/Ac + NOM
Ac	$Ac(CO_3)_2(-)$	
Cm	$Cm(CO_3)_2(-)$	
Sm	$Sm(CO_3)_2(-)$	
Pu	$Pu(CO_3)_2(-)$	
U	$U(OH)_4(aq)$	Tetravalent Ln/Ac+ NOM
Th	$Th(OH)_3(CO_3)(-)$	
Np	$Np(OH)_4(aq)$	
Pa	$Pa(OH)_5(aq)$	

3.3. Description of migration behaviour in Boom Clay

As described in SCK·CEN's strategy, next to similarities in aqueous speciation and sorption behaviour also similarities in migration behaviour were observed which lead to a categorisation of the radionuclides. Each group of radionuclides displays a similar migration behaviour reflecting different underlying processes.

This section is structured according to the different major transport processes observed for radionuclides in the Boom Clay.

3.3.1. Reference conservative tracer: HTO

HTO is used as a reference tracer to study the overall transport properties of the Boom Clay.

HTO is treated as a conservative tracer, hence no sorption occurs and the retardation factor, R, is equal to 1. Moreover, HTO has neutral charge and will distribute itself over the entire pore space. Therefore HTO migration data allow information to be extracted about the diffusion accessible porosity (η) in the Boom Clay and the ratio δ/τ^2 (constrictivity/tortuosity). HTO was used to study the influence of compaction, ionic strength, upscaling, as well as the vertical and lateral variability on the general transport parameters of the Boom Clay.

3.3.2. Migration of anions – anion exclusion

Several anions, such as chloride (Cl^-) and iodide (I^-), also behave as conservative tracers but because of their negative charge, their transport paths are different compared to neutral species as HTO and the ratio δ/τ^2 will be different for anions and HTO. Because of charge repulsion by the negatively charged solid matrix of the clay [Bruggeman et al., 2010a], these anions cannot penetrate the double layer covering the charged clay plates and as a result only part of the pore space is accessible for their diffusion. This effect is called "anion exclusion" or "Donnan exclusion". The diffusion accessible porosity for anionic species in Boom Clay, determined using iodide as tracer, is about half the porosity of the neutral HTO.

The decreased diffusion accessible porosity for anions is a well-documented observation that applies also to other argillaceous formations and to compacted clay systems [Bruggeman et al., 2010a], [Kozaki et al., 2001], [Kozaki et al., 1998], [Pusch et al., 1990], Van Loon et al., 2007]. The current understanding and modelling of that phenomenon is summarized in Section 2.4.1.

For some anions like HCO_3^- and SO_4^{2-}, retardation is observed ([Aertsens et al., 2008b], Canniere et al., 2010] This retardation is mainly invoked from the fitting of rather high values of ηR (higher than the corresponding value for HTO) to the diffusion profiles of these anions. In these cases, no information is available from batch sorption experiments which could substantiate the degree of retardation, or could allow the observed retardation factor to be coupled quantifiably to specific uptake mechanisms. However, the consistent observation of these high ηR values is considered as sufficient evidence for uptake processes related to the chemical species in question.

3.3.3. Migration of cations adsorbed through ion exchange – surface diffusion

The adsorption of alkali and alkaline earth metals to ion exchange sites of montmorillonite and illite clay minerals is qualitatively well understood and can be qualitatively described and predicted using the 2 SPNE SC/CE (2 site protolysis non-electrostatic surface complexation/cation exchange) or 3-site IEX (Ion Exchange) models developed by Bradbury and Baeyens. The use of these (quasi-)thermodynamic sorption models is part of SCK·CEN's simplified component additivity strategy to describe and explain metal uptake in the Boom

Clay. These models reinforce confidence in measured K_d values on the whole Boom Clay. Moreover, no difference in K_d values has been shown to exist for Cs between suspended and compacted systems ([Altmann et al., 2012], [Durce et al., 2016], [Maes et al., 2011b], [Maes et al., 2008], [Van Loon et al., 2009]). This high confidence in adsorption modelling and K_d values in batch experiments should lead to a straightforward determination of R values in transport experiments. However, experience at SCK·CEN has shown that different types of migration experiments led to robust values for D_{app} only, while R values extracted from these experiments were less reliable. Nevertheless, the obtained values are still in line with values derived from sorption experiments ([Durce et al., 2016], [Maes et al., 2011b], [Maes et al., 2008]).

Despite the ability to obtain both good sorption data from batch experiments, and D_{app} data from migration experiments, the phenomenological description of the transport of cations sorbed through ion exchange in clays poses a problem. In the classical theory on transport through porous media, the following relationship is used to link the sorption (via R) to the diffusion coefficient:

$$D_{app} = \frac{D_{pore}}{R} = \frac{D_0}{R}\frac{\delta}{\tau^2} = \frac{D_{eff}}{\eta R}$$

It has been observed for cations diffusing in micaceous and/or smectite clays, and especially for ion-exchangeable cations, that this relationship might not be correct. D_{pore} values calculated on the basis of independently measured D_{app} and R (K_d) values lead to values which exceed the D_{pore} value for HTO, which seems physically impossible. This apparent enhanced diffusion is often referred to as “surface diffusion” and although it is systematically observed for all cations that adsorb through ion exchange, this phenomenon and its driving force were heavily debated ([Gimmi&Kosakowski, 2011], [Glaus et al., 2010], [Horseman et al., 1996], [Melkior et al., 2005], [Melkior et al., 2007], Muurinen, 1994], Van Loon et al., 2005], [Van Loon et al., 2004]).

The exact nature of this mechanism is not fully understood yet, but is linked to EDL phenomena.

The conceptual model which is currently being developed and which would explain these observations is called “double layer enhanced diffusion model” ([Appelo et al., 2010], [Altmann et al., 2014]). This model subdivides the pore space in “free water”, “double layer water” and “interlayer water”. The free water is to be found in the region outside the influence of the double layer. The concentration of a species in these 3 types of water is different and governed by double layer phenomena. This implies that the overall transport is composed of transport in the 3 different pore spaces each having a different concentration gradient. This has consequences for transport modelling as classical transport models only consider one concentration gradient. However, within this concept the sorption model for ion exchange cations and surface complexation remains valid. More information on the current understanding and modelling approaches of this phenomenon are summarized in Section 2.4.2.

With respect to predictive modelling (for changing chemical conditions), the surface diffusion mechanism poses a problem as chemically coupled transport models are based on the classical relation between diffusion and sorption. However, transport calculations can be based on experimentally determined and robust D_{app} values. Models requiring separate input for D_{pore} and R instead of D_{app} might be used by fixing one value and varying the other, ensuring that they combine to the known D_{app} value.

3.3.4. Migration of nuclides adsorbed through surface complexation and influenced by humic substances

As already pointed out, transition metals, lanthanides and actinides tend to show similar sorption behaviour when in presence of dissolved OM. Also in migration experiments it was observed that these elements show similar behaviour [Maes et al., 2011a].

Based on these experimental observations, a phenomenological model was conceived which captures the most prominent features of the geochemical behaviour.

In that model, two components per radionuclide are allowed to migrate: the dominant (as revealed by the speciation calculations) dissolved inorganic species under Boom Clay conditions (typically a neutral hydrolysed species or a negatively charged complex with carbonate and/or hydroxy ligands) and the species (i.e. radionuclide) associated with a humic substance colloid (figure).

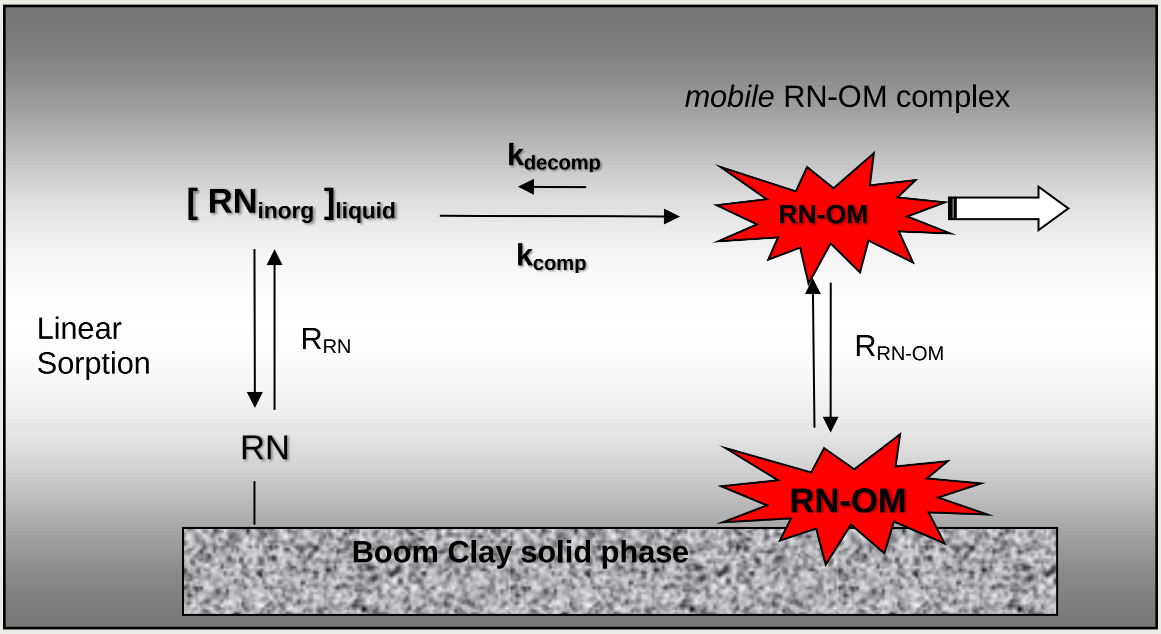

Figure 3-1 Schematic representation of phenomenology of humic colloid-mediated transport of radionuclides through the Boom Clay (Maes et al., 2011a)

The transport behaviour of these elements must therefore be described by two conservation equations for diffusive-reactive transport. The first equation corresponds to the classical diffusion-advection equation with linear reversible sorption, and is applicable only to the pure dissolved species of the element in question. The second equation corresponds to a simplified (single species of OM, no filtration) humic colloid transport equation and applies to the mobile radionuclide-humic substance colloid. Both equations also contain terms which correspond to the kinetic exchange between dissolved and humic colloid-associated species.

$$\frac{\partial C_{RN}}{\partial t} = \frac{D_{pore}}{R_{RN}} \frac{\partial^2 C_{RN}}{\partial x^2} - \frac{Q_{RN-OM}}{R_{RN}}$$

$$\frac{\partial C_{RN-OM}}{\partial t} = \frac{D_{pore,OM}}{R_{OM}} \frac{\partial^2 C_{RN-OM}}{\partial x^2} - \frac{Q_{RN-OM}}{R_{RN}}$$

$$Q_{RN-OM} = k_{comp} C_{RN} C_{OM} - k_{decomp} C_{RN-OM}$$

Radionuclides in solution will either be present as a mobile RN-OM complex or "free inorganic" radionuclide species in solution, $[RN_{inorg}]$. The relationship between $[RN_{inorg}]$ liquid and the RN-OM complex is described by a complexation constant or the ratio between the association and dissociation kinetics.

$$K_{RN-OM} = \frac{k_{comp}}{k_{decomp}} = \frac{[RN-OM]}{[RN_{inorg}][OM]}$$

$$[RN_{inorg}] + [OM] \underset{k_{decomp}}{\overset{k_{comp}}{\rightleftarrows}} [RN-OM]$$

The symbols k_{comp} and k_{decomp} are the kinetic rate constants for the RN-OM complexation/association and decomplexation/dissociation reactions, respectively and are linked to the equilibrium constant K_{RN-OM}. Slow dissociation of organic matter-bound radionuclides has been observed for many strongly bonding radionuclides. The kinetic dissociation constant, k_{decomp}, is of the order of 10^{-7} s^{-1}.

Both species can interact with the solid phase. It is assumed that this interaction in the case of $[RN_{inorg}]$ liquid is mainly due to sorption processes and can be described by a retardation factor (R_{RN}) that can be linked to batch sorption data. Most frequently, the dissolved species is characterised by a very strong retardation as shown through batch experiments. Typically, a retardation factor R_{RN} in the range of 10^3 - 10^5 is assumed.

With respect to RN-OM, the retardation factor (R_{RN-OM}) is considered as a lumped factor, accounting for both sorption and colloid filtration processes. In [Martens et al., 2010], it has been described how both these processes can account for the observed organic matter transport phenomena through the Boom Clay. Diffusive OM transport is characterised by weak, but non-negligible retardation, with retardation factors R_{OM} (determined mostly under advection conditions) ranging typically from (>)1-10 [Bruggeman & Craen, 2012a].

Within this transport model, the number of parameters remains limited and most of them can be obtained from independent measurements (batch complexation/solubility experiments, batch sorption experiments and organic matter transport experiments).

3.4. Migration parameters in Boom Clay @ Mol

Following the outlined phenomenological models that describe the transport behaviour of RN groups, migration parameter ranges are derived for the reference elements that apply for Boom Clay at the Mol site for current geochemical conditions. For details is referred to the topical reports on these reference elements as mentioned in Section 3.2.

Parameters that will be covered are:

- η	diffusion accessible porosity,
- D	apparent and pore diffusion coefficient,
- R	retardation,
- K_{RN-OM}	RN-OM complexation constant, and
- k_{diss}	RN-OM dissociation kinetic constant.

3.4.1. Transport parameters for dissolved species not influenced by organic matter

Diffusion accessible porosity

With respect to the diffusion accessible porosity, mainly two different types of nuclides are distinguished: (1) neutral and cationic species, and (2) anions. Nuclides of the first group will redistribute themselves over the entire pore volume accessible for diffusion. Therefore the results obtained from the transport modelling of the conservative reference tracer HTO may be used [Bruggeman et al., 2013], and assume that all other neutral and cationic species will likely have identical parameter ranges for η as HTO. The porosity range for HTO was obtained by a statistical analysis of the migration data for this tracer on Boom Clay cores gathered from the whole stratigraphical domain of the Boom Clay formation at the Mol site. This resulted in the range $0.34 < \eta < 0.40$.

The second group of nuclides will only use a restricted part of the pore volume accessible for diffusion. This restriction is due to charge repulsion (Donnan exclusion) of the negatively charged nuclides by the negative charges present in the solid phase. This charge repulsion causes, among other effects, the interlayer pore space associated with smectite minerals to be virtually inaccessible to anions. Based on the statistical analysis of the migration data for the conservative anionic iodide tracer on Boom Clay cores gathered from the whole stratigraphical domain of the Boom Clay formation at the Mol site, the range for the diffusion accessible porosity for anions is $0.12 < \eta < 0.20$ [Bruggeman et al., 2010a]. This range does not necessarily apply for other anions, because the effect of the charge repulsion may be dependent on the nature of the anion. Anions with double negative charge see their porosity even reduced to even lower values, e.g. in the case of SO_4^{2-} the porosity calculated according to Archie's law would be ~0.05 [De Cannière et al., 2010]. The considered range of the diffusion accessible porosity for all anions can therefore be taken as starting from 0.05 up to 0.40 (the upper limit for HTO).

Apparent and pore diffusion coefficient

Pore and apparent diffusion coefficient for HTO

Statistical analysis of the migration data for the (assumed) conservative HTO tracer on Boom Clay cores gathered from the whole stratigraphical domain of the Boom Clay formation at the Mol site resulted in the range 2.0×10^{-10} m²/s < D_{pore} < 2.6×10^{-10} m²/s. Because the diffusion coefficient of HTO in pure water, D_0, is equal to 2.20×10^{-9} m²/s [Li and Gregory, 1974]), and HTO is assumed to be a conservative tracer, the difference is explained by assuming a combined constrictivity/tortuosity factor δ/τ^2 ratio given by D_0/D_{pore} equal to ~0.10.

Pore and apparent diffusion coefficient for iodide and other anions

Because iodide is assumed to be a conservative tracer, the pore diffusion coefficient is equal to the apparent diffusion coefficient. From statistical analysis of the migration data for iodide on Boom Clay cores gathered from the whole stratigraphical domain of the Boom Clay formation at the Mol site, the observed range of the pore diffusion coefficient is: 1.2×10^{-10} m²/s < D_{pore} < 1.6×10^{-10} m²/s. Given a D_0 value of 2.06×10^{-9} m²/s, the ratio δ/τ^2 for iodide equals ~0.07. The lower δ/τ^2 ratio for I^- compared to HTO indicates that anions use a more tortuous migration path than neutral tracers.

For Cl^- and HSe^- and $Nb(OH)_6^-$ (all monovalent anions) it is assumed that the migration path is approximately equal to that of I^-, meaning that the same δ/τ^2 ratio can be used to scale the ranges for these nuclides based on the difference in D_0 value. All three tracers are also considered as conservative.

For divalent anions, migration data for SO_4^{2-} serve as a reference. From the study of SO_4^{2-} migration it was concluded that this species does not behave as a conservative tracer (the product of ηR was higher than that for I^-). Because no batch sorption data are available, it is not feasible to obtain independent measurements of D_{pore}, η and R. Therefore the apparent diffusion coefficient, which can be obtained directly from tracer profiles in transport experiments, is used instead of D_{pore}. The range for D_{app} of the sulphate species is chosen by statistical analysis of available migration data and amounts to 2.2×10^{-11} m²/s < D_{app} < 4.2×10^{-11} m²/s. The D_{app} ranges for other divalent anions (SeO_4^{2-}, MoO_4^{2-}) are taken equal to those of SO_4^{2-} (D_0 scaling is implicitly taken into account: D_0 values for SO_4^{2-} and SeO_4^{2-} are equal, but the D_0 value for MoO_4^{2-} is not known to the authors).

Also HCO_3^- does not act as a conservative tracer and the D_{app} ranges were deduced by statistical analysis of migration data: 3.0×10^{-11} m²/s < D_{app} < 9.0×10^{-11} m²/s. Hence the ratio δ/τ^2 can be calculated and amounts to ~0.08, which is slightly higher than the value for I^-.

Apparent diffusion coefficient for Cs(I), Sr(II) and other ion-exchange cations

As explained previously, surface diffusion processes make an independent determination of D_{pore} for ion exchange cations impossible. Similarly, it is not valid to carry out a simple scaling with respect to the D_{pore} for HTO, using scaling factors to account for the difference in D_0 values. Instead, D_{app} ranges are provided since this parameter can be obtained with good confidence from different types of migration experiments. It is also hypothesised that this D_{app} value can be related to the retardation factor, which can be calculated from batch suspension K_d values. For Cs(I) and Sr(II) the basic ranges for D_{app} are taken from the statistical analysis of different migration experiments. These values amount to 1.0×10^{-13} m²/s < D_{app} < 1.8×10^{-13} m²/s and 6.9×10^{-12} m²/s < D_{app} < 8.9×10^{-12} m²/s, for Cs and Sr respectively. The lower D_{app} value for Cs(I) indeed reflects the higher retardation factor compared to Sr(II). The final ranges for D_{app} are then calculated as a scaling of the best estimate (BE) (or average) D_{app} value according to the range in R values that are selected for the nuclide in question. As D_{app} and R are inversely proportional, a simple mathematical rule can be applied: lower limit D_{app} = BE(D_{app})×BE(R)/UL(R) and upper limit D_{app} = BE(D_{app})×BE(R)/LL(R). This rule signifies a very robust D_{pore} = BE(D_{app})×BE(R) = LL(D_{app})×UL(R) = UL(D_{app})×LL(R).

For the other ion exchange cations a similar reasoning is used. D_{app} ranges for these cations are calculated based on a scaling with respect to the range in R values. In the case of Rb(I), the D_{app} range is equal and calculated with respect to the range for Cs(I) (the D_0 for Cs and Rb are approximately equal). In the case of Ca(II) a set of electromigration experiments resulted in a D_{app} equal to the value for Sr(II) (7.9×10^{-12} m²/s). Since the ranges for R of Ca and Sr are also equal, the D_{app} ranges are therefore also taken to match those of Sr(II). In the case of Ra(II) a set of electromigration experiments resulted in a D_{app} (9.1×10^{-13} m²/s) about 10 times lower than that for Sr(II). This factor 10 difference was also used to scale the parameter range. It is remarked that the D_0 values for Ca(II), Sr(II) and Ra(II) are also approximately equal, hence no additional scaling with respect to D_0 has been performed.

Pore diffusion coefficient for other cations

With respect to the cations for which transport behaviour is mostly determined by the formation of kinetically stable pseudocolloids with humic substances (HS), some assumptions have to be made in order to estimate the diffusion coefficient. Indeed, due to the very high retardation of the (non-organic matter-related) species of these cations, the transport parameters of these species are not easily determined. Firstly, it is assumed that no surface diffusion-type transport occurs for radionuclides bound mostly through surface complexation mechanisms. Therefore, the relationship between D_{pore}, D_{app} and R is valid. Secondly, it is assumed that retardation factors R may be calculated directly from batch K_d values obtained in the absence of DOM.

Under these two assumptions, the following working hypothesis is used: values for D_{pore} may be calculated from either HTO (in case of cationic and neutral species) or I^- (in case of anionic species) using the respective rock factor R_f and by scaling the D_{pore} values of these reference nuclides according to the difference in D_0 (if available). Using the value ranges given for R, apparent diffusion coefficients may then be calculated directly as $D_{app} = D_{pore}/R$.

3.4.2. Transport parameters for humic colloid mediated transport

Radionuclide-OM interaction coefficient

The reference elements that are influenced by organic matter-driven transport are Tc, Am and U. While trivalent Am forms coordinative bonds with functional groups embedded in the HS structure, the mechanism by which tetravalent Tc and U bind to humic colloids is much more disputed. Current knowledge considers that the strongly hydrolysed tetravalent Tc and U species bind to HS through a colloid-colloid interaction mechanism that is similar to hydrophobic sorption. More specifically, this means that the interaction constant at a given pH and ionic strength is independent of the occupancy (or loading) of the organic matter molecule as shown by Maes et al., 2003] in the case of Tc(IV).

For Tc, a considerable number of independent data points (obtained in Boom Clay suspensions under controlled conditions), covering several orders of magnitude in Tc and HS concentrations provided a good estimate of the interaction constant $\log K_{Tc\text{-}OM} = 5.3\pm0.3$.

In contrast, the overall interaction of Am with HS is dependent on the loading and decreases with increasing loading. Moreover, the different literature sources that studied Am complexation with Boom Clay HS cover more different geochemical conditions: different ionic strength, wider pH range, HS extracted under oxidising conditions, presence of ion exchanger, etc. Also, all data on Eu were considered in the data collection because the similarity between Eu and Am is generally recognised. Hence a value of $\log K_{Am\text{-}OM} = 5.6\pm1.0$ was derived.

For the other elements data are scarce. However, it is generally acknowledged that the differences between trivalent lanthanides and actinides are small. Therefore the interaction constant for Ac, Cm, Sm and Pu(III) are expected to be similar to those for Am and Eu.

For the tetravalent elements, it is hypothesised that the interaction mechanism is similar to that proposed for Tc, i.e. colloid-colloid interaction. However, not much experimental data exist to test this hypothesis both qualitatively and quantitatively. Like for the trivalent radionuclides, it is argued that it is expected that interaction constants between tetravalent radionuclides are similar within the margins of uncertainty. In Tipping (1998) the interaction constants $\log K_{Rn\text{-}OM}$ for Am(III) and Th(IV) are comparable, just like the interaction constant, $\log K_{Rn\text{-}OM}$, between Am(III) and Tc(IV). Therefore the interaction constants for Th, U(IV), Pu(IV), Np(IV), Zr and Sn are judged to be in line with the values obtained for Tc and Am.

Because this interaction constant is quite high, it is also assumed that the Pa(V)-OM interaction constant will be in the same range (a conservative assumption).

Both the log*K* and *R* values determined for Am and Eu(III) and Tc(IV) are in similar ranges. Also the modelling of “sequential” migration experiments with trivalent, tetravalent and pentavalent radionuclides [Maes et al., 2011a] showed that the behaviour could be described with parameter values lying in a very narrow range, regardless of the species considered. Therefore it is proposed to use the same ranges for both *R* and log*K* for all trivalent, tetravalent (and pentavalent) actinides and transition metals. This hypothesis was tested by plotting all available logK_d values (data for Np, Tc, Pu, Eu, Am, Tc, Th) as function of organic matter concentration together with simulations based on following value ranges : 15 000 < *R* < 150 000 (R range for Tc and Eu/Am) and log$K_{RN\text{-}OM}$ = 5.3±0.3 (Tc data).

All values (except 2 outliers) fall within the simulation curves. The range in log*K* is extended arbitrarily to log$K_{RN\text{-}OM}$ = 5.3±1 reflecting a typical one order uncertainty on an interaction constant.

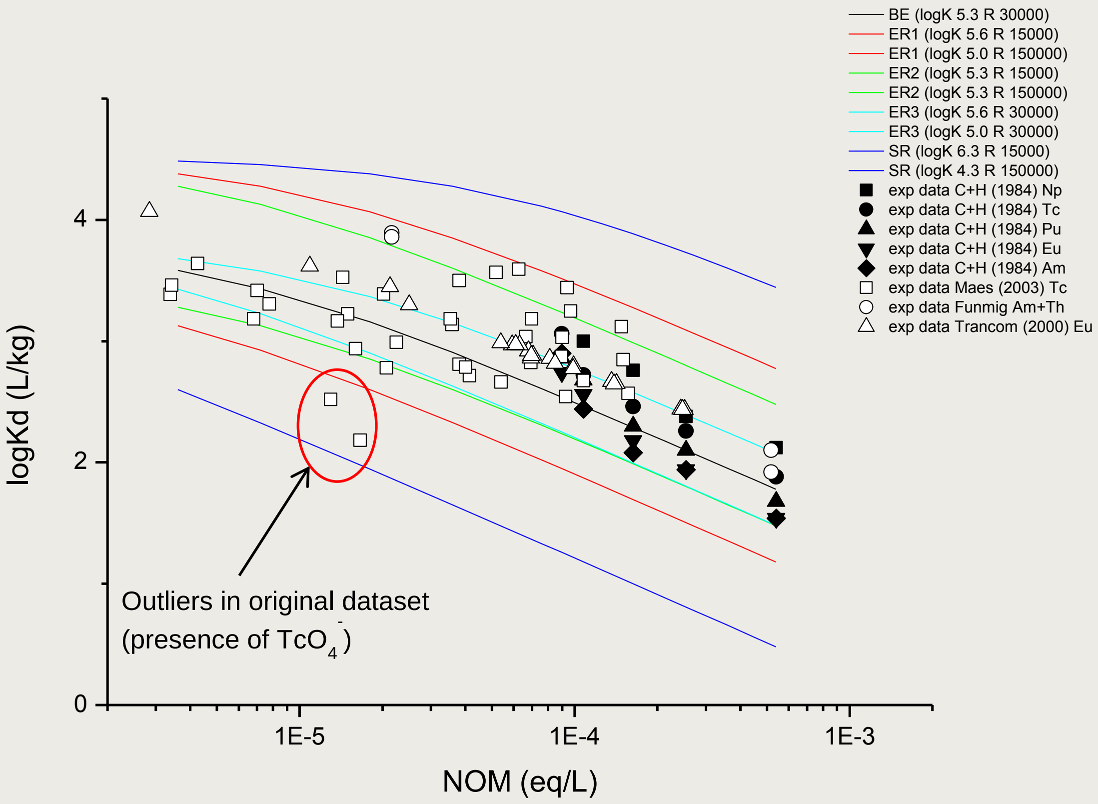

Figure 3-2 Summary of experimental K_d values obtained on Boom clay slurries for Np, Tc, Pu, Eu, Am and Th for different conditions: 10^{-12} M<[RN]<10^{-4}; 8.3<pH<9.2; 2g/l<S/L<500g/l, 10^{-6} eq/l<OM<10^{-3} eq/l. The lines correspond to simulated logK_d values based on combinations of an RN-OM interaction constant log*K* and a retardation value.

For mono- and divalent transition metals (Ag, Pd, Ni), a similar log*K* value is considered (despite the fact that it is known that they have a lower affinity). Furthermore, they are bound with less affinity to illite and montmorillonite (3 < log K_d < 5 in the 8-10 pH range, 0.01 mol/l $NaClO_4$ inert background electrolyte) and therefore it was chosen to adapt the *R* ranges. A simple scaling of the *R* range is proposed with respect to the illite logK_d range to obtain a range for R for these nuclides (150 < *R* < 15000).

Kinetic dissociation constant

Apart from the radionuclide-organic matter interaction constant, K_{RN-OM}, the binding to Boom Clay HS is also characterised by slow association and dissociation reactions. These latter parameters essentially control how far organic matter-associated (and therefore colloidal) radionuclides will migrate through the formation before being made available to sorption sinks on the Boom Clay solid phase. Unfortunately, this concept is quite novel within the research on radionuclide migration in the Boom Clay. Therefore, the amount of data concerning this mechanism and its parametric representation is limited. Essentially, almost all available data (and certainly the quantification of the dissociation rate) are gathered from a set of so-called sequential migration experiments. These experiments were first set up some 10 years ago and data are now available for the elements Tc(IV), Cm(III), Np(IV), Pu(III/IV), Pa(V), U(IV). Apart from these migration experiments, also the results from selected batch experiments allow insight into the existence of kinetic processes related to organic matter binding. Among these are batch experiments with Tc(IV), Th(IV), Eu(III), Am(III) and U(IV).

An assessment of this parameter revealed that for this parameter range, the model uncertainty is quite low (i.e., calculated breakthrough curves are not much dependent on the uncertainty related to this parameter). Therefore it is proposed to use the same value of 10^{-7} s^{-1} as the k_{diss} for all nuclides dependent on HS-related transport. Especially with respect to the mono- and divalent transition metals this may be assumed to be a conservative choice.

Transport of humic substance colloids

The colloidal transport process of humic substances in Boom Clay is simplified in such a way that it can be described by a simple diffusion-advection equation similar to the one used for dissolved radionuclides.

From laboratory-scale transport experiments, values of the product of the diffusion accessible porosity (η) and the retardation factor (R) can be deduced, as well as values for the apparent dispersion (D^{i}_{app}) and/or diffusion (D_{app}) coefficient. According to [Martens et al., 2010], modeling of the in-situ ^{14}C-DOM diffusion experiment revealed that these “lumped” parameters can be transferred to larger scale experiments. Furthermore, the modeling showed that a classic diffusion-advection description gives quite good results for describing the colloidal transport behaviour of DOM in Boom Clay.

R_{OM} is considered as a “lumped” constant in which several colloid retention processes are represented, although it was acknowledged that current understanding of these processes in Boom Clay is too limited to be able to discern and treat them separately.

Diffusion accessible porosity and retardation factor

Because of the similarities between the diffusion accessible porosity for negatively-charged colloids and negatively-charged anions, the range for η , accessible porosity for dissolved organic matter is judged to correspond to the one for iodide, except for the lower ranges, which are taken equal to that of divalent anions: 0.05-0.40.

The retardation factor for the larger size fraction of DOM, which is most relevant for long-term radionuclide transport, lies within the range 20-60. The smaller size fraction of DOM is less likely to interact with the Boom Clay solid phase and less prone to colloid filtration processes, and is therefore characterised by a range for R equal to 3 – 20.

Diffusion coefficient

Based on results of DOM migration experiments in the Boom Clay at small scale, a large-scale range of 4×10^{-12} – 1×10^{-10} m²/s is obtained reflecting the heterogeneity in size.

3.5. Transferability

The bulk of information related to the transport (retention and migration) properties of radionuclides in Boom Clay has been gathered by way of experiments and modelling under geochemical conditions which are relevant for the Boom Clay in the Mol area. However, the Boom Clay formation is not restricted to the Mol area and stretches west to east from Oost-Vlaanderen to the Limburg province, and south to north from Vlaams Brabant to the Netherlands. Given the relatively small area from which most of the data haven been gathered, relative to the vastness of the geological formation, an assessment is required regarding the possibility of using the data obtained on “Mol” samples for predicting/describing radionuclide transport at other locations within the Boom Clay (i.e., “Transferability” of data from Mol to other locations).

The influence on transport will be discussed starting from the point of view of the underlying phenomenological models described in previous sections. Where possible and whenever available, experimental data will be shown to support the theoretical discussions.

The parameters which are used to describe transport are 1) the porosity, and 2) the (apparent, effective or pore) diffusion coefficient. With respect to porosity, both the water content and the porosity organisation (pore size distribution, pore transport pathways, constrictivity and tortuosity, formation factor or geometrical factor) are of interest. Both parameters might change according to, e.g., burial depth and history. But probably more important, the changes in pore water chemistry will influence the extent of the diffuse double layer which has an influence on the transport of both anions and cations. Furthermore, the differences in OM content, either from “nature” or induced by changed pore water composition will have an important impact on the transport behaviour of many RN.

At Mol, the porewater composition has a low ionic strength (low salinity) and is a bicarbonate type of water. However, more towards the North where Boom Clay is buried deeper, the water changes to a sea-water type with higher ionic strength and salinity. The remainder of the text will merely concentrate on the effect of higher ionic strength/salinity on the transport parameters.

3.5.1. Diffusion accessible porosity – anion exclusion

[Moors, 2005], Aertsens et al., 2009], [Bleyen et al., 2014] studied the effect of the ionic strength (either by adding salts or by using pore waters of different origin) on the diffusion parameters for HTO in Boom Clay cores. No significant change of the apparent diffusion coefficient nor the diffusion accessible porosity was observed for widely varying range of ionic strength.

For anions, an increase in ionic strength will increase the anion accessible porosity. A higher ionic strength implies a decrease of the thickness of the diffuse double layer. This will be accompanied by an increase of the fraction of free pore water. The Debye length, which gives the thickness of the diffuse double layer, is a function of the ionic strength, *I*, according to following relationship [Appelo and Postma, 2005]:

$$\kappa^{-1} = 3.09 \big/ \sqrt{I}$$

For a 0.02 M solution the double layer thickness is ca. 2 nm. If the ionic strength of the interstitial solution is increased to 1 M, the double layer thickness decreases to ca. 0.3 nm and anion exclusion phenomena should become less pronounced. As diffusion is dependent on porosity, this higher anion accessible porosity will allow a faster diffusion of the anions.

[Moors, 2005], Aertsens et al., 2009], [Bleyen et al., 2014] studied the effect of the ionic strength (either by adding salts or by using pore waters of different origin) on the diffusion parameters for iodide in Boom Clay cores. With an increase in ionic strength, the diffusion accessible porosity for I^- in Boom Clay cores increased significantly. The process was also found to be reversible. On the other hand, the effect on the diffusion coefficient is low, if not negligible.

Van Loon et al., 2007] studied the diffusion of ^{36}Cl in compacted bentonite at different ionic strengths. Increasing the ionic strength of the external solutions resulted in an increase of both the effective diffusion coefficient and the Cl^- accessible porosity. This can be explained by anion exclusion effects (Donnan exclusion). Glaus et al., 2010 observed for the anionic tracer ^{36}Cl an increase of D_{eff} with one order of magnitude when increasing the ionic strength from 0.1 to 2 M in Na-montmorillonite.

3.5.2. Double layer enhanced diffusion of cations

A change in ionic strength has an effect on the diffusion of cations. The effective diffusion coefficient increases when ionic strength decreases. At low ionic strength, the double layers are thicker, so the amount of tracer present in the double layer (enriched because of sorption to surface) compared to the amount in the free pore water becomes more important and will dominate the radionuclide flux.

Different studies have shown that an electrostatic shielding of the surface charge due to the increase of the ionic strength implies an increase in D_{eff} for anionic species and a decrease in D_{eff} for cationic tracers.

[Van Loon et al., 2007] studied the diffusion of ^{22}Na in bentonite at different ionic strengths. The D_{eff} of the cationic tracer ^{22}Na D_{eff} decreased with a factor 10 for an increase of the ionic strength from 0.1 to 1 M. The same trends, albeit less pronounced, were observed for Na-illite. In an earlier study of Glaus et al., 2007 the effect of external salt concentration on the diffusion of Na and Sr in montmorillonite was studied. For the diffusion of Na, the same effect as in bentonite was observed. The diffusion decreased directly proportional with the increase in ionic strength. In kaolinite, diffusion coefficients were found to be independent of the external salt concentration.

More recently, in the EC project CatClay [Altmann et al., 2014], the diffusion and sorption of Sr, Zn and Co in purified illite was studied at different ionic strengths and at different pH values. The diffusion of Sr at pH 5 decreased two orders of magnitude when the ionic strength increased 100 times (D_{eff} 1.6×10^{-8} m²/s at 0.01 M - 1.1×10^{-10} m²/s at 1 M). The D_{eff} values were in this case directly proportional with K_d. At higher pH, the same decreasing trend of D_{eff} with increasing ionic strength was observed, although the K_d at pH 9 was much higher. This reveals that the slower diffusion at higher ionic strength is not only related to a pH effect. For Co and Zn, two cations which sorb mainly via surface complexation, this is even more pronounced. The decrease in D_{eff} with increasing ionic strength is much larger than the decrease in K_d. As illite is a main constituent of the Boom Clay, for the radionuclides similar behaviour in Boom Clay can be expected, when ignoring the effect of organic matter.

A precise appraisal of the magnitude of the changes in effective diffusion coefficient of cations related to changes in ionic strengthis at the moment difficult to make. However, it is known that the relative importance of double layer diffusion decreases as the ionic strength increases. Therefore, values of D_{eff} obtained under Mol conditions may be used as upper estimates for cation effective diffusion coefficients at other locations. Combination of D_{eff} values with calculated retardation factors, R, obtained from static batch sorption tests, and the diffusion accessible porosity, η, can then be used to obtain estimates for the apparent diffusion coefficient, D_{app}.

3.5.3. Effect of ionic strength on dissolved organic matter

DOM was observed to easily associate with several radionuclides enhancing or lowering their mobility in porous media ([Maes et al., 2006], [Maes et al., 2011a]). On the one hand, the association with large soluble organic species that are immobilized due to natural filtration or by sorption on the solid prevents the radionuclides from migrating. On the other hand, mobile organic species may act as a carrier of radionuclides through the Boom Formation. An increase of the salinity of Boom Clay pore water is expected to reduce both the concentration of mobile DOM and its size/molecular weight (MW) distribution. Considering that the affinity of radionuclides for DOM was in some cases reported to be higher for large organic species ([Matsunaga et al., 2004], [Zang et al., 1997]), the enhancement of radionuclide migration *via* colloid-facilitated transport may thus be foreseen to be limited at high ionic strength. Indeed, increasing the salinity increases the amount of Particulate OM that operates as an additional sorption sink for radionuclides. Furthermore, the sorption of DOM on clay minerals is also expected to be promoted at high ionic strength which is again favouring the retardation of radionuclides.

The extent of the association of radionuclides with DOM in solution as a function of ionic strength and of the nature of the counter ion can be described using the NICA-Donnan or Model VI approaches [Bruggeman et al., 2010c]. Even though some literature data may be used in a first attempt, it is necessary to characterize the Boom Clay DOM in detail to obtain a representative modelling. Furthermore, it is unclear how reaction (association/ dissociation) kinetics would change with a variation in ionic strength. These reaction kinetics dictate the importance of DOM as a colloidal carrier for radionuclides.

Describing the effect of ionic strength on the ternary system involving Boom Clay, Boom Clay DOM and radionuclides is even more challenging. Certain approaches such as the LCD (Ligand Charge Distribution) model for sorption of organic molecules to oxide surfaces, successfully reproduced the sorption of arsenate, phosphate and copper on goethite in presence of fulvic or humic acids [Weng et al., 2006, 2008a, b, 2009]. However, in these works, the sorption of the humic and fulvic acids was not predicted but given as input. Only the repartitioning of the species of interest between the solution, the sorbed humics and the goethite was modelled. Moreover, this model has not been applied to more complex structures such as Boom Clay.

Regarding the potential effects of increased ionic strength on DOM concentrations it is to be expected that an increase of ionic strength of the Boom Clay pore water up to seawater composition would significantly decrease the concentration of dissolved organic matter leaving only small organic molecules in solution. The resulting reduction of total dissolved organic matter concentrations and the reduction of its average molecular weight would limit the colloid-facilitated transport of radionuclides through the Boom Clay layer. However, it is obvious that the behaviour of DOM in Boom Clay under variable ionic strength is tremendously complex and cannot be predicted precisely by any existing model. A full assessment of the DOM impact on radionuclides at other locations of Boom Clay requires therefore a detailed knowledge of the Boom Clay, the pore water and the DOM present.

4. Molecular dynamics

The diffusion of radionuclides within the formation water of a clay matrix is strongly affected by many chemical and physical interactions between the aqueous species and the clay minerals. Diffusion parameters required for reactive transport modelling are often obtained by experimental studies, which cannot make a clear distinction between the different chemical and physical processes. A better understanding of the separate processes will allow improved predictions of the long-term migration of radionuclides within a clay matrix and better constrained diffusion parameters for reactive transport modelling. In addition, improved understanding of these processes could make expensive and time consuming experiments redundant.

Molecular modelling is a powerful tool for the evaluation of sorption and diffusion mechanisms on the molecular scale. A validated model can be used to calculate sorption and diffusion parameters under varying subsurface conditions. In subtask C of OPERA Task 6.3.1 the application and benefit of molecular modelling for the purpose of gaining improved insight in the interactions between charged clay surfaces on the diffusion of radionuclides is assessed.

The central objective of the subtask C is to:
- develop a molecular model of a clay mineral surface interacting with a fluid;
- develop a methodology for molecular modelling of the interaction between aqueous species and charged clay mineral surfaces, and the effect on diffusion;
- use the model for a series of simulations to test the methodology.

For the purpose of this task, focus will be on the anionic species and the influence of the fluid composition on diffusion. Molecular simulations result in time-dependent ion density profiles with distance to a clay surface. These can be used to calculate relevant parameters such as the diffusion ratio, which is the ratio between the modelled diffusion coefficient and the value in bulk water. The results will be compared to experimental studies. Due to the small scale of this type of modelling, a discussion of upscaling issues is given, as well as a discussion on the requirements for future cation diffusion simulations.

The recent progress in understanding of detailed chemical processes occurring at soil particle surfaces makes it possible to attribute observed overall diffusion behaviour to small scale chemical and physical process (e.g. extent and composition of double layers composition of pore solutions, estimation of diffusion accessible porosity, estimation of local molecular diffusion coefficients etc.). At this detailed level there is a strong interaction between chemical and physical processes, and studying both types of processes at this detailed level allows taking into account these interactions in a mechanistic way.

The sorption and diffusion of relevant radionuclides in Boom Clay has been assessed by TNO on a molecular scale. The work includes a determination of micro-scale diffusion coefficients including a literature study. Sorption and diffusion on a molecular scale will be compared to the experimentally determined values, as reported in the reference database. Molecular dynamics is ideally suited to compute sorption and diffusion parameters of ions in contact with charged surfaces. Molecular dynamics simulation takes into account the electrostatic properties of the Boom Clay and ion exclusion effects at the interface of the clay. In this way, molecular modelling gives insight into the mechanisms and processes at a molecular scale that underpin the empirical values determined in larger scale experiments. The study of clay surfaces on a molecular scale requires input of the local chemical conditions that is provided by the chemical model as described in Subtask B, variations in composition of the formation water and temperature can be imposed for a broad application to a wide range of conditions. The outcomes of the study into molecular dynamics will be compared with modelling results on larger scale (including the results of subtask B). The determined diffusion coefficients and diffusion coefficients from literature will be provided as input for the final database in Subtask D.

4.1. Model set-up and parameter selection

4.1.1. Clay mineral selection

The OPERA report of task 5.2.1 reports on the mineralogy of the Boom Clay in the Netherlands [Koenen and Griffioen 2014]. Bulk XRD analyses showed that the clay mineral fraction of the different samples varies significantly between ~10 and 68 wt%. The clay fraction XRD analysis indicated that the clay consists mainly of smectite and interstratified illite-smectite. Smectites are known to have a high cation exchange capacity (CEC) and an intermediate layer charge [Appelo & Postma, 2005]. Characterisation of the *type* of smectite requires additional techniques, which were not applied within the OPERA project. It may be assumed that the smectite consists primarily of montmorillonite which is suggested from the correlations between XRF and XRD results [Koenen and Griffioen, 2014]. Montmorillonite is the most common type of smectite and it is an important constituent of naturally occurring, clay-rich sediments and rocks. They form from weathering of base-rich parent rocks at high pH conditions [Galan & Ferrel, 2013]. This type of mineral, which is also the main constituent of bentonite, has a large surface area for interaction with water and aqueous species.

4.1.2. Radionuclide selection

For the purpose of this task, the approach as used by SCK·CEN is followed which allows different radionuclides to be divided into groups for which representative species were defined [Bruggeman et al., 2010a]. One of the radionuclide groups of interest identified by SCK·CEN are radionuclides which are preferentially present as anionic species. For this group iodine (I) can be used as a representative radionuclide [Bruggeman et al., 2010a]. Other groups identified include specific cationic species. Bruggeman et al., 2010a provide a detailed assessment of migration of iodine within Boom Clay at conditions representative for the Belgian subsurface at Mol. For the current study, it is assumed that iodine in the formation water is mainly present in the form of iodide (I^-). This is a reasonable assumption for low concentrations and low Eh values in the Boom Clay. In the presence of high amounts of organic matter, iodide can be transformed into organoiodine (organically bound iodine). This implies that iodine becomes covalently bound to the organic matter. These organoiodine species are not expected to form after release of radioactive iodine, in the form of iodide, from the repository. Potential organoiodine formation from oxidised iodine species would slow down iodine migration, making the assumption that all iodine is present as iodide a conservative approach [Bruggeman et al., 2010a].

4.2. Brine composition

The formation water considered in the simulations consists of NaCl, covering the range from 0 to 2.53 mol/L. Such a range encompasses commonly studied states of Boom Clay [Aertsens et al., 2009]. In terms of the computational model, the choice for the range in concentration was made following the same arguments as reported in [Bourg & Sposito, 2011]. They choose a similar but slightly smaller range (0.34-1.83 mol/L) based on typical applications where smectites might play a role in broader applications, such as high-level radioactive waste repositories, saline aquifers and seawater. Since smectites are abundant in a wide variety of subsurface conditions, it is important to understand the role of variations in fluid composition on diffusion processes.

4.2.1. Basic concepts of radionuclide diffusion

A detailed description of the basic concepts of radionuclide transport in sediments is given in ([Bruggeman et al., 2013], Bruggeman et al., 2010a]). Within the Boom Clay, it can be assumed that molecular diffusion is the main process for radionuclides to migrate away from a repository once they are released from their containment. Darcy flow is not predicted to occur in clay rocks with low hydraulic conductivity. The following empirical equation summarizes the main concepts relevant for molecular diffusion in clay host rocks:

$$D_{eff} = D_{pore} * \eta = D_{app} * \eta R = D_o * \eta R * G$$

Where D_{eff}, $D_{pore,}$ D_{app} and D_o are respectively the effective, pore, apparent and bulk diffusion coefficients (in $m^2 \cdot s^{-1}$), η is the diffusion accessible porosity, R is the retardation factor and G is an empirically determined, sediment specific correction factor for tortuosity and constrictivity. Except for G, each of these parameters are specific for the aqueous species as well as the type of sediment.

The bulk diffusion coefficient of iodide *in pure water* (D_0) is 2.0×10^{-9} m^2/s (at 25°C). With respect to D_0, D_{app} is corrected for the cementation of the rock, which is related to the tortuosity according to Archie's law. In addition to the tortuosity, D_{pore} is corrected for the retardation. The retardation factor is described as a result of adsorption [Bruggeman et al., 2013]. Since anions have negligible adsorption onto clays, R is assumed to be 1 and hence $D_{pore} = D_{app}$ ([Bruggeman et al., 2013], Bruggeman et al., 2010a]). The diffusion accessible porosity η depends on the host rock characteristics and the aqueous species.

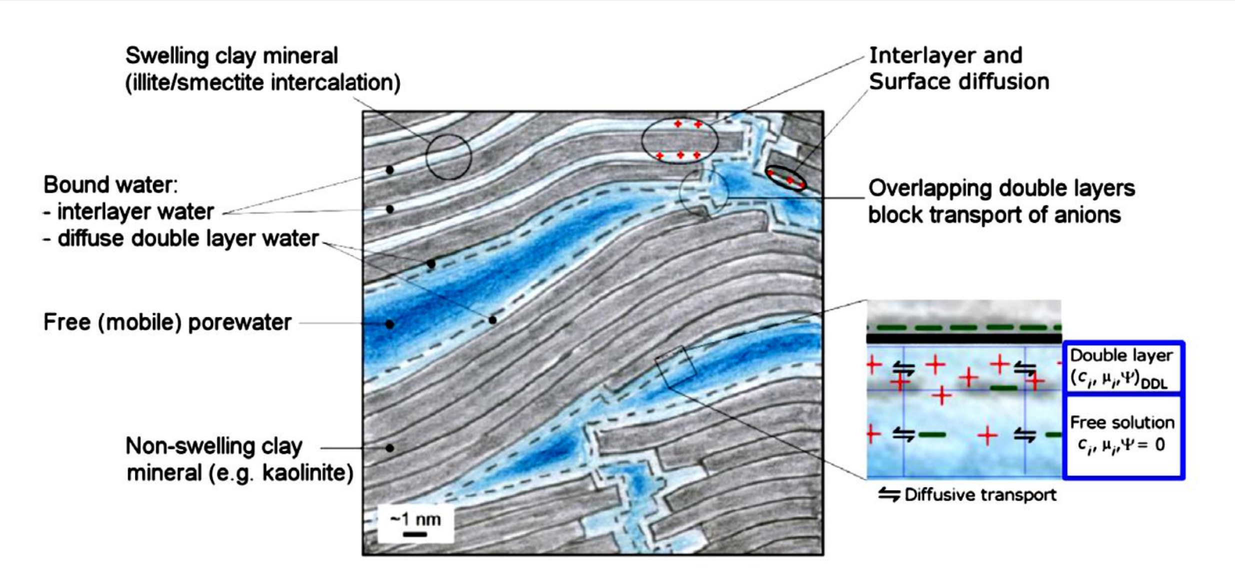

Figure 4-1 Schematic representation of microscopic clay (intercalated illite/smectite), showing the three types of water: interlayer water, diffuse double layer (DDL) water and free porewater. From [Appelo et al., 2010].

The total porosity in clay rocks is the sum of the interlayer space (between clay platelets of clay minerals) and interparticle pore space (Figure 4-1) ([Van Loon et al., 2007], [Appelo et al., 2010]). The interparticle pore space can be further subdivided into the diffuse double layer (DDL), sometimes also referred to as electrical double layer (EDL), and free pore water ([Van Loon et al., 2007], Appelo et al., 2010]). The DDL of a clay surface is the result of its negative surface charge. The principles of the DDL are described by the Gouy-Chapman and Stern models. These models include 1) a compact Stern layer adjacent to the clay surface, with compensating cations and complete anion exclusion and; 2) a diffuse layer with a high concentration of compensating cations and an anion concentration which increases exponentially away from the clay surface. The DDL gradually merges into the free water, or bulk solution (Figure 4-2 from (Leroy et al., 2007], Tournassat et al., 2009]).

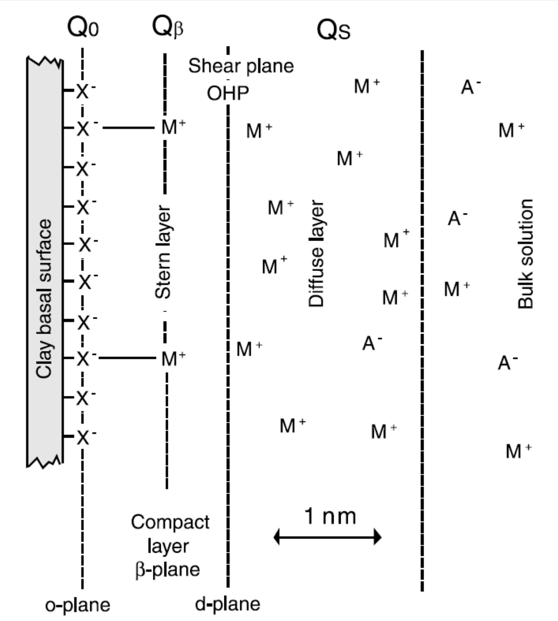

Figure 4-2 Sketch of the triple layer model based on the Gouy-Chapman model. M represents the cations, A the anions. For further details, (see [Leroy et al., 2007]).

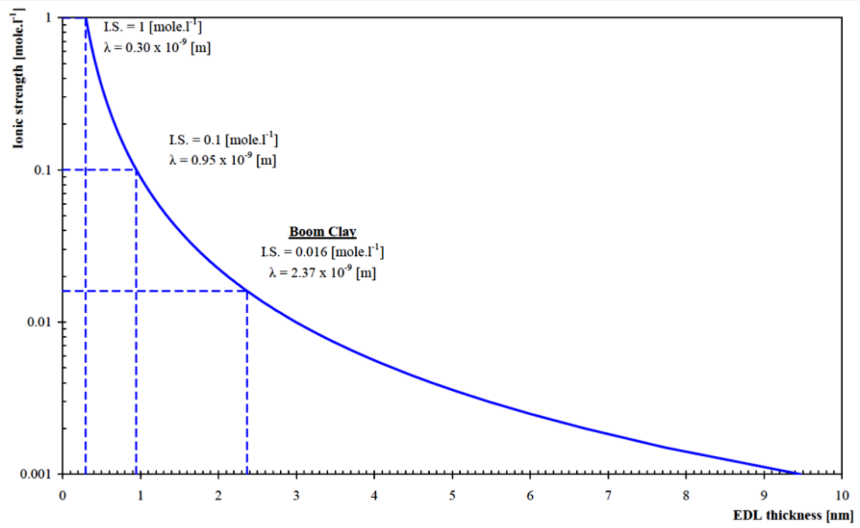

Figure 4-3 Calculated thickness of the diffuse double layer based on the Gouy-Chapman model. This model only includes a diffuse layer, without taking into account a Stern layer. The Boom Clay conditions are based on the Belgian case. From [Moors, 2005].

Due to the negative charge of clay surfaces anions are expelled from the DDL, a process which is called anion exclusion. The interlayer space, which is maximally ~10-12Å wide, consists of overlapping DDLs and is not accessible for anions [Van Loon et al., 2007]. The DDL thickness is a crucial parameter in the determination of η (diffusion accessible porosity) for anions [Moors, 2005] and is known to be highly dependent on the ionic strength (Figure 4-3).

The parameters for anions to be determined in order to define D_{eff} are D_{app} (= D_{pore}) and η. They can be determined experimentally. However, experiments are expensive and time consuming, and the results are sensitive to heterogeneity and quality of the sample material, which can be affected by sampling, storage and preparation processes.

4.3. Workflow development

4.3.1. Molecular modeling software

In the present work molecular dynamics (MD) simulations are used to calculate density profiles and diffusion coefficients of iodine radionuclide and different ionic species in solution when in close contact with a (charged) montmorillonite surface. For that purpose a purely atomistic description of the clay in a solution is adopted. This allows for a large number of choices for material configurations and system conditions, limited only by the total volume of the sample and the computational resources.

Numerous material descriptions have been developed to represent clay materials. For this study the so-called ClayFF force field developed in [Cygan et al., 2004], has been chosen, because of its versatility and successful implementations as shown in [Tournassat et al., 2009] and [Liu et al., 2007].

In its simple form the ClayFF force field assumes that the energy of the system is a contribution of 4 different terms, namely: Coulomb, van der Waals, bond stretching and angle bending interactions,

$$E_{total} = E_{coul} + E_{vdW} + E_{bond} + E_{angle}$$

Briefly, the Coulomb term takes care of the long range charged interactions characteristic of ionic systems. The van der Waals energy is responsible for steric repulsion and the attractive dispersion energy. The bond stretching term is mainly used for dangling hydroxyl groups in between clay sheets, and the angle bending energy gives water molecules its commonly known shape. In addition, ClayFF has an additional feature which is lacking in other software codes: when metal substitutions occur, it redistributes the excess or defect charge (locally) in the surrounding oxygen atoms. This allows for realistic clay systems to be modeled accurately.

In the following, all simulations were carried out conserving the number of particles, volume and temperature (NVT ensemble) for each configuration, unless stated otherwise. The time step to integrate the equations of motion was set to 0.5 femtoseconds (fs), and was chosen because it was sufficient to achieve energy conservation in preliminary systems. As equilibration period, before any relevant observable was computed there was at least a 5 ns relaxation time. The summation for the long-range Coulomb interaction was the particle-particle particle-mesh (PPPM) scheme. The MD software engine utilized was LAMMPS, see [Plimpton & Thompson, 2012] for more details. Total computer time to produce the obtained results surpassed 300 hours at TNO’s high performance cluster.

4.3.2. Model validation

To be able to compare results for different conditions, reference values are required that are intrinsic to the model. For that purpose bulk water was simulated and the self-diffusion coefficient, the density and the average volume occupied per molecule were calculated. In addition, these parameters were calculated for ions in diluted solutions.

Water self-diffusion

A system consisting solely of water molecules was constructed at a density of 0.99 g/cm^3, as shown in Figure 4-4 (left). The system was equilibrated at T = 300K for a duration of 1ns. After this, the system was allowed to evolve to a natural state so it was possible to measure its thermodynamically observables. Additionally the mean square displacement (MSD) was measured during the next 100 ps, taking averages over each consecutive interval of 2ps. The result of such quantity allows the computation of a diffusion coefficient from the Einstein-Smoluchowski relation [Pathria & Beale, 2011]:

$$D = \frac{1}{6}\lim_{t\to\infty}\frac{d < \Delta r^2 >}{dt}$$

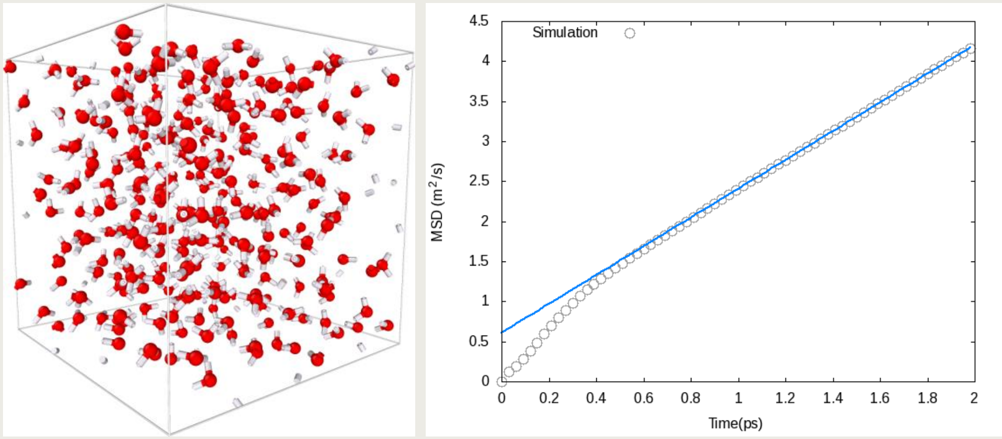

Figure 4-4 Schematic depiction of representative water volume (left). Mean square displacement as a function of time for a system containing only water at 0.99 g/cm^3 (right). The diffusion behaviour and the related quantities can be derived from this.

where D is the diffusion coefficient, t is the elapsed time and Dr^2 is the square relative distance for each particle compared with its initial position. In calculating the diffusion coefficient the approximation is used which is often used when examining bulk and isotropic (homogeneous) liquids. In such approximations the molecules in the liquid are assumed to distribute their energy equally in space. This makes it possible to separate linearly the three independent contributions to the diffusion coefficient for x, y and z directions.

A representative curve for the MSD is shown in Figure 4-4 (right), from which it is clear that before 1ps the system already reached the diffusive limit. Using the above mentioned expression the water self-diffusion coefficient was 3.0x10^{-9} m^2/s. Reported values in literature using the same software vary between 2.5 and 4.5x10^{-9} m^2/s. Hence, the present value falls within the lower side of this range. Compared to the experimentally established value of 2.3x10^{-9} m^2/s molecular simulations generally slightly overestimate the water self-diffusion coefficient [Lee, 2013].

Clay swelling

In order to build confidence in the developed models , swelling curves for hydration of montmorillonite were reproduced, as previously done in [Cygan et al., 2004]. In their study, a stacked layer montmorillonite was taken with both tetrahedral and octahedral substitutions of the form $Na_3(AlSi_{31})(Mg_2Al_{14})O_{80}(OH)_{16}$. Subsequently, the water content was gradually increased by introducing water in the interlayer spacing. This resulted, as expected, in an increase in the mean separation distance between montmorillonite layers. In Figure 4-5, the interlayer separation is shown as a function of the content of water-per-layer. At very low concentrations, when water is added, the interlayer spacing quickly reaches a plateau where it can accept more water for up to a water/clay ratio of 0.15. Spanning that plateau, there is virtually no change in volume. The results are consistent with previous experiments and theoretical findings (e.g. [Cygan et al., 2004]). Hence, it is shown that the smectite model describes accurately the swelling after hydration.

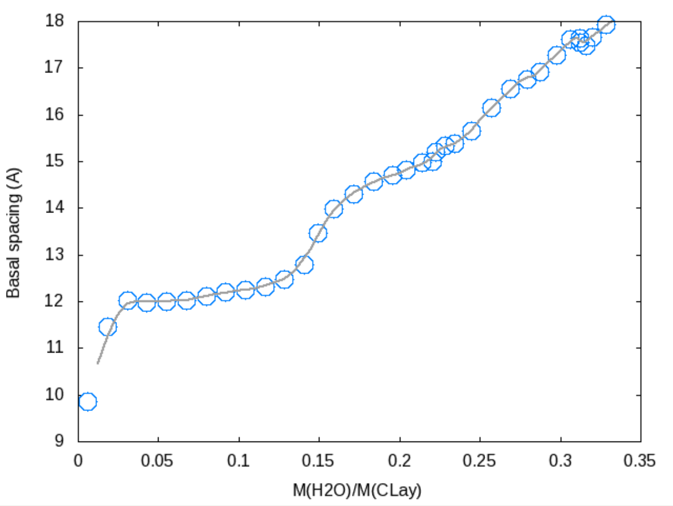

Figure 4-5 Basal interlayer spacing as a function of the water-in-clay mass ratio. At very low concentration the interlayer spacing reaches a plateau where it can accept more water for up to a ratio of 0.15. This result is consistent with previous experiments and theoretical findings.

Interlayer spacing

Different simulations were carried out using systems of stacked layers with additional water in the interlayer spacing to evaluate the basal spacing (Figure 4-6).

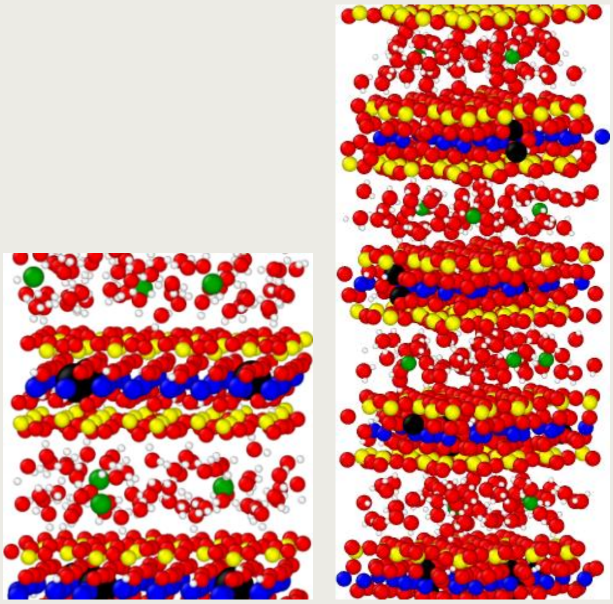

Figure 4-6 Typical arrangements used for the computation of the mean interlayer spacing in montmorrillonite. In this simulations boundary conditions are such that the clay particle is considered infinite. The coloring scheme used in these depiction follows: Red for O, white for H, green for Na, blue for Al, yellow for Si and black for Mg.

Imposed boundary conditions were such as to recreate an infinite particle with periodically separated layers. The model then calculates the average separation between clay layers. For this, the hydration of the clay was fixed at a water/clay mass ratio of 0.185 water content per layer. The excess of charge per layer was set to 0.5e with only octahedral substitutions, resulting in montmorillonite with the form $NaSi_{16}(MgAl_7)O_{40}(OH)_8$. These choices followed similar settings like the ones used in other studies for uranyl(VI) adsorption onto smectites (e.g. [Greathouse & Cygan, 2005]). Moreover, since [Maes et al., 1979] have shown that, depending on pH, different charge densities could be found in the range of 0.3e to 0.9e for reduced charge montmorillonite, a mean charge of 0.5e was considered without loss of generality. The results for the montmorillonite system are shown in Table 4-1. The dimensions of the crystal lattice agree with measured values.

Table 4-1 Calculated interlayer spacing and sheet dimension for hydrated montmorillonite.

Number of layers	Interlayer spacing (Å)	A cell length (Å)	B cell length (Å)
2	15.31	5.19	4.50
4	15.29	5.20	4.49

4.3.3. Clay model system

For this study, the main system of interest is iodine diffusion through montmorillonite clays (Figure 4-7). As such, focus is on negatively charged iodine ions, iodide (I^-) in solution at close proximity to montmorillonite particles. In the solution presence of an electrolyte was allowed for: sodium chloride. Since I^- and Cl^- are equally charged, iodide replaces chloride when it enters the solution, thus maintaining the entire system at electro neutrality.

To represent clay particles in solution an atomistic model was used inspired by [Greathouse & Cygan, 2005]. In a nutshell, the entire system can be subdivided into two major parts. The major part is made up by a large solution space where ions in water can be found, named “A” in Figure 4-7. The remaining part is a limited set of montmorillonite layers representing the edge of a particle submerged in solution. In this case this set was composed of two montmorillonite layers each with 0.5e excess charge per unit cell. The interlayer spacing was set to the one found previously for the bulk in the same structure. In the same manner, the volume in between layers was filled with water to satisfy a 0.185 mass ratio per layer, signaled “B” and “B’” in Figure 4-7. The total balancing charge (Na^+) per layer was distributed as follows. The regions called “A” and “B’” together received 50% of the charge in equal amounts. The remaining 50% was introduced in interlayer spacing “B”. This distribution obeyed a more symmetrical configuration than simply assigning 50% of the charge to regions “B” and “B’”. The balancing charge to compensate for the negative charge of the montmorillonite surface is equal to 0.22 mol Na^+/L. Hence, to maintain electroneutrality the anion concentration in the brine in mol/L is equal to $[Na^+]$ - 0.22 and in every simulation, 0.22 mol/L more Na is present than Cl. For this system periodic boundary conditions in the directions parallel to the clay layers were used. In the perpendicular direction two fixed walls were used to confine the particle plus solution system, implying that particles cannot leave the modeled area at these ends. This boundary condition was chosen to avoid poorly-minimized configurations which can destroy the system’s stability. A disadvantage is that peaks might appear at the end of the model system as an artefact. Figure 4-8 shows a typical ion density profile characteristic for the complete system as shown in Figure 4-7.

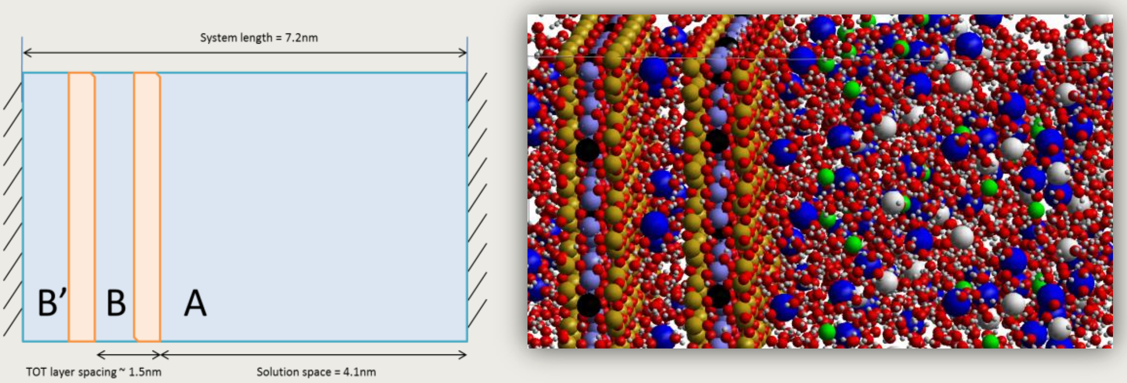

Figure 4-7 Schematic representation of the simulated system representing two stacked clay sheets (orange), interlayer space B and B’, and interparticle space A occupied by brine (Left). Snapshot of the corresponding atom distribution (right). Atoms in the montmorillonite sheets Al, Si, O and Mg are colored respectively light blue, yellow, red and black. Na, Cl and I in the solution are colored blue, green and white. Hydrogen atoms are also colored white but with tiny sized spheres.

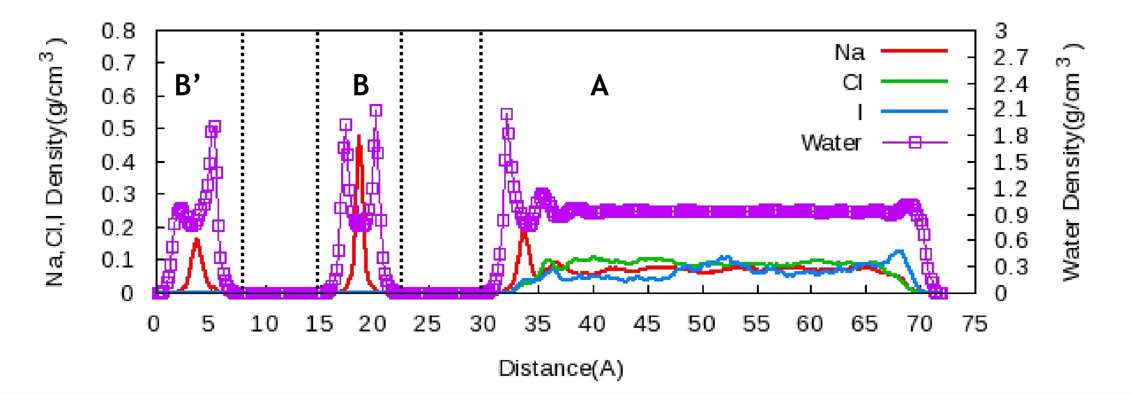

Figure 4-8 Typical ion density profiles. In this example [I-] is 0.44M, [Cl-] is 1.09M and [Na+] is 2.75M. Note the surface bound water and adsorbed sodium in the interlayer space and at the contact with the interparticle space. The chloride and iodide concentrations increase away from the clay sheet surface.

Iodine parameters

As initially published, ClayFF does not contain parameters for the radionuclide of interest: iodine. Nevertheless, ClayFF is compatible with the SPC/E model for water and other ions in solution. Because of this, the ionic radius for I^- was chosen in agreement with the values previously used in Koneshan et al., 1998. In their work parameters are chosen based on binding energies of ions in solution while making sure that the result is compatible with the water model SPC/E (also adopted by ClayFF). It was also ensured that in the translation to ClayFF the interaction energy and the effective ionic radius maintained the appropriate ratio so that the relation between Na^+, Cl^- and I^- properties is kept.

Brine composition

The behavior of different properties of the clay will vary according to the ionic concentration in both the interlayer and interparticle spacing. The cation concentration in the interlayer space is fixed (Van Loon et al., 2007), related to the clay charge defined for the model. However, for the solution in the interlayer space the ionic strength was varied and therefore properties are expected to change accordingly. In these simulations only the fluid is taken into account and hence $[Na^+] = [Cl^-]$. Figure 4-9 (top left) shows the density of the solution with increasing concentrations of NaCl. This model predicts that there is a linear increase in the density of the solution when NaCl is increased. In the same manner, the concentration of iodine in the system can be changed resulting in a different solution density. As an example, the density of a solution with initial NaCl concentration of 2.76 M has been computed, in which Cl^- is substituted increasingly by I^-. The ionic strength does not change, but the density increases significantly with increasing I^- substitution for Cl^- (Figure 4-9, right). The results are slightly lower than experimentally determined values.

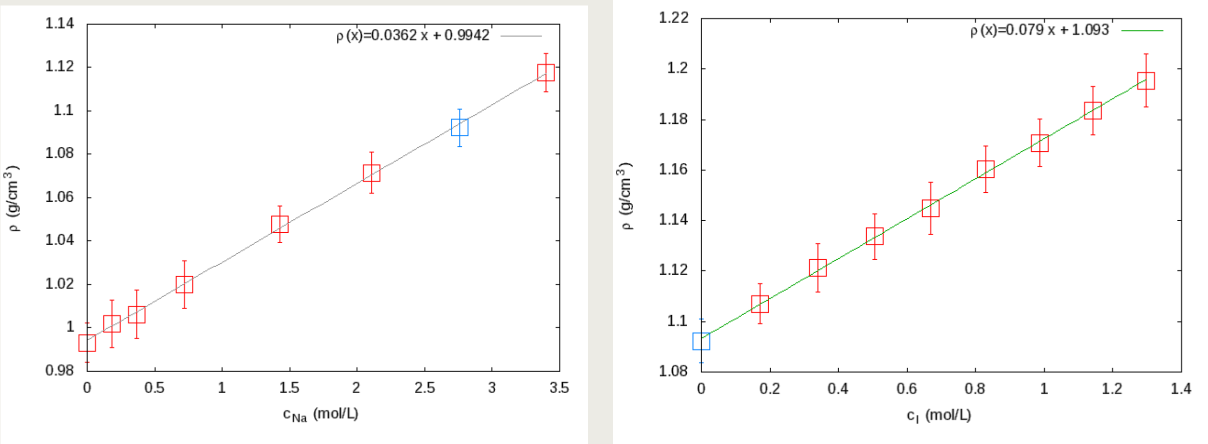

Figure 4-9 The solution density as a function of NaCl concentration calculated using molecular dynamics (left). Influence of increasing iodine substitution for chloride on solution density with fixed [Na+] = 2.76 M (right). The blue box in left image with 2.76 M NaCl is starting point in the right image.

Sampling and relaxation

Long duration simulations were carried out in order to evaluate the relaxation time for the ions to be distributed as they would in equilibrium in solution in the presence of the clay surfaces. Figure 4-10 shows the concentration profiles for Cl^- and Na^+. This profile is calculated for different times during the simulation: 4, 5 and 6 ns. It is clear that there is a slight difference between the profiles calculated at 4 and 5 ns. However, this difference is much smaller when the average profiles are compared for 5 and 6 ns. A total equilibration time of 7 ns was decided to be sufficient for ions to explore their local environment and obtain their equilibrium state.

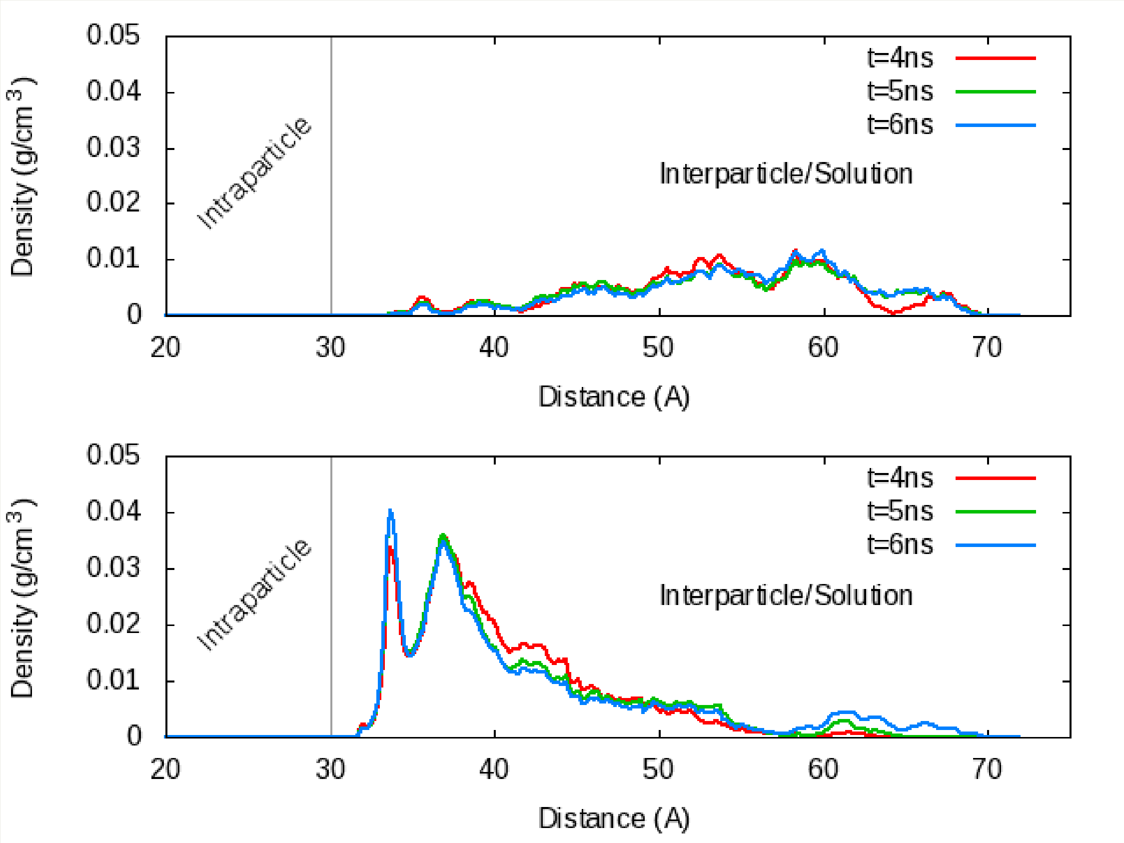

Figure 4-10 The Cl- (top image) and Na+ density profiles (bottom image) for 0.1 M NaCl in the pore solution. Relaxation after 4, 5 and 6 ns is shown. Averages are taken every 1 ns.

4.3.4. Sensitivity analysis

In the sensitivity analysis 3 distinct cases were considered to assess the effect of fluid composition on the ion behavior with regard to the charged clay surface. These cases are:

1. No iodine in solution and variation of NaCl concentration: The concentration of sodium ions considered in this case were: [Na$^+$] = 0.22, 0.33, 0.77, 1.32, 1.87 and 2.42 mol/L. The chloride concentrations are equal to the sodium concentrations minus 0.22 mol/L. Hence, in the case of [Na$^+$] = 0.22, no chloride is present in the solution since all sodium ions are compensating for the negative clay charge.

2. Variation of iodine concentration while maintaining Na constant (with [Na$^+$] = 2.75 mol/L): The concentration of iodide ions considered in this case were [I$^-$] = 0.11, 0.44, 0.88 and 1.32 mol/L and the chloride concentrations were decreased accordingly to retain electroneutrality. These concentrations for iodine are much higher than expected to occur and represent hypothetical accumulations.

3. Fixed iodine concentration of 0.77 mol/L and variation of NaCl: The concentration of sodium ions considered in this case were [Na$^+$] = 1.11, 1.54, 1.98 and 2.42 mol/L.

For each of these scenarios was computed:

- The ion density profiles with distance from the charged clay surface.
- The ratio between simulated diffusion coefficients (D, averaged over the total simulated pore space) and coefficients in bulk water (D$_0$).
- Diffuse double layer thickness for chloride and iodide.

Since the chloride and iodide concentration profiles show increasing concentrations from the clay surface (Figure 4-8), a definition for the DDL thickness is required (see also the discussion on DDL in Section 4.2.1). In order to have a quantitative measure of how large the excluded region is, the mean double layer thickness is estimated as the distance at which half of the concentration in free solution is reached for each anionic species. The method utilized here consists in fitting smooth functions for each profile, in order to smear small fluctuations. These functions can then be used to find the best fitted distance at which half of the concentration in solution would be found. Error bars are taken to be equally spaced at 1 standard deviation from the mean values.

The diffusion coefficients D and D_0 are calculated from the simulation results using the same relation as described in Section 4.3.2 for the water self-diffusion coefficient. The computed values of D_0 for sodium, chloride and iodide are 1.6×10^{-9} m/s^2, 2.0×10^{-9} m/s^2 and 1.7×10^{-9} m/s^2, respectively. These values are somewhat higher than the values reported in literature. The computed average diffusion coefficients parallel to the clay surface (D) only include the effect of the charged clay surface and do not take into account the pore morphology. Therefore, this coefficient has no value by itself but the ratio D/D_0 can be interpreted as an acceleration/retardation value. All simulations are performed at T = 300K.

4.4. Model results

4.4.1. Case 1: Effect of ionic strength without iodide

Figure 4-11 shows the density profiles for water at increasing sodium (and chloride) concentration. The resulting water distribution with distance from the clay is characteristic of water in proximity of charged surfaces, showing surface bound water (density peak) and a ‘normal’ water density in the bulk water away from the clay surface. These results are consistent with those reported in literature for similar systems [Greathouse & Cygan, 2005]. Starting from the clay outer surface (at 30 Å), water progressively increases its density until it reaches a maximum of ~2 g/cm^3 at a distance of 2.2Å. The maximum value of this surface bound water corresponds to approximately twice its value in the bulk. The amplitude and location of this peak is not significantly modified when altering the sodium concentration. At 4.2 Å from the surface, a region exists which is slightly depleted in water (0.8 g/cm^3), followed by a second, but much smaller peak at 5.6 Å (1.15 g/cm^3). At a distance of approximately 10 Å, the mean water density in solution for each sodium concentration is reached.

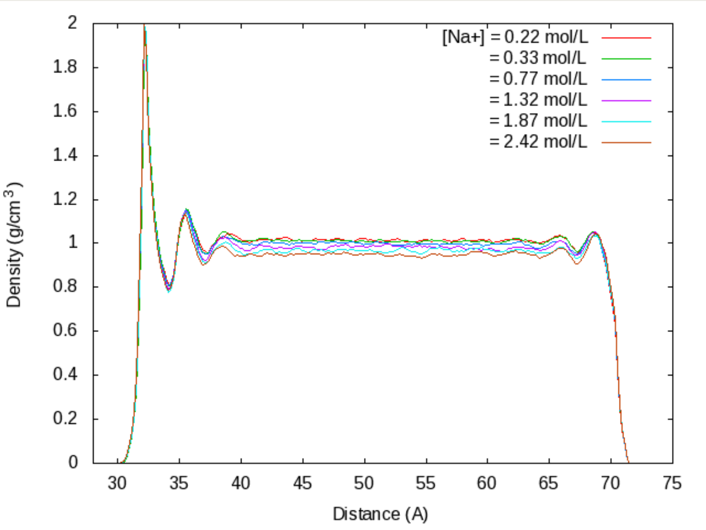

Figure 4-11 Water profiles in the interparticle pore space for different [Na+] concentrations in the absence of iodine with distance from the montmorillonite clay sheet boundary, which is located at 30Å.

Density profiles for Na^+ and Cl^-, are presented in Figure 4-12. Note that in the simulation with the smallest sodium concentration ($[Na^+]$ = 0.22 mol/L) no chloride is present. By its nature in Na-montmorillonite, sodium is initially present as adsorbed ions to compensate for the excess of charge in the clay surfaces, therefore it is possible to have sodium in a electroneutral system without additional anions in the pore water.

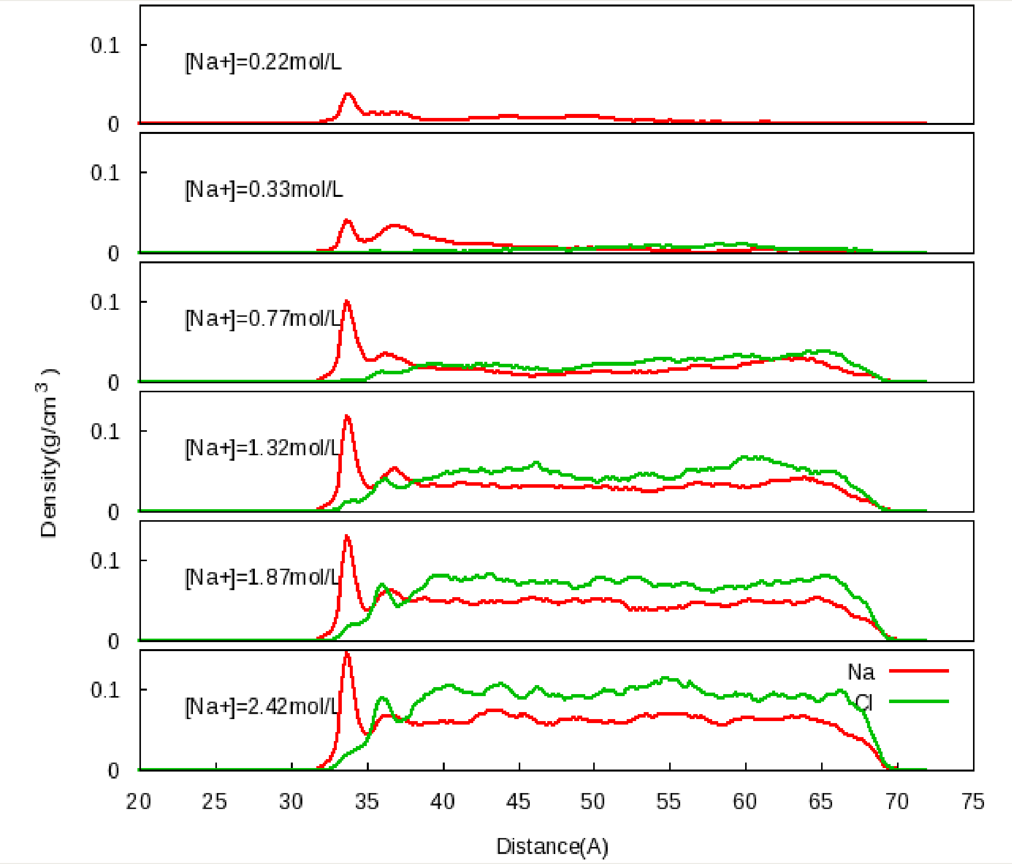

Figure 4-12 Sodium and chloride profiles in the interparticle pore space for different [Na+] concentrations in the absence of iodine.

With increasing ionic strength the sodium concentration increases in the bulk water at a distance >10 Å from the clay sheet. Near the clay surface the cations behave very distinctively with increasing ionic strength. At a concentration of 0.22 mol/L sodium appears mostly at the surface of the montmorillonite in an adsorbed state, with a first peak at a distance of ~3.8 Å from the clay surface. This is the result of the attraction between the negatively charged clay surface and the positive charge of the ions. Hardly any cations are found in the bulk pore space. After increasing the concentration slightly to 0.33 mol/L, the first peak is not significantly modified only slightly broader, the second peak follows at ~6.5 Å with a similar concentration. When the ionic strength is further increased, the concentration of the first peak at 3.8 Å rises considerably to ~0.15 g/cm^3 at an ionic strength of 2.42 mol/L. The second peak remains much smaller. As expected, chloride is excluded from the clay surface. Like sodium, the chloride concentration in the free pore water goes up with increasing ionic strength. Because of the increasing concentration in the free pore water, the chloride ions are forced more strongly towards the negatively charged surface. At a sodium concentration between 0.77 and 1.32 mol/L a chloride peak starts to develop at ~5.8 Å, which might be explained by the attractive forces by the positively charged, adsorbed sodium layer. The peak is located slightly closer to the clay surface than the second sodium peak.

The ratios of simulated diffusion coefficients (averaged over the total simulated pore space) over coefficients in bulk water are presented in Table 4-2 and Figure 4-13. The ratios are mostly well above 1, implying an acceleration with respect to diffusion in bulk water. This was not expected and is difficult to explain. Possibly the model is not very accurate in the calculation of this particular coefficient, and further fine tuning of the model is required in the future. In addition, no trend can be observed of the coefficients with increasing sodium content.

Table 4-2 Calculated average, relative diffusion ratios for ions in montmorillonite interparticle pore space in the plane parallel to the interface calculated for Cl^- and Na^+ ions at different [Na^+], when no I^- is present in solution.

[Na+] (mol/L)	Na^+	Cl^-	H_2O
0.22	1.19	-	1.32
0.33	1.05	1.49	1.40
0.77	1.18	1.25	1.25
1.32	0.98	1.06	1.11
1.87	1.59	1.52	1.43
2.42	1.19	1.03	1.17

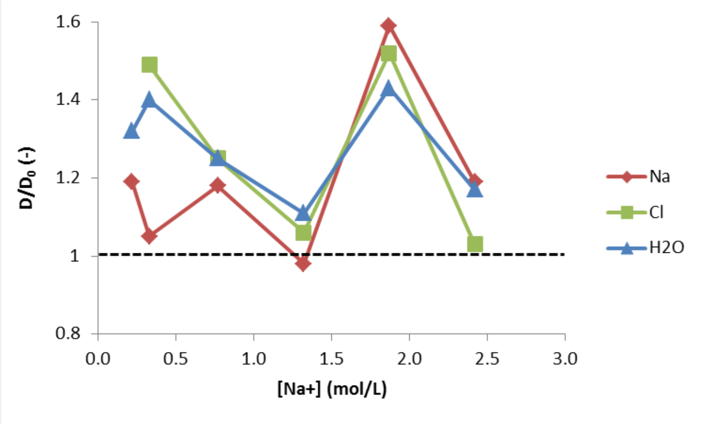

Figure 4-13 Graph with D/D$_0$ for Na+, Cl- and H2O as a function of the sodium concentration.

Figure 4-14 shows the results obtained for the mean DDL thickness of chloride at increasing ionic strength. The overall trend is that with increasing [Na+] the excluded region quickly narrows down. When both the concentration of Na+ and Cl- ions is small, chloride is only found in significant concentrations at a distance > 2.2 nm from the clay surface. However, the DDL thickness decreases exponentially with increasing ionic strength. Eventually, it appears that there is a limiting thickness for higher concentrations at 5 Å.

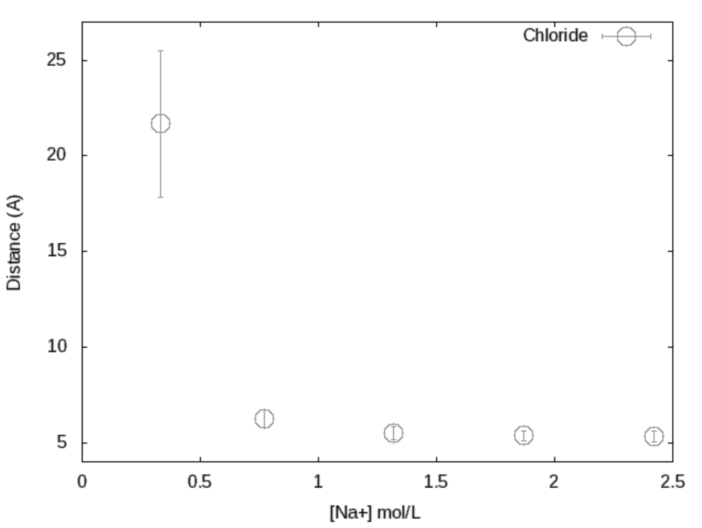

Figure 4-14 Mean DDL layer thickness as a function of increasing ionic strength, without iodide.

4.4.2. Case 2: Effect of iodine concentration at fixed ionic strength

Iodide replacement for chloride was systematically increased from 0.11 to 1.32 mol/L at a fixed sodium concentration of 2.75 mol/L. In this way the ionic strength of the system remained constant. In Figure 4-15 the density profiles for water are presented. The distributions are very similar to case 1 as shown in Figure 4-11. Like for case 1, the main peak appeared at 2.2Å from the clay surface. The maximum concentration at this location increases slightly with up to 5 % when iodide is present (not visible in the figure).

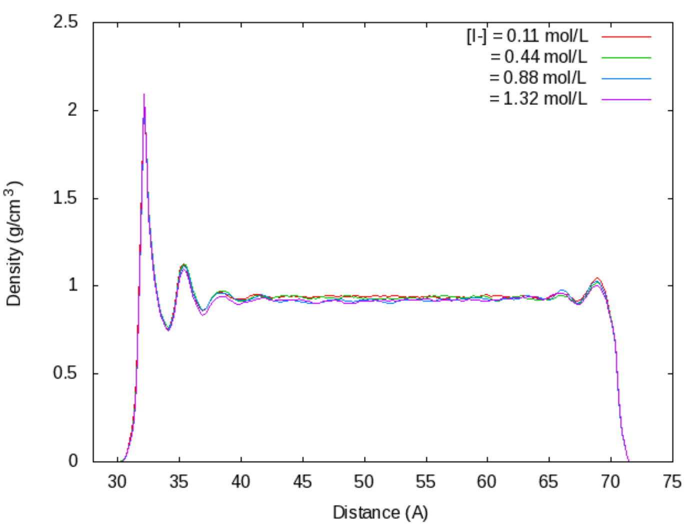

Figure 4-15 Water profiles in the interparticle pore space for different [I-] concentrations at a constant sodium concentration of 2.75M.

The density profiles for the ionic species are shown in Figure 4-16. The profiles for sodium are similar to the high sodium scenario in case 1 with slightly higher peak concentration due to the higher sodium concentration. The profiles are very consistent with increasing iodide concentration. The sodium peak intensity increases slightly with increasing iodide concentration.

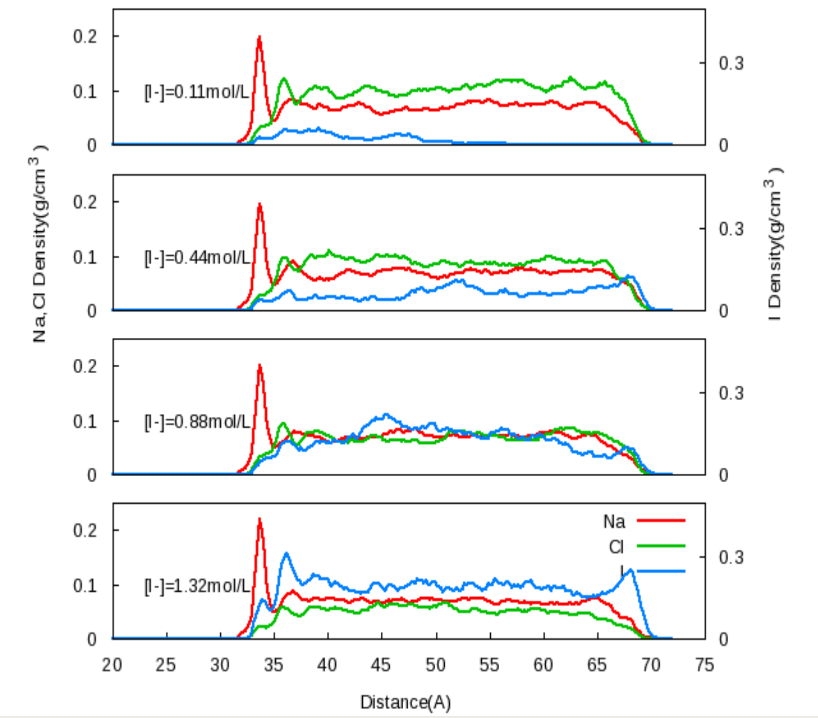

Figure 4-16 Sodium, chloride and iodine ions profiles in the interparticle pore space for increasing I- concentrations. Note that the I- concentration is shown on the right y-axis.

Due to the increasing replacement of chloride by iodide, the chloride concentrations in the free water (at a distance >10Å) decrease when the iodide concentrations increase. Like chloride, iodide shows exclusion effects near the surface of the clay sheet. Yet, in contrast to chloride, iodide shows higher concentrations between ~2.5 and 20 Å from the clay surface, than at a distance >20 Å (compare the graph of [Na$^+$] = 0.33 mol/L in Figure 4-12 and [I$^-$] = 0.11 mol/L in Section 4.4.1. In addition, at increasing concentrations iodide starts to form a small peak at the same location of the adsorbed sodium ions (3.8 Å), which chloride does not. A second and main iodide peak is located in between the main chloride peak and the second sodium peak, around 6 Å.

Diffusion ratios for each ionic species and water are shown in Table 4-3 and Figure 4-17. At low iodide concentrations, all ratios except for iodide itself are below one, implying a deceleration with respect to the diffusion in bulk water. At higher iodide concentrations, the ratios increase to values mainly above 1. Compared to case 1 the ratios for all species are lower.

Table 4-3 Diffusion ratios for each ionic species and water at increasing iodide concentration and a fixed sodium concentration [Na$^+$] at 2.75 mol/L.

[I-] (mol/L)	Na	Cl	I	H_2O
0.11	0.93	0.82	1.36	1.00
0.44	0.88	0.94	1.05	0.92
0.88	1.14	1.05	1.24	1.09
1.32	1.18	0.91	1.21	1.13

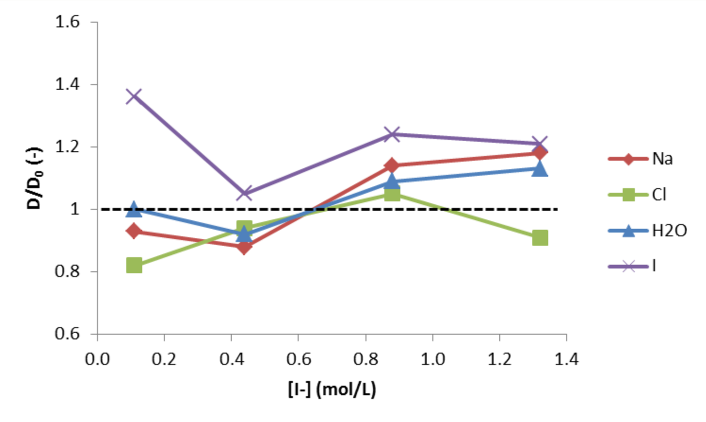

Figure 4-17 Graph with D/D0 for Na^+, Cl^-, H_2O and I^- as a function of the iodide concentration.

The DDL thickness results for increasing iodide concentration at fixed [Na+] are shown in Figure 4-18. Contrary to case 1, this time there are no statistically relevant differences when iodide is progressively increased and chloride diminished. Both iodide and chloride are present in significant concentrations at a distance of >3-5 Å from the clay surface at [Na+] = 2.75 M, independent of their relative concentrations.

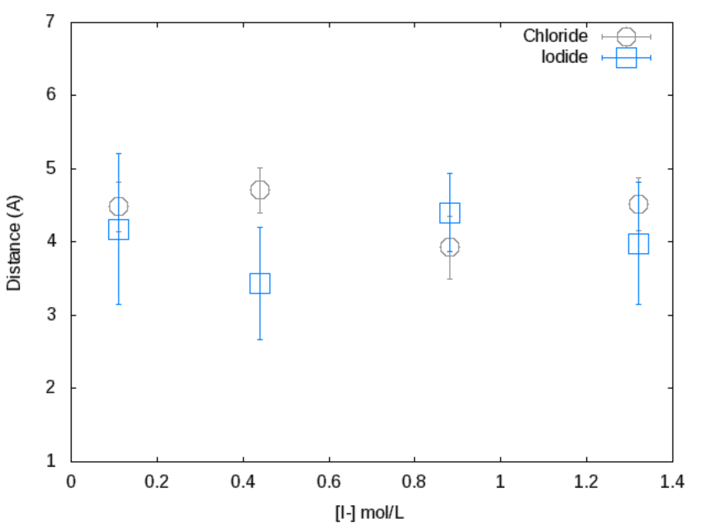

Figure 4-18 Mean DDL layer thickness as a function of the iodide concentration.

4.4.3. Case 3: Effect of ionic strength at fixed iodide concentration

In this scenario the NaCl concentration was increased at a fixed iodide content of 0.77 mol/L. In a similar way as it was done for case 2, chloride is added to the system in a sufficient amount to, together with iodide, counter balance the excess sodium ions. Similar to the previous cases, water profiles are very consistent with slightly higher peak concentrations than in case 1 (Figure 4-19).

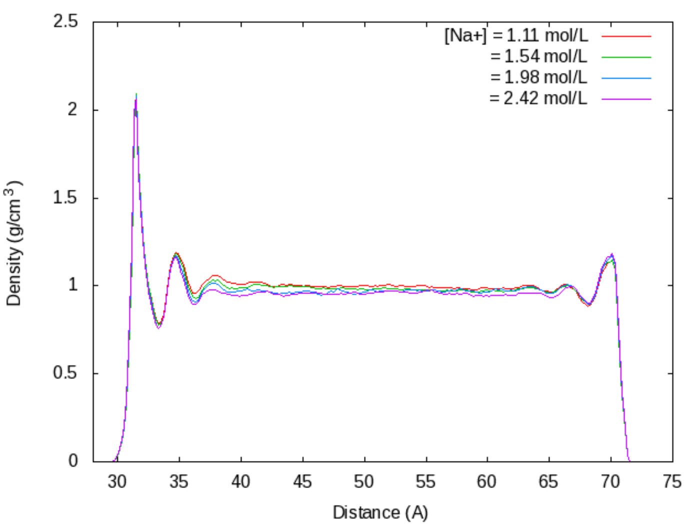

Figure 4-19 Water profiles in the interparticle pore space for different [Na+] concentrations at fixed [I-] of 0.77M.

The behaviour of the sodium ions is similar to case 1 for increasing sodium concentrations with increasing peak concentrations (Figure 4-20). The behaviour of the anions is more complex. At [Na$^+$] = 1.11 mol/L, iodide is found preferentially far away from the clay surface and hence the exclusion effect is strong. Yet, iodide is not completely absent near the clay surface, and the concentration increases with distance. At this concentration, barely any chloride ions are present. At increasing concentrations to [Na$^+$] = 1.54 mol/L, the iodide density profile does not change initially, but chloride shows an opposite distribution to iodide with a *decreasing* concentration away from the surface. At even higher sodium (and chloride) concentrations, both iodide and chloride become more evenly distributed over the free pore water. Close to the clay surface the two iodide peaks start to form, similar to those at high iodide and sodium chloride concentrations in case 2. At the highest concentration with [Na$^+$] = 2.42 mol/L, the iodide concentration has shifted more towards the clay surface, while chloride concentration increases away from the surface. Hence, the distribution of chloride and iodide is now opposite to the distribution at lower sodium concentrations.

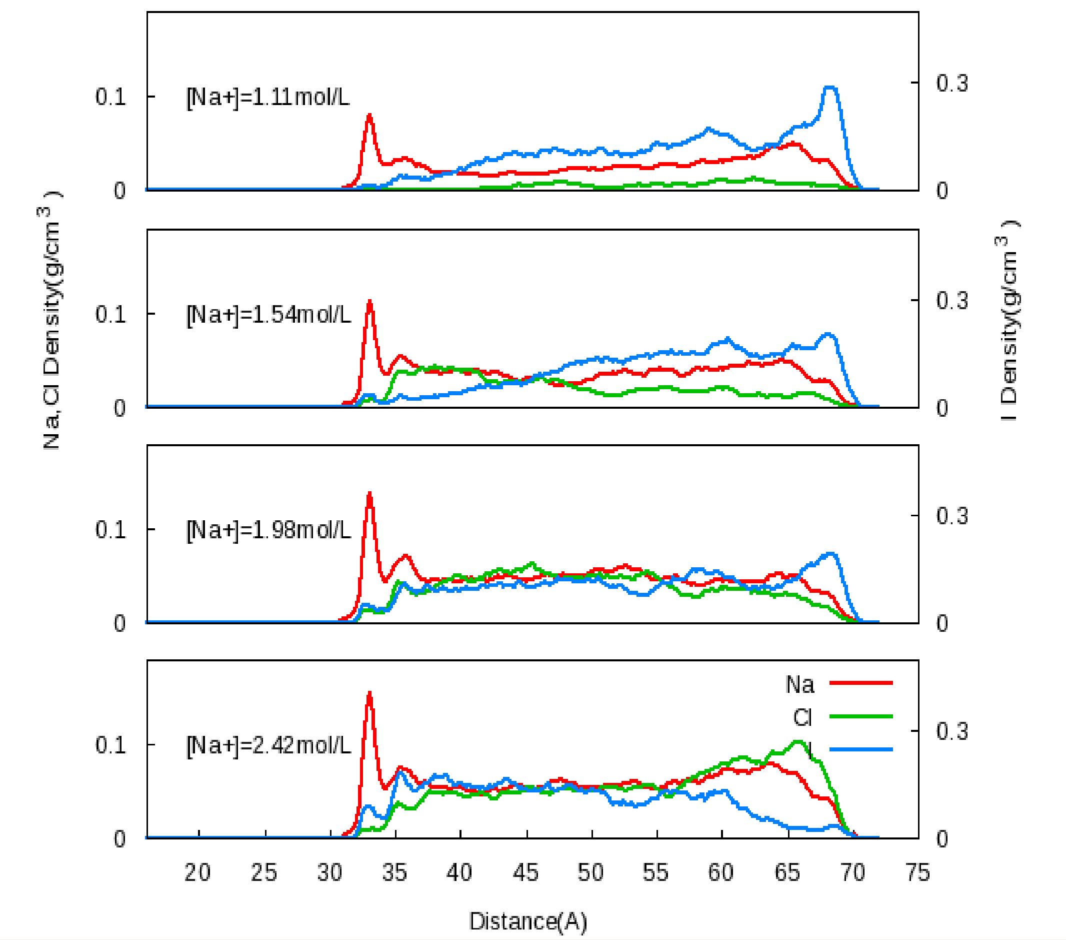

Figure 4-20 Sodium, chloride and iodine profiles in the interparticle pore space for different Na+ concentrations at fixed [I$^-$] of 0.77mol/L.

The diffusion ratios for each species in this case are presented in Table 4-4 and Figure 4-21. Again, no clear trend can be observed between the ratios and the sodium concentration. The ratios are mostly well above 1 and reach values for iodide as high as 1.6.

Table 4-4 Diffusion ratios for each ionic species and water when iodide concentration is kept constant while increasing the concentration of sodium ions.

[Na+] (mol/L)	Na	Cl	I	H_2O
1.11	1.42	0.60	1.62	1.35
1.54	1.03	1.40	1.18	1.11
1.98	1.26	1.06	1.66	1.21
2.42	1.08	0.89	1.14	1.10

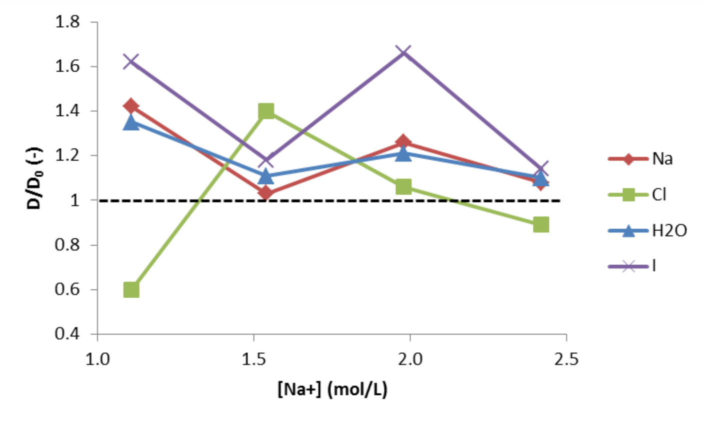

Figure 4-21 Graph with D/D_0 for Na^+, Cl^-, H_2O and I^- as a function of the sodium concentration at fixed [I-] of 0.77M.

The thicknesses of the DDL for case 3 are presented in Figure 4-22. Similarly to case 1, at low ionic strength both anionic species are excluded significantly from the clay surface. With increasing [Na+] the excluded region narrows down. However, the DDL thickness as defined in this project, decreases quicker for chloride than for iodide. This would imply the requirement of ion specific DDL thicknesses. At [Na+] = 1.5 M the chloride double layer has been reduced to 30% of its value compared to [Na+] = 1.1 M. In contrast, iodide DDL mean thickness is still 80% at this point. For values larger than [Na+] = 2.0 M it seems that they both reach their minimum values of ~4 Å, similar to the values obtained for case 2.

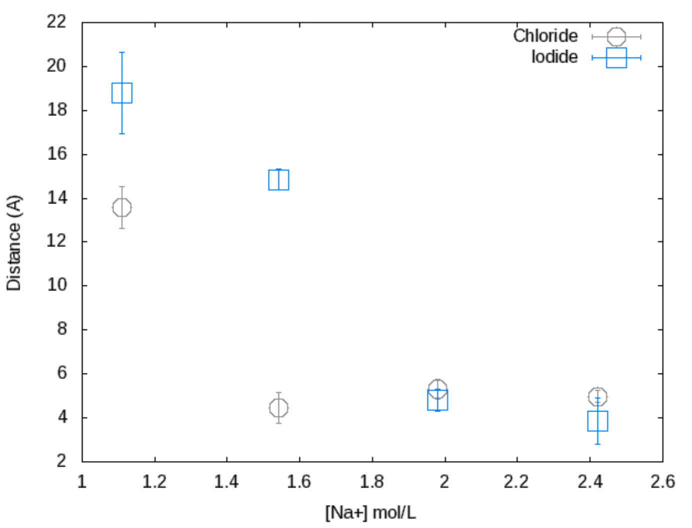

Figure 4-22 Mean DDL layer thickness as a function of the ionic strength at fixed iodide concentration.

4.5. Discussion

4.5.1. Model results

The molecular simulations resulted in ion density profiles and allowed the assessment of two important parameters for ionic species within the presence of a charged smectite mineral, as a function of ionic strength and iodide concentration: the acceleration/ retardation with respect to the diffusion in bulk water and the DDL thickness for diffusion accessible porosity.

The density profiles from the molecular simulations show water and ion distributions which overall correspond with the basic principles related to charged clay surfaces, as described by the Gouy-Chapman and Stern models. These include the Stern and diffuse layer (together they form the DDL) and the free pore water.

In the simulation results, surface bound water and adsorbed cations (sodium in this case) can be found in the *interlayer or intraparticle* pore space, as shown Figure 4-7. Complete anion exclusion occurs, consistent with overlapping Stern layers. In the *interparticle* pore space, the simulations show surface bound water and adsorbed sodium ions located at a short distance to the charged clay surface, visualized by the concentration peaks at respectively 2.2Å and 3.8Å. The locations of these peaks are more or less fixed regardless of the brine composition, while the peak concentration can vary slightly. Consistent with [Tournassat et al., 2009] the surface bound water and main sodium peak occur in the Stern layer. The simulations show that the peak width, and hence the thickness of this layer, is not affected by the ionic strength. According to the calculations in [Tournassat et al., 2009] the diffusion of both the surface bound water and the adsorbed cations is slowed down by the clay surface charge.

For case 1, at low ionic strength ($[Na^+]$ = 0.33 mol/L and $[Cl^-]$ = 0.11 mol/L), the chloride is practically absent in the zone of surface bound water and adsorbed sodium, which is consistent with the definition of the Stern layer (Leroy et al., 2007). The chloride concentration starts to increase from a distance of ~5 Å (= 0.5 nm), consistent with a diffuse layer. These results are similar to the molecular simulation results from [Tournassat et al., 2009] at 0.1 mol/L who also found a Stern layer with a thickness of ~0.5 nm.

At higher ionic strength ($[Na^+]$ > 0.33 mol/L), the simulations predict that the chloride is 'forced' towards the clay surface and chloride becomes present in the zone of adsorbed sodium. This is also true for iodide in case 2 and 3. The results show a layer of complete anion exclusion which is maximally 1-2 Å (0.1-0.2 nm) thick. The chloride and iodide are present at a distance >1-2 Å, even if it is in low concentrations. If the definition of the Stern layer is based on the location of the adsorbed cations (instead of the zone of complete anion exclusion) this would imply that anions enter the Stern layer. Simulations with iodide were only performed at intermediate ($[Na^+]$ = 1.11 mol/L) to high ionic strength ($[Na^+]$ = 2.75 mol/L). The iodide concentration profile depends both on the ionic strength and the chloride concentration. At intermediate ionic strength and low chloride concentrations the iodide is forced away from the clay surface. It is present in very low concentrations at the location of the adsorbed sodium. At high ionic strength and intermediate to high chloride concentrations the iodide becomes more attracted to the positively charged, adsorbed sodium. A concentration peak can be found at the same location as the main sodium peak, and a second, larger peak is located close to the second sodium peak. It might be expected that the diffusion coefficient of the iodide goes down as a result of this attraction. The mean DDL thickness, as calculated for this study, decreases exponentially with increasing ionic strength for chloride, and more slowly for iodide, to a minimum value of ~4-5 Å for both species. *The presence of iodide seems to decelerate the decrease in DDL thickness for chloride* (compare Figure 4-13 and Figure 4-21). More simulations at varying concentrations, including at low ionic strength, are required to verify this hypothesis.

The diffusion coefficient ratios as computed from the model simulations are mainly >1, suggesting enhanced diffusion with respect to diffusion in bulk water. In literature on cation diffusion, the term 'surface diffusion' is generally described as diffusion *acceleration*. This term is somewhat confusing, since the acceleration of cations in this definition is *relative to the diffusion of a neutral species* and not relative to the diffusion of the specific cation *in bulk water*. Acceleration with respect to the bulk water is not likely, especially for water and sodium ions which are for a large part respectively bound and adsorbed onto the negatively charged clay surface.

Improved diffusion coefficient calculations are probably required to obtain more realistic values. Averaging the diffusion coefficients in specific layers parallel to the clay surface, consistent with the methodology applied by Tournassat et al. (2009), would improve the calculations. In addition, when other than free boundary conditions are imposed, such as in interfaces of dissimilar materials, the ordinary diffusion equation is not accurate. In reality, when such heterogeneous regions are considered, molecules will distribute differently than in the bulk. They will spend limited time within each distinct region, where locally the distribution is different from other parts of the system. As a consequence, by using the conventional diffusion equation in such systems, the interpretation of the results is prone to inaccuracies. For an extensive discussion on the calculation of diffusion coefficients, and for more sophisticated methodologies to obtain more accurate values, see [Liu et al., 2004]. Future improved post-processing of these model results is necessary. It would allow the assessment of iodide diffusion under varying conditions. The ion density profiles show that the behavior of iodide in the proximity of the charged clay surface is complex and changes upon variations in fluid composition.

4.5.2. Implications for anion diffusion

Diffusion coefficient

The assessment of the diffusion coefficient ratios by molecular simulations is only related to the charged clay surface in contact with free pore water. The pore morphology is not taken into account. This way, the effect of the clay charge can be investigated separately from any other effect. As explained above, the calculations gave unrealistic results. However, Tournassat et al. (2009) obtained reliable diffusion coefficients from molecular model simulations for sodium and chloride at low ionic strength (0.1 M) for the interlayer, Stern layer, diffuse layer and free water separately. Their results showed that, due to the negative charge of the clay surface, cation diffusion in the Stern layer is much lower than the diffusion in bulk water ($D/D_o = 0.5$) but faster than diffusion of adsorbed water (neutral species) ($D/D_o = 0.4$). In the diffuse layer the diffusion for sodium, chloride and water is close to the value in bulk water ($D/D_o = 0.9\text{-}1$).

In addition to the effect of the charged clay surfaces, D_o (and hence D_{app} and D_{eff}) depend on the temperature: D_o has a temperature dependency according to the Arrhenius equation. D_{app} values for iodide increase by a factor of three when the temperature increases from 24 to 80˚C [Bruggeman et al., 2010]. Hence, this effect should be taken into account and corrected for if relevant. D_{app} (and hence D_{eff}) is affected by the tortuosity and constrictivity of the sediment or rock. These parameters vary with orientation. Due to the preferred orientation of clays perpendicular to the compaction direction, the tortuosity and hence the pore diffusion coefficient is higher parallel than perpendicular to the bedding. In heavily consolidated clay this anisotropy factor can be up to 3.5-5.0 [Bruggeman et al., 2010a). A change in the pore water chemistry can affect these parameters. For example, Ca^{2+} released from cement, might replace Na^+ as the main exchangeable cation in clay minerals. Ca-bentonite has larger pores and hence tortuosity decreases and D_{app} increases. The other way around, flushing of low ionic clays with high sodic water would result in the formation of Na-bentonite and consequently more, but smaller sized pores and hence a larger tortuosity. The tortuosity decreases, and thus the D_{app} increases, in the following order: Na-montmorillonite, Ca-montmorillonite, kaolinite, Ca-illite, Na-illite [Bruggeman et al., 2009)].

Diffusion accessible porosity

It is commonly agreed that the DDL thickness, comprising of the Stern and diffuse layer, directly affects the diffusion accessible porosity of anions due to the anion exclusion effect (e.g. [Van Loon et al., 2007], [Appelo et al., 2010]). The higher the ionic strength, the smaller the DDL [Moors, 2005] and hence, the larger the diffusion accessible porosity. the simulation results are consistent with this principle, as shown by the large influence of ionic strength on the calculated mean DDL thickness.

Yet, a challenge regarding the determination of the DDL thickness is that it is a theoretical parameter. Mathematical equations based on e.g. Gouy-Chapman model are used to calculate the DDL thickness [Moors, 2005]. The DDL gradually merges into the free pore water and the boundary is basically at the location where the concentration of both the anions and cations are stable. The anion concentration in the diffuse layer increases exponentially away from the clay surface and a precise definition for the thickness in the light of anion exclusion is therefore rather arbitrary. Yet, the DDL is generally treated as a zone which is inaccessible to anions (e.g. [Moors, 2005], [Van Loon et al., 2007], [Appelo et al., 2010]), thereby not differentiating between a Stern layer and a diffuse layer. However, as described in section 4.2.1, the zone with complete anion exclusion (the Stern layer) comprises only a minor part of the DDL zone. The thickness of the Stern layer depends on the concentration and size of compensating cations, which is fixed for a specific clay charge. According to the simulation results, anions were predicted to enter the Stern layer at higher ionic strength. The main part of the DDL is made up by the diffuse layer, the thickness of which decreases with higher ionic strength. Anions are present in the diffuse layer, even if the concentrations are lower than in the free pore water, and is therefore part of the anion accessible porosity. The thickness of the complete exclusion zone (equal to or thinner than the Stern layer) is hardly affected by the ionic strength. Based on these insights, the diffusion accessible porosity does not decrease with increasing ionic strength due to a significant increase in DDL thickness, but due to a slight increase of the thin Stern layer! For the low ionic strength in the Boom Clay in Belgium, a DDL thickness of 2.37 nm is assumed (Figure 4-3), while the actual exclusion zone is only ~0.5 nm thick.

The interparticle pore space within a sediment or rock consists of isolated pores, pore bodies and pore throats. Isolated pores are not accessible for migrating ions. Pore bodies can have various sizes and they are connected with each other through narrow pore throats [Nakashima, 1995]. Pore bodies connected by very narrow pore throats might be inaccessible to anions if the anion exclusion zones overlap in the narrow throats (Figure 2-1).

Hence, the thickness of the anion exclusion zones does not only influence the pore volume excluded for anion diffusion, but can also exclude part of the free water in the pore bodies if narrow pore throats do not allow excess.

This implies that there is no linear relationship between the free pore water volume (water volume not present in the double layer) and the observed anion diffusion accessible pore volume.

This also implies that the pore morphology plays a crucial role in the effect of DDL (or anion exclusion zone) on anion exclusion. The pore morphology of rocks can be investigated by means of mercury injection capillary pressure (MICP, also referred to as mercury injection porosimetry (MIP)) measurements. MICP analyses allow the calculation of pore throat size distributions and total porosity, up to a resolution of ~3 nm. Hence, if the anion exclusion zone is >1.5 nm, MICP measurements allow the estimation of the pore size fraction which is inaccessible for anions.

Leroy et al. (2007) calculated a diffuse layer thickness of 2 nm for the Callovo-Oxfordian argillite in France at low ionic strength, using theoretical models. According to the authors, the minimum thickness of the Stern layer is 1-2 nm based on the mean diameter of various hydrated cations. Combining a Stern layer of 2 nm with a diffuse layer of 2 nm, they defined a critical pore fraction with a diameter of 8 nm (80Å) which still allows diffusion. Using MICP measurements, they calculated that 50% of the pore space is inaccessible to anions. However, a Stern layer thickness of 2 nm is quite extensive and this is much higher than what is observed by the molecular simulations as well as those from [Tournassat et al., 2009]. The hydrated diameter of sodium and corresponding thickness of the Stern layer is only 0.37 nm, which is more in line with simulation results. Considering that they overestimated the thickness of the Stern layer by at least 1 nm, and the fact that anions are not excluded from the diffuse layer, this value for the critical pore fraction seems highly overestimated.

Hemes et al. (2013) investigated pore morphology of Belgian Boom Clay samples by MICP as well as by broad-ion-beam scanning electron microscopy (BIB-SEM). With BIB-SEM the microstructures of the clay rock, including pore morphology, can be visualized. The porosity values derived from MICP were between 27 and 35%. The visualization of the pore morphology showed that for fine grained samples, 85-88% of the total BIB-SEM visible porosity is located within the clay matrix. For the Opalinus Clay in Switzerland it was also shown that the main part of the pore space was present within the clay matrix [Houben et al., 2014]. This is important information, since ions will be affected by the charged clay surfaces bounding the pore space. MICP results showed that the Belgian Boom Clay samples have peaks at pore-throat diameters <100 nm and that 94% of the porosity is made up of pores of < 300 nm. Even higher porosities (34 – 40%) were determined by water content measurements and HTO diffusion experiments, implying that an additional 1 - 13 vol% of the porosity is made up by interlayer pore space and/or by interparticle pore space which is only accessible by pore throats <3.6 nm [Hemes et al., 2013]. Assuming that the smallest pore space is located in the clay matrix, that the clay matrix consists of montmorillonite and considering the DDL thickness inaccessible for anions assumed for the Belgian Boom Clay (2.37 nm), this pore volume would not be accessible. Based on the hypothesis that the anion exclusion zone is maximally 0.5 nm, the pore space inaccessible because of narrow pore throats would be much lower.

4.5.3. Comparison to experimental studies

Many laboratory experiments have been published which aimed at the understanding of transport properties and migration behavior of radionuclides through clay-rich sediments [Aertsens et al., 2008)]. Depending on the required parameters and the type of radionuclide, these experiments were designed in various ways: percolation, pulse injection, through-diffusion or in-diffusion experiments ([Van Loon et al., 2007], [Aertsens et al., 2008]). Most of these studies aimed for the determination of D_{app} (= D_{pore}) and η. For a detailed description of the experimental designs and the determination of the diffusion parameters be referred to [Van Loon et al., 2007] and [Bruggeman et al., 2009, 2010] and references therein.

Experiments with tritiated water (HTO), considered to be a non-sorbing tracer (R = 1), are performed to evaluate migration parameters of the sediments. Due to its neutral charge, HTO can distribute itself over the entire pore space, including interlayer and DDL pore space [Bruggeman et al., 2009]. As a result, the accessible pore space defined for HTO from experiments represents the total pore space of the sediment. For the Boom Clay in Mol (Belgium) the HTO diffusion accessible porosity is defined as 0.38-0.40 (38-40%), and D_{app} as $2.0\text{-}2.6 \times 10^{-10}$ m/s^2 for diffusion perpendicular to the bedding, regardless of the ionic strength [Aertsens et al., 2009]. D_o for HTO is 2.44×10^{-9} m/s^2 and hence, for these samples, *the effect of tortuosity on the diffusion coefficient is a decrease by one order of magnitude*.

Laboratory tests using percolation experiments (with Darcy flow) allow the estimation of D_{app} and ηR for tracer concentrations such as iodide with time [Aertsens et al., 2013]. Since R is equal to 1 for iodide, η can be determined from the experiments. With regard to anions, the effect of the charged clay surface will probably mainly have an effect on η. At least for chloride, at low ionic strength, the chloride ions are being expelled from the clay surface. In the diffuse layer and free pore water the diffusion coefficient, as calculated from molecular simulations, is close to the value in bulk water [Tournassat et al., 2009]. At higher ionic strength, when anions are forced towards the clay surface, the effect of the charged clay surface on the diffusion coefficient might play a role.

Table 4-5 Summary of pore diffusion coefficient D_{pore} and diffusion accessible porosity η for iodide in Boom Clay at currently prevailing conditions found in Mol (see Section 3.4.1]).

	D_{pore} [m^{2}s^{-1}]	
	Min	Max
D_{pore} (m^2/s)	1.2×10^{-10}	1.6×10^{-10}
η	0.12	0.20

Table 4-6 Percentage of the *total* porosity available for iodide diffusion. Based on experiments performed by [Van Loon et al., 2007].

Bulk dry density **Ionic strength**	**1300 kg/m^3**	**1600 kg/m^3**	**1900 kg/m^3**
1 M	20.9%	14.9%	7.5%
0.01 M	3.2%	0.9%	0.3%
	% of *interparticle* pore space inaccessible for diffusion		
0.01 M	84.7%	94.0%	96.0%

For Belgian Boom Clay, experiments have been performed using cores from several boreholes at varying locations in the Campine Basin [Aertsens et al., 2004, 2013]. Both lateral and vertical variations were assessed at the prevailing low ionic strength. The obtained η values for HTO and iodide are 0.34 to 0.47 and 0.14 to 0.28 respectively. The difference in values between the two species is thought to be the result of anion exclusion. The D_{app} values are 1.2×10^{-10}-3.1×10^{-10} m/s^2, and 9.1×10^{-11}- 1.9×10^{-10} m/s^2 respectively [Aertsens et al., 2013].

Van Aertsens et al. (2009) experimentally showed that the average η value for iodide in Belgian Boom Clay *at the Mol* site increases from ~17% to 28% when increasing the ionic strength from 0.016 to 1.0 M (with corresponding theoretical DDL thickness of 2.37 and 0.30 nm respectively (Figure 4-3)). Bruggeman et al. (2010) summarized the available data for D_{pore} and η for iodide in Boom Clay at currently prevailing conditions found in Mol (very low ionic strength)(Table 4-5).

Van Loon et al. (2007) performed several types of diffusion experiments on compacted bentonite to better understand anion diffusion and exclusion effects. The average total porosity of the bentonite was 53.6%, 42.9% and 32.2% for samples with a bulk dry density of respectively 1300, 1600 and 1900 kg/m^3. Their results are summarized in Table 4-6.They show that the diffusion accessible porosity decreases with increasing bulk density, and increases with increasing ionic strength of the brine. Assuming that the DDL thickness is minimal at an ionic strength of 1 M, the remaining part of the porosity is made up of interlayer pore space. At a low ionic strength of 0.01 M, the main part of the interparticle pore space is inaccessible for diffusion, interpreted to be the result of anion exclusion. These results suggest a huge effect of the DDL thickness on the diffusion of anions.

Yet, this is not consistent with the observations from molecular simulations which show only a minor anion exclusion zone. Considering the pore sizes of Belgian Boom Clay, as investigated in [Hemes et al.,2011], the effect of changes in DDL thickness might not be the crucial process in the anion accessible porosity. Other phenomena resulting from changes in fluid water composition might play a role in the diffusion accessible porosity:

- Flushing with low ionic waters can enhance *crystalline clay swelling* [Laird, 2006]. This implies that more hydration layers form in the interlayer space, thereby increasing the interlayer thickness to maximally 10-12 Å. Hence, this would imply that a larger fraction of the water is bound to the clay minerals. The clay mineral with the highest potential for crystalline swelling is Na-montmorillonite.
- In the presence of large volumes of low ionic water *osmotic clay swelling* can occur, resulting in the formation of so called quasi-crystals (Laird, 2006). This is due to the detachment of clay sheets upon cation hydration, thereby adsorbing additional cations on the liberated clay surface. The electric forces between the opposite cation layers forces the clay sheets apart and can result in a significant increase in interlayer thickness up to 130 Å [Anderson et al., 2010]). As a result of osmotic clay swelling, *the volume of the clay minerals can increase up to a factor of 10* [Laird, 2006]. The mechanisms of osmotic clay swelling are currently not well understood, but the smectite with the highest swelling potential is Na-montmorillonite [Zhou et al., 1996, 1997].
- Flushing can result in the migration of clay particles, a process which is called *fines migration*. This process can be enhanced by osmotic clay swelling. The migrating clay particles can block pore throats and thereby lower the diffusion accessible porosity.

Clay swelling, both in the crystalline and the osmotic regime, affects the proportion of interlayer, DDL and free water pore space, and thereby the diffusion accessible porosity. The combined effect of clay swelling, fines migration and the changes in DDL thickness might explain the large influence of the ionic strength on the diffusion accessible porosity of anions but the processes are complex. Whereas changes in DDL thickness upon fluctuations in ionic strength are reversible [Bruggeman et al., 2010a], deterioration of the microstructures upon sodic flushing is considered as irreversible [Moors, 2005)]. Investigation of changes in pore structure by MICP and BIB-SEM before and after flushing experiments should give improved insight in the various processes that play a role when the ionic strength of the fluid is changed.

4.5.4. Upscaling - Implications for reactive transport modelling

In reactive transport models, an effective diffusion coefficient needs to be considered, which implicitly considers tortuosity, (diffusion accessible) porosity and clay charge effects other than adsorption (adsorption is explicitly included in the model). This means that a D_{eff} needs to be defined.

Nakashima (1995) determined values of D_{eff} for iodide in varying rock types experimentally. Results showed a linear relation between D_{eff} and porosity, regardless of the rock type, but only when the porosity was roughly corrected for ‘storage porosity’ (porosity not accessible for diffusion). This so called ‘transport porosity’ was measured using MIP with a pore-size limit of 5 nm, assuming that pore space connected by pore throats <5 nm is inaccessible for iodide. Their obtained relation between D_{eff} and transport porosity does not consider the potential effect of anion exclusion and is thus implicit. The scatter in the datapoints could therefore partially be explained by the anion exclusion. Yet, MIP measurements can be used to roughly estimate the D_{eff} for iodide by the relation obtained in [Nakashima, 1995]:

$$\log D_{eff} = \log (0.53*10^{-9}) + 1.3\log \varphi_{transport}$$

where $\varphi_{transport}$ is defined as the transport porosity, which is used in a similar way as the diffusion accessible porosity. For an improved identification of the D_{eff} such a relation could also be defined specifically for Boom Clay for various radionuclides. A critical pore size unavailable for anion diffusion for specific fluid compositions, based on calculated or simulated DDL thicknesses, should be taken into account. The parameter $\varphi_{transport}$ could be defined as a function of the smectite content and the fluid composition.

4.5.5. Boom Clay in Belgium versus the Netherlands

The potentially targeted Boom Clay in the Netherlands is located at greater depth compared to Mol in Belgium. A higher degree of compaction will most probably result in a decrease of the total porosity, the pore sizes and throat widths [Bruggeman et al., 2009]. The fraction of interlayer space of the total pore space increases upon sediment compaction, due to a significant decrease in interparticle pore space. However, also interlayer space decreases when the hydration layers of montmorillonite decrease from 3 to 2 (and possibly 1) with increasing compaction [van Loon et al., 2007].The experimental study by Van Loon et al. (2007) clearly showed that an increase in material density, resulting from increased compaction, will drastically lower the diffusion accessible porosity for anions. A higher degree of compaction could also result in greater preferential orientation of the clay minerals and hence in higher anisotropy [Bruggeman et al., 2009]. The tortuosity perpendicular to the bedding would increase and therefore the apparent and effective diffusion coefficient in that direction would decrease. Hence, a detailed study on the pore morphology of the Boom Clay in the Netherlands would improve the present insights in the diffusion accessible porosity and as a result, also in the potential diffusion behaviour of radionuclides from a repository.

4.5.6. Cation diffusion

Cation diffusion deals with different processes than anion diffusion. Cations are attracted by the negative clay charge, resulting in adsorption in the interlayer and the DDL layer. The retardation effect due to cation adsorption is covered by the retardation factor in the diffusion equation:

$$D_{eff} = D_{pore} * \eta = D_{app} * \eta R = D_o * \eta R * G$$

The retardation factor depends on the dry bulk density, the diffusion accessible porosity and the distribution of the cation over solid and liquid ($K_d = S_i/C_i$, with S_i defined as the mass on solid and C_i as mass in solution) [Bruggeman et al., 2010a]:

$$R = 1 + (\rho \times K_d)/ \eta$$

Adsorbed cations are not immobile. They are known to diffuse faster than neutral species (like HTO) in the presence of a negatively charged clay surface. This is called the cation 'acceleration' phenomenon [Robinet et al., 2011]. The adsorbed cations in the Stern layer are accelerated with respect to neutral species in this zone (Tournassat et al., 2009], [Robinet et al., 2011]). However, compared to diffusion in bulk water, the diffusion is much lower. Hence, the acceleration phenomenon has a slightly misleading name. Since the main part of the cations in solution are located in the Stern layer, the diffusion of cations is much slower than in bulk water. The acceleration parameter, used to assess the acceleration with respect to the neutral species, is:

$A = (D_{ec} \times D_{wn}) / (D_{wc} \times D_{en})$

where D_{ec} and D_{en} are the effective diffusion coefficients of the cation and neutral species respectively, and D_{wc} and D_{wn} the diffusion coefficients in bulk water of the cation and neutral species respectively. Similar to the acceleration calculated from the simulation results for anions in the current study, the acceleration parameter for cations can be determined from molecular simulations. As explained above, the calculation of this acceleration parameter requires further processing, but the study by Tournassat et al. (2009) showed the value of the determination of these values for a better understanding of ion migration in clay rocks.

4.6. Conclusions and recommendations

Molecular simulations were used to assess the effect of negatively charged clay surfaces on anion diffusion and exclusion effects. The simulations resulted in ion density profiles as a function of distance from the clay surface. These profiles allowed the assessment of the thickness of the DDL layer for the diffusion accessible porosity. In addition, calculations based on ion movement allow the determination of an acceleration/retardation parameter. The simulation results showed unreliable values for the acceleration/ retardation parameter and require further post-processing according to complex calculations reported in literature. The ion density profiles show that the anion exclusion effect decreases with higher ionic strength. At increasing ionic strength the anions were shown to approach the clay surface and hence the effect of the charged clay surface on the diffusion coefficient might be stronger than at lower ionic strength. Future work on improved calculations need to confirm this.

The DDL thickness is generally assumed to be a crucial parameter in the determination of the diffusion accessible porosity due to the anion exclusion effect. The molecular simulations showed the strong effect of ionic strength on the DDL thickness. In addition, the presence of iodide seems to affect the DDL thickness of chloride, suggesting the importance of interaction between the various aqueous species present. Yet, the actual anion exclusion zone is limited. The main part of the DDL zone, the diffuse layer, was shown to be accessible to anions, even if concentrations are lower than in the free pore water, and the diffuse layer would therefore not affect the anion accessible porosity. The changes in thickness of the actual anion exclusion zone with varying ionic strength are lower than the changes in the DDL thickness. Yet, it would be interesting to simulate two negatively charged clay surfaces and the effect on anion exclusion when the surfaces approach each other.

A change in the exclusion zone thickness as a result of changing conditions (e.g. ionic strength) can enhance or limit the pore space available for diffusion by respectively opening up or blocking pore throats which connect the pore space. Hence, the pore morphology plays a crucial role in the diffusion accessible porosity. Considering the small effect of ionic strength on the anion exclusion zone, the effect on the anion diffusion accessible porosity is possibly minor. Future model studies should couple molecular simulations to a pore scale model in order to assess the combined effect of pore morphology and clay surface charge on anion exclusion.

In addition to DDL effects, a change in pore water chemistry can also result in processes such as clay swelling and fines migration, which subsequently affect the pore morphology and hence the ratio of interlayer, DDL and free pore water space, significantly. These effects should not be neglected and need further study. Especially when interpreting experimental results, these effects should be taken into account. The initial state of the rock samples and clay minerals and the potential effect of changing fluid conditions on pore morphology should be evaluated prior to the start of lab experiments.

5. Towards a modelling approach for OPERA

In this chapter, an approach is developed to address radionuclide migration in Boom Clay within the safety assessments of the OPERA Safety Case. A sequential set-up is used, where:

1. General considerations are given (Section 5.1);
2. Relevant processes to be covered are defined (Section 5.2);
3. The range of parameters to be considered is defined (Section 5.3);
4. The radionuclides of interest and their assignment to different phenomenological groups are discussed (Section 5.4).

5.1. General considerations

The generally accepted and applied approach for modelling migration of ions through argillaceous rock is by assuming simple Fick's diffusion, in which the combined chemical and physical effects of the clay porous medium are incorporated by adding a number of additional factors (e.g. accessible porosity, molecular diffusion coefficient, tortuosity, constrictivity, retardation).

Of these factors the ion accessible porosity, molecular diffusion coefficient, tortuosity and constrictivity together represent processes of physical nature, and together define the effective diffusion coefficient, D_{eff}. The retardation R, summarizes the interactions between dissolved ions and the solid particle surfaces, and so summarizes the chemical processes.

The application of such an effective diffusion coefficient combined with a linear sorption model provides a numerically simple and computationally efficient approach that is very suitable for incorporation in assessment calculations. Although it assumes linear sorption behaviour, which is of course a simplification, it has the advantage of enabling to obtain a closed analytical solution for coupled transport, and is easy to use in a safety assessment modelling.

However, this modelling approach does not discriminate between the chemical and physical factors underlying the observed behaviour because in fact observed diffusion behaviour can usually be explained by various modelling assumptions; i.e. retarded ion diffusion can be explained by sorption, ion exclusion, or other effects. As long as the net migration is not affected by such choices, this might be mainly an academic discussion. However, for the safety case it is of importance to understand the effects of different interpretations and to provide evidence that a chosen approach is sufficiently conservative.

A proper understanding on the processes behind observed diffusion behaviour is of particular importance for the OPERA safety assessment, because currently only limited experimental support exists for the properties range of Boom Clays present in the Netherlands. Therefore, existing data, mainly provided by the Belgian research programme on radioactive waste disposal, need to be 'translated' or extrapolated to the range of physico-chemical conditions expected in the Netherlands. In order to do so, insight into the individual contributions of these physical and chemical factors is necessary to allow a proper estimation of how these effective diffusion coefficients can potentially vary, and how they are affected by changing chemical conditions.

The recent progress in understanding of ion interactions occurring at geo-surfaces present in Boom Clay (i.e. sorption, see [Schröder et al., 2016a, Schröder et al., 2016b]) allows to analyse observed overall diffusion behaviour by modelling, and to distinguish individual contributions of different chemical and physical process discussed here and in Tasks 6.1.2 and 6.1.4. This is of importance because experiments not only reflect diffusion processes 'sec' as discussed in the previous chapter, but other processes can be of relevance, too. Therefore, in this chapter an attempt is made to integrate understanding on diffusion processes as discussed in Chapter 2 with the outcomes of Task 6.1.2 [Schröder et al., 2016a, Schröder et al., 2016b] and Task 6.1.4 [Durce et al., 2016]. Hence, the term 'migration' is used for the integrated approach proposed in this chapter.

Current modelling approaches are evaluated with respect to their applicability. Based on the above, a phenomenological instead of mechanistic modelling approach is recommended.

To this end, the overall observed D_{eff} must be split up into (assumed) individual contributions of different physical migration and electrochemical sorption processes. The present Task 6.1.3 concentrates on the physical processes (so, all processes apart from R, determined by electrochemical sorption processes). This makes it possible to evaluate the potential effects of different conditions in the Netherlands, and come up with adapted values of physical migration parameters. These values can afterwards again be combined with R into new summarized D_{eff} values that are relevant for Dutch conditions. The electrochemical interactions, or R values, allowing evaluating the effect of chemical conditions are investigated separately in Task 6.1.2.

5.2. Processes influencing the radionuclide transport in porous media

The main processes influencing the radionuclide transport in porous media are:

- chemical speciation (distribution of elements over different chemical forms);
- diffusion;
- sorption;
- anion exclusion;
- surface diffusion (cation diffusion);
- presence and mobility of colloids.

Sorption and the presence and mobility of the colloids are investigated in WP 6.1.2 and 6.1.4 of the RANMIG project. The remaining processes will form the object of the present study. The results of the investigations will be combined to serve at the end as input for the WP7.

5.3. Definition of required parameters

Four phenomenological migration parameters that describe the migration of radionuclides within the Boom Clay formation can be identified [Bruggeman et al, 2010, p3]:

1. The concentration/solubility limit which represents the maximum concentration of a nuclide present in the aqueous phase under undisturbed conditions,
2. The retardation factor which represents the uptake of a nuclide by the inorganic and organic phases (minerals, kerogen, etc.) present in the Boom Clay formation,
3. The diffusion accessible porosity which is the total physical space available for transport of a nuclide, and
4. The diffusion coefficient (the pore diffusion coefficient, D_{pore}, or the effective diffusion coefficient $D_{eff,}$ their values are interrelated).

The chemical interactions of radionuclides within the Boom Clay formation are described by the solubility limit and retardation and form the subject of WP6.1.2 ([Schröder et al., 2016a] and [Schröder et al., 2016b]) and WP6.1.4 [Durce et al., 2016] (see Figure **5-1**).

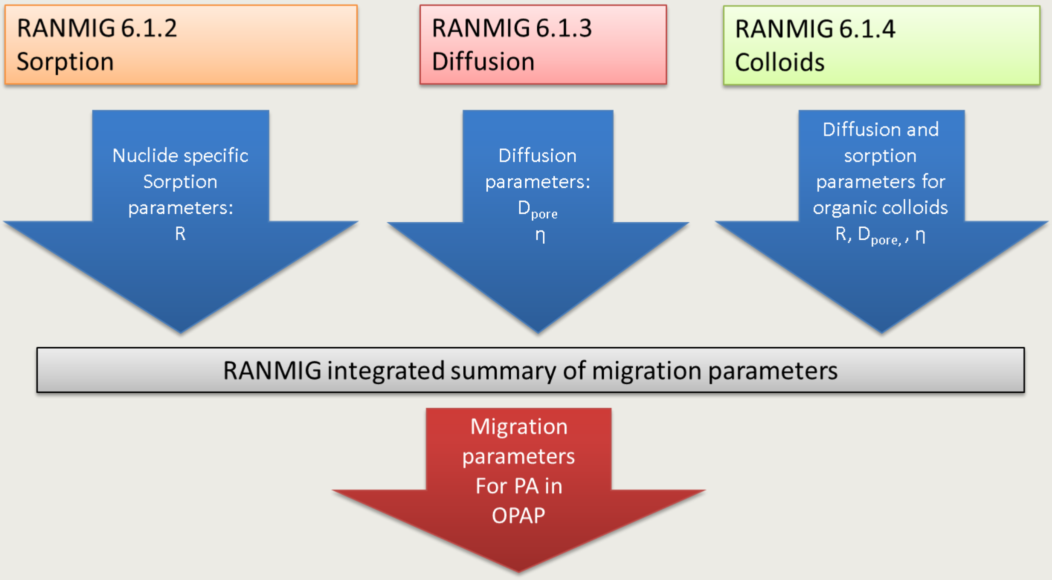

Figure 5-1 Schematic representation of the overall approach and interaction with other tasks

The diffusion accessible porosity and the diffusion coefficients are of physical nature and are subject of the work presented here. Together these factors determine the physical part of the mobility of radionuclides, so the part that is independent of the chemical properties. The combination of chemical and physical factors covers the complete mobility of the radionuclides.

In summary, the combination of physical factors that regulate the migration of radionuclides is represented by the equation:

$$D_{eff} = \eta D_{pore} = \eta \frac{\delta}{\theta^2} D_0$$

with:

D_{pore} - pore water coefficient (or bulk diffusion coefficient) accounting for the effects of tortuosity [m^2/s],
D_0 - diffusion coefficient in free water [m^2/s],
θ^2 - tortuosity factor [-],
δ - constrictivity factor [-],
η - diffusion accessible porosity [-].

In this work package values for the pore-diffusion coefficients (D_{pore}) and diffusion accessible porosity (η) will be provided for each radionuclide considered in the safety assessment. For the elements that are strongly bound to colloidal particles, the diffusion of the colloidal particles will be considered. The significance of this process depends on the amount, mobility and reactivity of the colloidal particles, which is the subject of WP 6.1.4. Therefore, some preliminary results of the WP6.1.4 are used in the present work.

5.4. Radionuclides and phenomenological groups to be considered

The complete list of radionuclides based on the inventories given in in [Hart, 2014, Table 6-1, p.36-38] and [Verhoef et al., 2016] contains 69 radionuclides distributed over 42 elements. All these radionuclides will be considered in the PA model and subsequent PA calculations.

Because of the similarities in reactive (chemical) and migration behaviour between different nuclides, different phenomenological groups of nuclides with the same migration parameters can be considered. A similar approach is used in the Belgian programme.

Ranges of values for the migration parameters will be provided for each phenomenological group. These parameter values will be assigned to each radionuclide belonging to a particular group. For this, the radionuclide classification approach currently followed in the Belgian programme on geological waste disposal will be followed (see Section 3.1). In this approach the safety-relevant radionuclides are grouped according to their similarities in chemical behaviour (speciation, sorption, transport) under Boom Clay reference conditions in following four groups:

- neutral species;
- anionic radionuclide species;
- cationic radionuclides;
- radionuclides that can form complexes with natural organic matter.

Within the last group three sub-groups with different radionuclide behaviour are identified in the Belgian programme: the heavy metals, the trivalent lanthanides/actinides and the tetravalent lanthanides/actinides. The transport behaviour of the radionuclides in these groups is determined by radionuclide affinity for DOM colloids (see Section 3.2).

For the purpose of this work, the radionuclide classification approach currently followed in the Belgian programme on geological waste disposal will be followed. The distribution of radionuclides over different groups will be assessed again at a later stage based the outcomes of chemical interaction calculations carried out within Task 6.1.2. In case the results from that task will indicate that the dominant chemical form or the interactions between certain nuclides and organic matter differ from what is assumed here, the radionuclides in question will be reattributed to the corresponding group.

The radionuclides that are not considered in the Belgian programme but present in OPERA-inventory are: Si-32, Ar-39, K-40, Ti-44, Kr-81, Kr-85, Ba-133, Pb-202, Pb-210, Cd-113m, Eu-152, Ho-166m, Bi-207, Po-209, Re-187, Cf-249.

Considering their neutral properties the radionuclides Kr-81, Kr-85, Ar-39 will be assigned to the first group, comprising also the conservative tracer HTO.

Speciation calculations show that under soil solution conditions Si is present in the form of $H4SiO_4$, so probably will behave as neutral species and therefore Si-32 will be attributed to the first group.

The radionuclides K-40, Ba-133 are present in solution in cationic form and manifest no interaction with the dissolved organic matter and therefore will be assigned to the group containing cationic radionuclides.

The transition metals Ti (Ti-44), Pb (Pb-202, Pb-210), Cd (Cd-113m) are attributed to the group of NOM linked radionuclides, sub-group ‘Transition metals’ and the trivalent lanthanides and actinides - Eu (Eu-152), Ho (Ho-166m), Cf (Cf-249), Pm (Pm-145) - are correspondingly attributed to the sub-group Trivalent Ln/Ac.

There are no thermodynamic and chemical data on Bi, Po and Re in the standard databases so it is difficult to estimate the form in which they might occur. For these radionuclides the most conservative migration parameters will be assumed.

The grouping of the radionuclides found to be relevant for the long-term safety and considered in the OPERA program is summarized in Table 5-1.

Table 5-1 Assignment of the radionuclides to different groups based on the considered phenomenological model

Group	Nuclide
Neutral	**HTO (H-3)** , Kr (Kr-81, Kr-85), Ar (Ar-39), Si (Si-32)
Anions	**monovalent**: I (I-129), Cl (Cl-36), Se (monovalent Se-79), Nb (Nb-93m, Nb-94), C (C-14) **divalent: Se (**divalent Se-79), Mo (Mo-93)
Cations	**monovalent: Cs (**Cs-135, Cs-137), K (K-40), **bivalent: Ca (**Ca-41), Sr (Sr-90), Ba (Ba-133), Ra (Ra-226)
NOM linked radionuclides	**NOM** **Transition metals:** Tc (Tc-99), Ag (Ag-108m), Be (Be-10), Ni (Ni-59, Ni-63), Pd (Pd-107), Zr (Zr-93), Sn (Sn-121m, Sn-126), Ti (Ti-44), Pb (Pb-202, Pb-210), Cd (Cd-113m) **Trivalent Ln/Ac:** Am (Am-241, Am-242m, Am-243), Ac (Ac-227), Cm (Cm-243, Cm-244, Cm-245, Cm-246, Cm-247, Cm-248), Sm (Sm-146, Sm-147, Sm-151), Pu (Pu-238, Pu-239, Pu-240, Pu-241, Pu-242, Pu-244), Eu (Eu-152), Ho (Ho-166m), Cf (Cf-249), Pm (Pm-145) **Tetravalent Ln/Ac:** U (U-232, U-233, U-234, U-235, U-236, U-238), Th (Th-229, Th-230, Th-232), Np (Np-237), Pa (Pa-231)

6. Migration parameters and model

The current developments/approaches in diffusion modelling (Chapter 2) were analysed by NRG and SCK·CEN with regard to their relevance for overall diffusion of radionuclides in Boom Clay (section 5.1). Based on the processes discussed in the Tasks 6.1.1 and 6.1.3 and the physical transport processes discussed in Chapter 2 a mathematical model is established (Section 6.1) and implemented numerically by NRG (Section 6.2). In Section 6.3 the related migration parameters are derived . In Section 6.4 the parameter values are summarized in a database of migration parameters. Particular attention has been paid to translating the data provided by SCK·CEN to the specific conditions expected in the Netherlands.

6.1.Mathematical model

Migration of nuclides from the waste compartment through the Boom Clay layer can be approximated by assuming a one dimensional diffusion process, where all waste is assumed to be located in a plane in the centre of the clay layer. This one dimensional approximation implicitly assumes that there is no horizontal concentration gradient and represents a worst case in terms of calculated nuclide concentrations at a certain distance from the source at any moment in time. The one dimensional approach does not require a specific spatial layout or selected site, is relatively easy to couple with transport and chemical reaction models and is much less computing time intensive than a two- or three-dimensional alternative would be.

In one-dimensional geometry, the diffusive flux of dissolved species through a horizontal plane will be calculated using Fick's first law:

$$J = -\eta A\ G\ D_0 \frac{dC}{dx}$$

With:

J - diffusive mass flux through a horizontal plane [mol/s],
D_0 - diffusion coefficient or diffusivity of the solute in free water or 'free-solution' diffusion coefficient (in absence of porous medium) [m^2/s],
η - total porosity [-],
A - horizontal plane area [m^2],
G - geometry factor accounting for the pore structure (i.e. tortuosity, constrictivity), [-]
C - aqueous phase concentration of the solute [mol/m^3],
x - distance in the direction of transport [m].

In this equation the dissolved concentrations are used as input. It is also convenient to calculate these fluxes based on total concentrations. To be able to do so an extra factor 1/R is required in the equation.

$$J = -\eta\ A\ G\ D_0\ \frac{1}{R}\frac{dC_{tot}}{dx}$$

This retardation factor (R) can be used when adsorption is assumed to be a linear process.

Assuming no advective transport, no presence of a gas phase/two phase flow and an indirect approach to address the presence of soluble colloids, for reactive behaviour of the dissolved radionuclides summarized into an effective retardation process, the diffusion equation takes the form:

$$\frac{\partial C}{\partial t} = G\frac{D_0}{R}\frac{\partial^2 C}{\partial x^2} - \lambda C + \lambda_p \frac{R_p}{R} C_p$$

where:
R - retention or retardation factor [-],
λ - radioactive decay constant [s^{-1}],
λ_p - radioactive decay constant of the parent nuclide [s^{-1}],
R_p - retention or retardation factor of the parent nuclide [-],
C_p - aqueous phase concentration of the parent nuclide [mol/m^3].

6.2. Model implementation

The mathematical model described above was implemented within the ORCHESTRA modelling framework [Meeussen, 2003]. The ORCHESTRA platform was chosen because it allows setting up all the necessary features and processes in order to perform the analyses and offers a high flexibility in anticipation of the (yet unknown) outcome of WP6.1. The ORCHESTRA platform allows combining the external water flow models with state-of-the-art detailed chemistry and mass transport models, and also allows using simplified alternative models for the PA calculations in WP7. Furthermore, ORCHESTRA is computationally very efficient and flexible in defining input parameters. Both are essential properties for performing the uncertainty analysis within OPERA.

The numerical representation of the mathematical model applies the explicit finite difference method – i.e. forward in time, central in space – and models the clay layer as a series of 50 mixed cells. Each of these cells contains a set of chemical physical state variables that summarize the average chemical conditions in that mixed volume in terms of physical parameters and nuclide concentrations present.

Examples of these state variables are:

- each cell *n* has a geometric factor $tortuosity_n$,
- for *k* elements X_k, a diffusion coefficient D_k is defined, and
- for each element and cell a porosity factor $porosity_{n,k}$ are defined.

Using discrete time steps the model calculates nuclide concentrations in each of these cells and nuclide fluxes in and out of these cells as a function of time.

At each of these time steps the following calculations are carried out:

- calculation (potentially time dependent) of feed and sink concentrations,
- calculation of net solid-solution partitioning for each of the nuclides in each of the cells,
- the calculated dissolved concentrations from the previous step is used to calculate the diffusion flux for each nuclide between cells,
- calculation of the nuclide mass change rates as a result of radioactive decay in each cell,
- update of the masses in the cells using the combined dmass/dt from the diffusion and decay processes.

Calculation of feed and sink concentrations

The first cell of the Boom Clay representation is linked to a source term. This term can be either defined as a fixed nuclide concentration, or a given total amount in a given volume. It is also possible to give an explicit expression for time dependent release rates for nuclides. The upper part of the Clay layer is linked to the aquifer system where migration by convection takes place. Effective diffusion fluxes out of the clay system are determined by concentration gradients between the last (uppermost) cell of the clay layer and the first (lowest) cell of the connected aquifer system.

Calculation of solid-solution partitioning

In this calculation the total amount of nuclide is used as input, and distribution over the mobile and immobile forms is calculated based on retardation coefficients for each element.

The retardation coefficients are determined through separate speciation calculations based on complete sets of thermodynamic reactions for the aqueous, adsorbed, colloids and precipitated species.

In principle it is possible to use the complete set of thermodynamic reactions in this module, but for the PA calculations within OPERA these reactions are summarized by a single linear adsorption reaction for each nuclide that describes the adsorption according to the R/K_d approach.

Based on the outcome of OPERA Task 6.1.2, the K_d-approach is followed, with:

$$X_{k\_ads} = K_{d,k} * X_{k\_diss}$$

with:

X_{k_ads}	- total concentration in the adsorbed phase (mol/kg) of the element *k*,
X_{k_diss}	- total concentration (of all species) of the element *k* in solution (mol/l),
$K_{d,k}$	- adsorption constant for each element *k [l/kg]*.

The retardation factor R is calculated by dividing the adsorption constant K_d by the liquid solid ratio (LS):

$$R_{n,k} = 1+K_{d,n,k}*(1/LS_n)$$

The liquid solid ratio is calculated for each cell *n* by:

$$LS_n = porosity_n/(density_n-(porosity_n * density_n))$$

with:

LS_n	- liquid solid ratio (kg/volume of dissolved phase) in the cell *n* [-],
$density_n$	- solid material density for each cell *n* (kg/l),
$porosity_n$	- the porosity of each cell *n* [-].

Calculation of diffusion flux between cells

First, the (dissolved) concentration gradient between cell *n* and cell *n+1* is computed according to:

$$dc_{n,k}dx_{n,k} = (X_{n+1,k\_diss} - X_{n,k\_diss})/((x_{n+1-}-x_n)*tortuosity_n)$$

with:

$dc_{n,k}\ dx_{n,k}$	- dissolved concentration gradient for the element k in the cell n [mol/l/m]
x_n	- cell position [m]
$tortuosity_n$	- tortuosity [-]

The fluxes are computed according to:

$J_{k,n} = -D_{k,n} * dcdx_{k,n} * (porosity_{k,n}) / (tortuosity_{n})$

with:
$J_{k,n}$ - flux [mol/s]
$D_{k,n}$ - diffusion coefficient in free water [m^2s^{-1}]

Calculation of radioactive decay in cells
In the last step, the mass changes for each nuclide as a result of radioactive decay and or ingrowth in each cell are calculated according to:

$dXdt_{n,k} = X_{n,k\_tot} * ln(2) / T_{1/2,k}$

with:
$dXdt_{k,n}$ - *mass change of element k as a result of radioactive decay/ingrowth* [mol/s]
X_{n,k_tot} - the total amount of an element *k* in a cell n: $X_{n,k\_tot} = X_{n,k\_ads} + X_{n,k\_diss}$ (mol)
$T_{1/2,k}$ - the half-life of the element *k* [s_s^{-1}]

It is also possible to provide decay reactions complete with formed daughter products. In that case the calculated mass fluxes are multiplied with the yield and added to the daughter nuclides.

D_{mass} daughter = $-d_{mass}$ mother * yieldfactor

In this way ingrowth of daughter nuclides is take into account, including the accompanying changes in chemical, migration and radioactive behaviour.

Note that all mass changes resulting from dynamic processes such as transport and decay processes are summed to a single value over-all per element per cell.

Calculation of mass update in cells
In final last step, which is performed after all mass fluxes by transport and decay/ingrowth processes are calculated, the amounts of all elements are updated for each time step *dt* in each cell:

$X_{n,k\_tot} = X_{n,k\_tot} - dXdt_{n,k} * dt$

The accuracy of the numerical solution, as applied within ORCHESTRA, is treated in more detail in [Grupa et al, 2015, p.21-22].The numerical results for a system with a point source in an infinite medium were compared with an analytical solution for the same system. The results showed that the numerical ORCHESTRA results agree very well with the analytical solution. Although careful observation shows that there are small differences in initial breakthrough times, these do not affect height and time of maximum concentrations.

6.3.Derivation of migration parameters

The influence of factors such as temperature, anisotropy, compaction and/or confinement pressure, pore water chemistry, up-scaling from laboratory to in situ measurements, spatial variability and near-field effects on the migration parameters was extensively studied within the Belgian programme and reported in the topical reports on the representative elements of each radionuclide group [Bruggeman et al., 2013, Bruggeman et al., 2010a, Bruggeman et al., 2010d, Bruggeman et al., 2012b, Canniere et al., 2010; Maes et al. 2011b, 2012, Salah et al., 2015]. The processes/phenomena having significant effect on the radionuclide migration were determined for each representative element. Each of these processes/phenomena will be assessed and (if possible) the values for the migration parameters will be adapted to the conditions expected in the Netherlands.

The main differences between the Dutch and Belgian cases are caused by the depth of the repository. The Dutch reference concept considers a repository situated at a depth of minimum 500 m, more than two times deeper than in the Belgian concept. The Boom Clay at a greater depth will have a higher degree of compaction which will most probably result in a decrease of the total porosity, the pore sizes and throat widths.Towards the North where Boom Clay is buried deeper, the pore water chemistry changes to a sea-water type with a higher ionic strength and salinity which will influence the extent of the diffuse double layer and the transport parameters of both anions and cations. Because of a higher depth the temperature of the host rock will be higher than in the Belgian concept. For the average value of the geothermal gradient of 25 ºC per kilometer of depth the difference in depth will be responsible for an increase of temperatures with a minimum of 25*(0.50-0.22)=7 ºC resulting in a temperature of 23 ºC at 500 m depth.

In the following each of these differences will be assessed and (where possible) the values for the migration parameters established for the Boom Clay at the Mol site will be adapted to the conditions expected in the Netherlands. The estimation of parameters values is based on the general consideration on the transferability given in Section 3.5. Belgian data ranges serve as starting point.

6.3.1. Diffusion accessible porosity

With respect to the diffusion accessible porosity, four types of nuclides will be considered, equivalent to the four phenomenological groups having the same migration parameters (see Section 5.4):

- Neutral species
- Anions
- Cationic species
- Dissolved organic matter (DOM) and organic matter associated nuclides

The nuclides belonging to the first group will distribute themselves over the entire pore volume accessible for diffusion. The porosity range for the conservative reference tracer HTO will be assumed to be the same for all other neutral and cationic species.

The anions are repulsed by the negatively charged solid matrix of the clay and cannot penetrate the double layer covering the charged clay plates. Only part of the pore space is therefore accessible for anion diffusion, lower diffusion accessible porosity than the neutral species. The diffusion accessible range for iodine does not necessarily apply for other anions, because the effect of the charge repulsion may be dependent on the nature of the anion. Anions with double negative charge will manifest even lower diffusion accessible porosities. The SO_4^{2-} ion will serve as reference ion for the group of anions with double negative charge.

Because of the similarities between the diffusion accessible porosity for negatively-charged colloids and negatively-charged anions, the value ranges for accessible porosity for dissolved organic matter (OM) and OM associated nuclides is judged to correspond to the diffusion accessible porosity for anions: the upper limit will be taken equal to the diffusion accessible porosity estimated for iodide, and the lower limit will be taken equal to that of divalent anions.

Neutral and cationic species

The retention and migration behavior of tritiated water in Boom Clay was extensively studied within the Belgian program on geological disposal of radioactive waste. The most up to date understanding and data on tritiated water transport in the Boom Clay are reported in [Bruggeman et al., 2013].

The effect of following factors on the diffusion accessible porosity of HTO was analyzed:

- Anisotropy
- Compaction and consolidation pressure
- Pore water chemistry
- Upscaling from *lab* to *in situ*
- Spatial variability over the entire formation
- Near-field effect

The **anisotropy** was found to have no effect on the diffusion accessible porosity [Bruggeman et al., 2013, p.41]. The **consolidation pressure** was found to have a limited influence on the diffusion accessible porosity of the HTO. The diffusion accessible porosity for HTO was found to not be affected by the changing ionic strength conditions [Bruggeman et al., 2013, p.43-45] so the proposed values are judged to be applicable also for other pore water chemistry conditions. The upscaling from *lab* to *in situ* showed a very good agreement with the *in situ* experiments [Bruggeman et al., 2013, p.45], [Weetjens et al., 2014]. The spatial variability over the entire formation host rock formation, both vertically and horizontally was assessed and showed similar values for diffusion accessible porosity at a specific location. The conclusion was that the Boom Clay may be considered homogeneous with respect to vertical transport by diffusion [Bruggeman et al., 2013, p.47]. No significant spatial influence of the near-field on the value of the diffusion accessible porosity was established.

From the information above it is clear that the degree of compaction or the consolidation pressure of the formation has only a limited influence on the value of the diffusion accessible porosity for neutral species. On the other hand, the anisotropy, pore water chemistry, upscaling from lab to situ, spatial variability and the near field have no significant effect on this value.

The diffusion accessible porosity for Boom Clay at the Mol site is expected to lie between 0.34 and 0.40 with a best estimate value of 0.37 [Bruggeman et al., 2013, p.3]. This range covers the uncertainties related to upscaling and applies only to the Boom Clay formation located in the Mol-Dessel area. For other locations, another range is needed, mainly because of difference in the degree of compaction and pore water chemistry/mineralogy [Bruggeman et al., 2013, p.4].

The Boom Clay in the Netherlands contains 28-58 % clay (see Table 6-1).

Table 6-1 Regional average mineralogical composition of Boom Clay samples of the Netherlands as reported in [Koenen & Griffioen, 2014, Table 13]

region	*Total clay [%]*	*Kaolinite [%]*	*K-S [%]*	*Chlorite [%]*	*Smectite [%]*	*I-S [%]*	*Illite [%]*	*G-S [%]*
north	58.1	5.5	8.4	1.2	47.5	18.6	10.7	13.2
middle	41.9	7.2	7.4	1.3	37.6	25.3	15.2	13.3
south	28.4	4.8	3.4	1.6	36.8	36.2	17.2	0.0

The total porosity of Boom Clay can be calculated based on its clay content and using the equations for void ratio (see [Vis &Verweij, p.24-25]):

$e = e_{100} - \beta \ln[(\sigma_v - P_w)/100]$
$e = \theta/(1 - \theta)$

with:
e_{100} - void ratio at 100 kPa effective stress, $e_{100} = 0.3024+1.6867clay+1.9505clay^2$,
clay - clay content (fraction) [-],
β - β=0.0407 + 0.2479clay +0.3684clay^2,
e - void ratio [-],
θ - porosity (fraction) [-],
$\sigma_v - P_w$ - effective stress [kPa],
σ_v - vertical stress [kPa],
P_w - formation water pressure (kPa).

The effective stress, the vertical stress and the pore water pressure for 500 m depth are estimated from the following relationships (see [Vis &Verweij, p.25] for more detail):

$(\sigma_v - P_w) = 9.9*z$

$\sigma_v = 19.9*z$

$P_w = 10.0*z$

with:
z - depth [m TVDss]

Table 6-2 Calculated total porosity at 500 m depth based on a clay content of 28-58% [Koenen & Griffioen, 2014, Table 13] and using the formula for void ratio given in [Vis &Verweij, p.24-25].

z *[m]*	*clay content* *[-]*	*σv-Pw* *[kPa]*	*beta* *[-]*	*e100* *[-]*	*e* *[-]*	*total porosity* *[-]*
500	0.3	4950	0.15	0.98	0.41	0.29
500	0.6	4950	0.32	2.02	0.76	0.43

For 500 m depth the total porosity is between 0.29 and 0.43 (see Table 6-2 for total porosity calculations results). Only a part of the total porosity is available for radionuclide transport. The diffusion accessible porosity in porous media is considerable lower than the total porosity excluding the fraction of pores that are not interconnected and thus not-available for mass transport (dead-end pores). The quantification of the diffusion accessible porosity is not straightforward and is usually carried out by fitting experimental data to mathematical models.

There is a lack of diffusion accessible porosities estimated for Boom Clay for conditions characteristic to the OPERA reference concept. The experimental results with reconsolidated clay samples and bentonites show a general decreasing trend in the value of diffusion accessible porosity with increasing consolidation pressure ([Henrion et al., 1991], [Garcia-Gutierez et al., 2004]). For HTO the experimental results show a decrease from 0.36 at a consolidation pressure of 0.98 MPa to 0.25 at 6.85 MPa. The *in situ* effective stress corresponding to -224 m level in the formation where the HADES underground research laboratory at SCK·CEN is located, is about 2.4 MPa [Bruggeman et al., 2013, p.24]. The experimental results on the influence of compaction on the diffusion of non-sorbed species in reconsolidated clay samples [Henrion et al., 1991] show for HTO a diffusion accessible porosity of 0.14-0.24 for a consolidation pressure of 6.86 MPa and 0.24 for 4.41 MPa [Bruggeman et al., 2013, Table 6]. Based on the data for HTO given in [Henrion et al., 1991] and Table 6 in [Bruggeman et al., 2013] the following regression line is obtained (Figure 6-1): ηR=-0.0281*Pconsol [MPa]+0.3874.

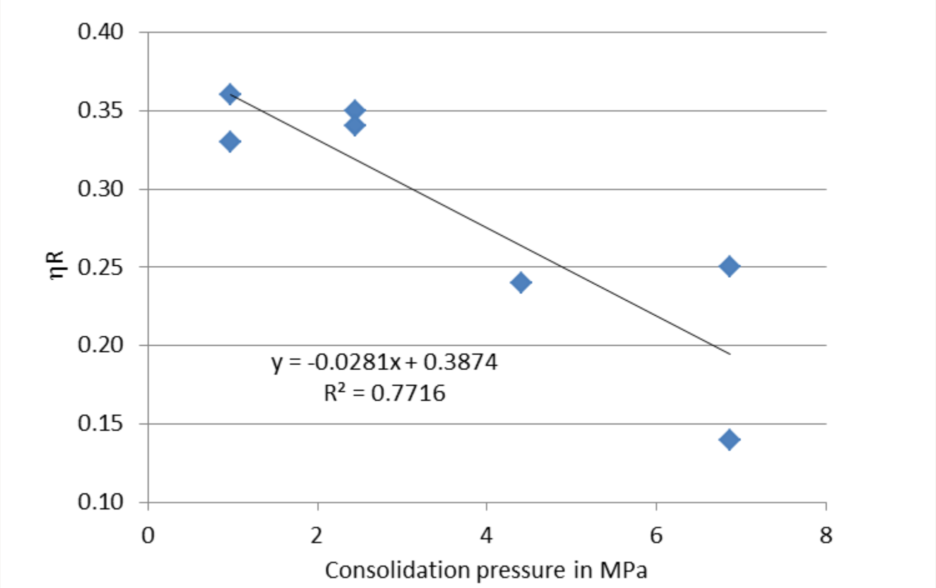

Figure 6-1 ηR measured in reconsolidated Boom clay pastes as a function of reconsolidation pressure (MPa) for HTO (data from [Henrion et al., 1991]).

In [Wisseal at al., 2016, p.11] reference pressure conditions for a Dutch Boom Clay repository were calculated based on a repository depth of 500 m, as well as for a shallower and deeper case (400 m and 600 m respectively), to allow for uncertainty in relation to burial history and glaciation [Wisseal at al., 2016, p.10]. For a depth range between 400-600 m, the likely value for total vertical stress was found to lie in the range of 8.0 to 11.9 MPa with a resulting estimated total vertical stress for a depth of 500 m of ≈ 10 MPa [Wisseal at al., 2016, Table 1-2]. Based on the hydrostatic pressure at this depth of 5 MPa the effective stress would lie between 3.0 and 6.9 MPa. Using the data for a consolidation pressure of 6.86 MPa reported in [Henrion et al., 1991] and the derived regression coefficient (Figure 6-1), at a depth of 500 m a diffusion accessible porosity of 0.14-0.36 can be expected. However, it should be noted that the samples in [Henrion et al., 1991] consisted of reconsolidated clay pastes, therefore the derived data should be regarded with conservatism when applying them to real systems.

The combination of the range established for the Mol location with the range estimated for an effective stress corresponding to 500 m depth results in diffusion accessible porosity range of 0.14-0.40 will be adopted for HTO in the Dutch situation. The chosen interval will be used for all the neutral and cationic species.

Anions

Iodine is considered as representative element for the radionuclide group of anionic species. The migration parameters for iodine were investigated by SCK·CEN and the results of these investigations are summarized and documented in [Bruggeman et al., 2010a]. The effect of following factors on the diffusion accessible porosity for iodine was analyzed:

- Upscaling from *lab* to *in situ*
- Spatial variability over the entire formation
- Ionic strength

- Compaction and consolidation pressure
- Anisotropy

The **ionic strength** was found to have a significant effect on the diffusion accessible porosity for anions [Bruggeman et al., 2010a, Section 5.1]: an increase in ionic strength would increase the diffusion accessible porosity. Another influential factor on the anion exclusion effect is the degree of compaction: the **degree of compaction** (or **the consolidation pressure**) was found to have an inverse effect on the diffusion accessible porosity. Also the pore structure would change, which might have an impact on the anisotropy. Large scale ***in-situ*** migration experiments with I^- showed an acceptable agreement with the laboratory data. The diffusion accessible porosity was found to be independent of **anisotropy**.

The effect of the ionic strength on the diffusion accessible porosity for anions will be taken into account by translating the change in the thickness of the diffuse double layer as function of the ionic strength into the change in the fraction of free pore water and thus a change of the diffusion accessible porosity.

The data for anion accessible porosity for the Boom Clay at the location Mol will serve as starting point. The main differences between the water chemistry at the location Mol and that for the Netherlands will be established. The thickness of diffuse double layer for Boom Clay in Mol and the Netherlands will be estimated. The change in the thickness of diffuse double layer will be translated into change of diffusion accessible porosity.

For Iodide the relationship is $\eta R=-0.011*P_{consol}[MPa]+0.128$ with $R^2=0.55$) (see Figure 6-2).

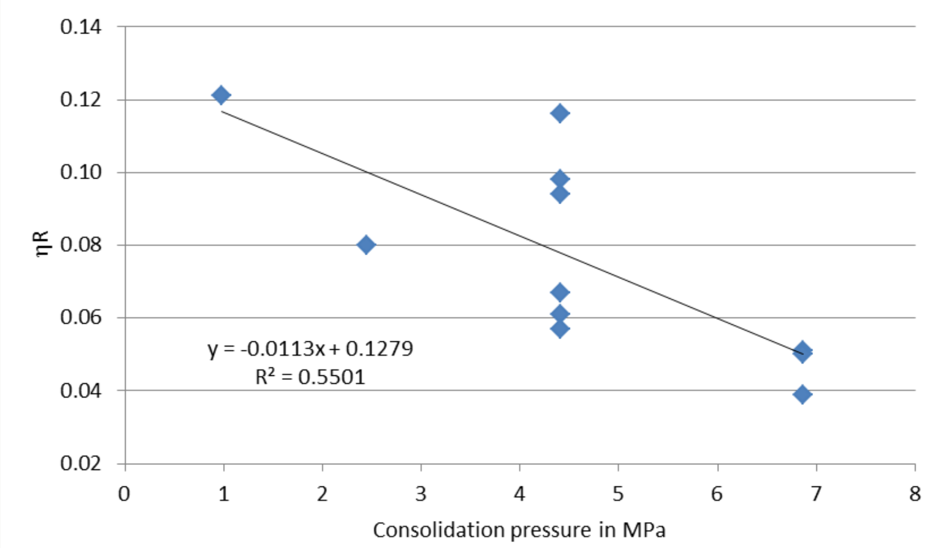

Figure 6-2 ηR measured in reconsolidated Boom clay pastes as a function of reconsolidation pressure (MPa) for I^- (data from [Henrion et al., 1991]).

Using the data of [Henrion et al., 1991] in Figure 6-2 and the expected range of effective stress at 500 m depth between 3.0 to 6.9 MPa, for the diffusion accessible porosity of I^- a range of 0.03 to 0.13 can be estimated. However, it should be noted that the samples in that study consisted of reconsolidated clay pastes and therefore should be regarded with conservatism when applying the results to real systems. Furthermore, the derived range would only apply for Mol type pore water.

The pore water chemistry of the Boom Clay in the Netherlands will differ from the water chemistry established for the Boom Clay at the Mol site. Table 6-3 and Table 6-4 summarize pore water properties as reported in [Behernd et al., 2015] and [Griffioen, 2015]. Please note that the low pH and high sulphate concentrations of samples 101 and 104 are most likely caused by exposure of samples to air and resulting oxidation. However, the measured salt (Na, Cl) concentrations in these samples are not affected and can still be used.

Table 6-3 Composition of pore water measured in Boom Clay samples from a location in the middle region as reported in [Behernd et al., 2015] (Table 4.1).

region	*sample name*	*depth*	*pH*	*Ca*	*Na*	*Cl*	*Mg*	*K*	*Fe*	*SO_4*
		[m]	**[-]**	**[mg/l]**	**[mg/l]**	**[mg/l]**	**[mg/l]**	**[mg/l]**	**[mg/l]**	**[mg/l]**
middle	**101**	73	3.17	2,421	5,451	14,464	1,028	407	41,6	5,472
	103	79	6.70	2,794	3,061	13,967	1,419	145	182	374
	104	76	3.05	1,884	10,189	19,356	1,256	623	16,6	6,240

Table 6-4 Regional average pore water composition above the Boom Clay as reported in [Griffioen, 2015] (Appendix 2).

region		*depth*	*pH*	*O_2*	*DOC*	*Ca*	*Na*	*Cl*	*Mg*	*K*	*Fe*	*Mn*	*SO_4*
		[m]	**[-]**	**[mg/l]**	**[mg/l]**	**[mg/l]**	**[mg/l]**	**[mg/l]**	**[mg/l]**	**[mg/l]**	**[mg/l]**	**[µg/l]**	**[mg/l]**
average	**north**	254.2	7.4	0.2	5.7	44	109	104	7.5	8.9	2.2	97	3.6
	middle	372.4	7.7	0.1	3.4	112	3324	5222	132	67	1.6	1678	157
	south	346.1	6.9	0.5	0.8	92	366	604	24	8.7	4.5	497	4.2
sd	**north**	46.9	0.5	0.1	6.3	30	97	81	3.4	8.3	2.7	71	7.7
	middle	80.2	0.3	0.1	0.5	113	2882	4652	115	28.4	1.2	1374	235
	south	72.1	0.4	0.4	0.4	47	1296	2218	44	20	2.4	462	2.1
rsd	**north**	18	7.1	78	111	67	89	78	46	93	123	73	215
	middle	22	4.2	72	16	100	87	89	87	43	75	82	150
	south	21	5.6	99	54	51	354	367	182	231	54	93	50

The maximum salinity corresponding to the regional average pore water composition above the Boom Clay (Table 6-4) varies from 0.02 M to 0.46 M. The salinity corresponding to the pore water of Boom Clay from a location in the middle region (Table 6-3) varies between 0.54 M and 0.83 M, the upper limit being much higher than the salinity of the sea water. The pH values for the samples 101 and 104 are below 4, which indicates that these samples are most likely significantly oxidized during storage and therefore not representative for the natural situation. This can also be seen in the very high concentration of SO_4^{2-}. For these reasons, the upper salinity limit will be chosen equal to the average salinity of sea water which is approximately 0.6 M.

For a solution with an ionic strength of 0.016, corresponding to the water composition at the Mol site, the extension of double layers at clay particle surfaces is estimated to be about ± 2.4 nm. For these conditions the anion accessible porosity is measured to be about half that of neutral species.
For Boom clay pore water conditions in the Netherlands, with estimated ionic strength levels up to 0.6 M, the calculated diffuse double layer thickness will be much thinner (± 0.40 nm) and the volume of the diffuse double layer will only be a small fraction of the total pore volume. As a result the anion exclusion zone will be small and the accessible porosity will thus be virtually the same as the effective porosity for neutral species (0.40).

The anion accessible porosities for anions with double negative charges were found to have lower values, e.g. in case of SO_4^{2-} the porosity calculated according to Archie's law would be ~0.05 (Canniere et al., 2010). Although it is expected that the diffusion accessible porosity of SO_4^{2-} will decrease further for a higher degree of compaction, there are no reported experimental studies that would allow an accurate quantification of this change. The diffusion accessible porosity of 0.05 as determined for SO_4^{2-} for the Boom Clay at the Mol site will therefore be adopted for the Dutch situation as well. The estimated range of the diffusion accessible porosities for anions with double negative charge can therefore be taken as starting from 0.05 up to 0.40 (the upper limit for HTO).

Cations

Similar to the approach adopted in the Belgian programme, the diffusion accessible porosity range determined for the conservative reference tracer HTO will be used for all cationic species as well (see Section 3.4.1).

Dissolved organic matter and organic matter associated nuclides

For dissolved OM the diffusion accessible porosity is estimated to range from 0.05 to 0.40 by the Belgian programme (see Section 3.4.2). Accurate values for the specific effect of tortuosity on the migration of colloidal organic matter particles are not available. However, measured migration rates are the result of a combination of molecular diffusion coefficient, tortuosity, retardation and accessible porosity.

Information on estimated binding will also follow from the sorption modelling in Task 6.1.2. In case the results from that task will indicate that interaction between certain nuclides and OM is less than assumed here, the migration properties of the dominant chemical form will be taken into account in the OPERA model.

6.3.2. Pore diffusion coefficient

Neutral species

The pore diffusion coefficient for HTO in Boom Clay at the Mol site is expected to lie between 2.0×10^{-10} and 2.6×10^{-10} $m^2 s^{-1}$ with a best estimate value of 2.3×10^{-10} [Bruggeman et al., 2013, p.3]. This range covers the related uncertainties and applies only to the Boom Clay formation located in the Mol-Dessel area. For other locations, another range is needed, mainly because of differences in pore water chemistry/mineralogy. Also an increase in temperature is expected to alter this range [Bruggeman et al., 2013 p.4].

The effect of following factors on the pore diffusion coefficient was analyzed:

- Temperature
- Anisotropy
- Compaction and consolidation pressure
- Pore water chemistry
- Upscaling from *lab* to *in situ*
- Spatial variability over the entire formation
- Near-field effect

The HTO diffusion coefficient in Boom Clay was found to be mainly influenced by the temperature and the anisotropy of the Boom Clay formation. The compaction pressure, pore water chemistry and near-field effects do not affect significantly the pore diffusion coefficient. The model predictions based on laboratory experiments were in very good agreement with a large scale in situ test. The Boom Clay formation showed also a very good homogeneity with respect to migration parameters [Bruggeman et al., 2013, p.37].

In the Belgian concept the Boom clay layer is situated at a depth of about 220 m while in the Dutch concept a depth of minimum 500 m is required. Because of a higher depth and thus a higher temperature of the host rock, the pore diffusion coefficient for HTO for Boom Clay in the Dutch conditions is expected to be higher than in the Belgian concept. For the average value of the geothermal gradient of 25 ºC per kilometer of depth the difference in depth will be responsible for an increase in temperature with a minimum of 25*(0.50-0.22) = 7 ºC resulting in a temperature of 23 ºC at 500 m depth. This temperature is in line with the initial conditions (295 K) used in the initial thermal assessment for the OPERA design carried out within WP3.1.1 and documented in [Arnold et al., 2014, p.253]. The thermal response as result of the disposal of heat-generating wastes showed an increase in temperature at the Boom Clay-tunnel lining interface as well as in clay self, the spent fuel having the highest thermal output. The peak temperatures would occur approximately 30 years after disposal and thereafter decline relatively fast (hundreds to thousands of years) making this temporary temperature increase negligible for migration calculations where time intervals of tens to hundreds of thousands of years are considered. The thermal response [see Arnold et al., 2014, Fig.8.4] declines also with increasing distance from the waste container so it can be assumed that the most part of the host rock will have a negligible thermal response (both in magnitude and duration) to the emplacement of heat-generating radioactive waste. The thermal response of the host rock will be therefore neglected when estimating the value of the diffusion coefficients.

The parameter ranges estimated in [Bruggeman et al., 2013] are based on laboratory experiments conducted at room temperature (25 ºC) [Bruggeman et al., 2013, p. 24] therefore no temperature-related correction of these estimates was used. For a repository situated at depths greater than 500 m, the temperature of the host rock will be higher, corresponding to an increase of about 2.5 ºC per 100 m depth. In that case a correction of the diffusion coefficients values would be necessary. For temperature ranges between 0 and 70 ºC the dependence of the effective diffusion coefficient on temperature was found to be of an Arrhenius type. The correction can therefore be carried out using the formula:

$$D_{T_2} = D_{T_1} e^{\frac{E_{a,wc}}{R}(\frac{1}{T_1} - \frac{1}{T2})}$$

with:
D_T - diffusion coefficient at a given temperature (m^2/s);
T - absolute temperature (K);
R - gas constant (8.31451 J mol^{-1} K^{-1});
$E_{a,wc}$ - activation energy (J mol^{-1}) for self-diffusion in confined water.

Each 100 m additional depth would lead to a host rock temperature increase of about 2.5 ºC corresponding to an increase of the diffusion coefficient value by approximately 10%. This increase is dependent on the activation energy of the diffusing particle: the higher the activation energy of the diffusing particle - the higher the increase of the diffusion coefficient value. To be able to determine this increase, data on its self-diffusion coefficient in confined water for each of the considered nuclides are needed.

Anisotropy was found to influence the migration parameters values in both confined and consolidated Boom Clay samples considerably [Bruggeman et al., 2013, p.22-24], [Moors, 2005]. For HTO diffusion parallel to the stratification of the formation the pore diffusion coefficient was found to be two to three times higher than for diffusion perpendicular to the stratification. Only in the case of highly consolidated clay rocks (e.g. Opalinus clay (OPA)), the anisotropy increases beyond 3. For the Boom Clay conditions in the Netherlands it will probably not come to this highly consolidated state. So, the anisotropy range will not be dramatically influenced.

Results of experimental studies on the influence of compaction on the diffusivities show that increasing pressure results in a generally small decrease of diffusion coefficient values [Henrion et al., 1991], [Van Loon et al., 2003a], [Van Loon et al., 2003b]. Experiments with reconsolidated clay pastes [Henrion et al., 1991] show a decrease of the pore diffusion coefficient of HTO by ~15 % when consolidation pressure increases from 2.4 MPa to 4.4 MPa and a further decrease of 0-40 % when consolidation pressure increases from 4.4 MPa to 6.9 MPa (see [Bruggeman et al., 2013, Table 6]). Experimental results on highly consolidated clays [Van Loon et al., 2003a], [Van Loon et al., 2003b] show also a decrease of the pore diffusion coefficient of HTO by ~17 % when increasing the pressure from 1 to 5 MPa [Van Loon et al., 2003a] and a decrease of ~20% for an increase in pressure from 4 to 15 MPa [Van Loon et al., 2003b].

For the Dutch situation a decrease of the pore diffusion coefficient in comparison with the pore diffusion coefficients determined for the Mol site could be expected. This decrease is small and for conservative reasons, but also because of the lack of migration data on the Boom Clay in The Netherlands, will not be taken into consideration in this study.

The pore diffusion coefficient for HTO in Boom Clay at the Mol site (between 2.0 10^{-10} and 2.6 10^{-10} m^2s^{-1}, see [Bruggeman et al., 2013, p.3]) can be therefore adopted for HTO also in the Dutch situation.

Anions

The value ranges of the pore diffusion coefficient for iodine determined for the Boom Clay at the Mol site are between 1.2 10^{-10} and 1.6 10^{-10} m^2 s^{-1} (see Section 3.4.1).

In [Bruggeman et al., 2010a] the effect of following factors on the pore diffusion coefficient for iodine were analyzed:

- Temperature
- Anisotropy
- Compaction and consolidation pressure
- Pore water chemistry (Ionic strength, major cations)
- Iodine speciation
- Upscaling from *lab* to *in situ*
- Spatial variability over the entire formation

In case of iodine which manifests no retardation the apparent diffusion coefficient is equal to the pore diffusion coefficient. It was observed that the degree of compaction has a large influence on the value of the pore diffusion coefficient and that the anisotropy factor, that is partly related to the degree of compaction, amounts to 2-3 in the case of the Boom Clay at the Mol site. The pore water chemistry was found to have no significant effects on the pore diffusion coefficient. Large scale in-situ migration experiments for iodide diffusion did show acceptable agreement with the laboratory data.

The values determined for the Boom Clay at Mol site are given for room temperature (25 ºC). Temperature related correction of the diffusion coefficients values for iodine is therefore not necessary. For greater depths the temperature of the host rock will be higher than 25 ºC therefore a correction of the diffusion coefficients values would be needed (see previous section).

Many literature sources [Henrion et al., 1991; De Preter et al., 1992; Oscarson et al., 1992]) show that the value of the diffusion coefficients of anionic species depend on the consolidation pressure of both Boom clay or pure clay samples. The D_{app} for I^- as function of the consolidation pressure can be estimated using the regression equation for D_{app} given in

[Bruggeman et al., 2010a, p. 40] which is based on the data from [De Preter et al., 1992] and Henrion et al., 1991]:

Log D_{app} (m^2s^{-1}) = -0.038·P_{consol}(MPa) - 9.53

The apparent diffusion coefficient for I^- at in-situ pressure corresponding to 400-600 m depth (total vertical stress of 8.0-11.9 MPa, corresponding to an effective stress / consolidation pressure range of 3.0-6.9 MPa) is according to this regression equal to 1.6 10^{-10}-2.3 10^{-10} m^2s^{-1} at 6.9 and 3.0 MPa, respectively. It should be noted that the samples in that study consisted of reconsolidated clay pastes and therefore should be regarded with conservatism when applying the results to real systems. The overview of iodide migration experiments performed on Boom Clay given in Table 4-1 in [Bruggeman et al., 2010a] shows that the migration experiments on clay samples cored perpendicular to the stratification result in D_{app} values lower than the ones performed on clay pastes. The experiments on clay pastes and clay cores reported in [De Preter et al., 1992] result in D_{app} for samples clay samples cored perpendicular to the stratification 33-37 % lower than a D_{app} for clay paste. Assuming that this difference factor is valid for the entire range of the considered consolidation pressure range, this leads to an expected apparent diffusion coefficient range of 1.0 10^{-10} - 1.5 10^{-10} m^2s^{-1}.

The combination of the range established for the Mol location with the range estimated for an effective stress corresponding to the depth considered in the Dutch reference concept results in a pore diffusion coefficient range for I^- of 1.0 10^{-10}-1.6 10^{-10} m^2/s that will be adopted for anions in the Dutch situation.

To estimate the ranges for other monovalent anions the same migration path as that of I^- will be assumed, the tracers will be considered as conservative and the ranges will be scaled based on the difference in D_0 value. The D_o for $Nb(OH)_6(-)$ is not known so a diffusion coefficient equal to that of $HSO_4(-)$ will be adopted.

HCO_3^- does not act as a conservative tracer. The D_{app} ranges were deduced in the Belgian study by statistical analysis of migration data resulting in an apparent diffusion coefficient of 3.0 10^{-11} m²/s < D_{app} < 1.0 10^{-10} m²/s with a retardation factor R ~ 1.6-2. The resulting pore diffusion coefficient (D_p=D_{app}/R) is 1.5 10^{-11}-1.0 10^{-10} m^2/s. Although it is expected that the pore diffusion coefficient will decrease with increasing depth and pressure, there are no data to quantify this effect. The same D_p range will be adopted for the Dutch situation although it has to be kept in mind that these values are conservative.

For all divalent anions, migration data for SO_4^{2-} will be taken as a reference. The values of the diffusion coefficient of ions in pure water (D_o) were compared in [Canniere et al., 2010, p.56] for iodide and sulfate (see table below). A factor < 2 is observed between the aqueous diffusion coefficients (D_o) of iodide (monovalent monoatomic ion) and of sulfate (divalent oxyanion) in water. Since D_p depends on D_o, so a factor of 2 could be invoked for scaling the D_p range for SO_4^{2-}. The D_p ranges for other divalent anions (SeO_4^{2-}, MoO_4^{2-}) are taken equal to those of SO_4^{2-} (D_0 scaling is implicitly taken into account: D_0 values for SO_4^{2-} and SeO_4^{2-} are equal, but the D_0 value for MoO_4^{2-} is not known to the authors).

Table 6-5 Pore diffusion coefficients for monovalent non-retarded anionic species estimated for the Boom Clay in the Netherlands.

	D_o [m^2s^{-1}]	D_{pore} [m^2s^{-1}]
I(-)	2.06 10^{-9} [Canniere et al., 2010, p.56]	1.0 10^{-10} - 1.6 10^{-10}
Cl(-)	2.03 10^{-9} [Appelo et al., 2009]	1.0 10^{-10} - 1.6 10^{-10}
HSe(-)	1.73 10^{-9} [Canniere et al., 2010, p.59]	8.4 10^{-11} - 1.3 10^{-10}
$Nb(OH)_6(-)$	-	6.7 10^{-11} - 1.1 10^{-10}
$HSO_4(-)$	1.37 10^{-9} [Canniere et al., 2010, p.56]	6.7 10^{-11} - 1.1 10^{-10}

HCO_3(-)	1.20 10^{-9} [Li & Gregory, 1974]	1.5 10^{-11} - 1.0 10^{-10}
SO_4(2-)	1.07 10^{-9} [Canniere et al., 2010, p.56]	5.0 10^{-11} - 8.0 10^{-11}
SeO4(2-)	1.07 10_{-9}	5.0 10^{-11} - 8.0 10^{-11}
MoO4(2-)	-	5.0 10^{-11} - 8.0 10^{-11}

Cations

A quantification of the magnitude of the changes in effective diffusion coefficient of cations as function of changes in ionic strength and in compaction pressure is difficult to make which makes it difficult to extrapolate the values of D_{pore} obtained under Mol conditions to other locations. The values of D_{pore} obtained under Mol conditions may be used as upper estimates for cation pore diffusion coefficients at other locations. Combination of D_{pore} values with calculated retardation factors, R, obtained from static batch sorption tests, and the diffusion accessible porosity, η, can then be used to obtain estimates for the apparent diffusion coefficient, D_{app}.

Based on the value rages for D_{app} (1.0 10^{-13}-1.8 10^{-13} m^2s^{-1}) and R (2750-85000) established for Cs(+) in [Maes et al., 2011b, p.8] a range for D_{pore} of 8.5 10^{-9} to 4.95 10^{-10} m^2s^{-1} can be established for Cs(+) ($LL(D_p)=UL(D_{a)}*LL(R)$, $UL(D_p)=LL(D_a)*LL(R)$. The ranges for other cations are scaled based on the difference in D_0 value. This range valid for when considering the surface cation diffusion but does not consider the decrease of the diffusion coefficient at higher compaction pressure.

Table 6-6 Diffusion coefficients based on the Data on Boom Clay at Mol location considering surface diffusion.

	D_o [m^2s^{-1}]	D_{pore} [m^2s^{-1}]	
		min	max
Cs (+)	2.05 10^{-9} [Maes et al., 2011b, p.61]	5.0 10^{-10}	8.5 10^{-09}
K (+)	1.96 10^{-9} [Appelo et al., 2009]	4.7 10^{-10}	8.1 10^{-09}
Sr (2+)	7.94 10^{-10} [Appelo et al., 2009]	1.9 10^{-10}	3.3 10^{-10}
Ca (2+)	7.94 10^{-10} [Appelo et al., 2009]	1.9 10^{-10}	3.3 10^{-10}
Ba (2+)	-	1.9 10^{-10}	3.3 10^{-10}
Ra (2+)	7.5 10^{-10} [Van Loon, 2014, Tab.20]	1.8 10^{-10}	3.1 10^{-10}

It is known that the relative importance of double layer diffusion decreases as the ionic strength increases. Experimental studies show that the surface diffusion of cations decreases at high ionic strength ([Van Loon, 2014, p.36-37], [Altmann et al., 2014]) so at high salinities the surface diffusion of cations can be neglected and the pore diffusion coefficient in combination with retardation factors (D_pR) can be used in transport calculations. When the surface diffusion of cations is not considered the pore diffusion coefficient can be determined based on the geometric factor (or tortuosity) and the diffusion coefficient in water (D_o): $D_{pore}=D_o*G$.

A general slowly decreasing trend of the geometrical factor with increasing compaction pressure was reported in [Henrion et al., 1991.The samples in that study consisted of reconsolidated clay pastes and therefore should be regarded with conservatism when applying the results to real systems.

Geometrical factor (G) or tortuosity (δ/θ^2) is the effect when the average length of the diffusion route in porous media is longer than the shortest straight line, because ions have to travel through pores around solid particles. So effectively the length of the diffusion route through a porous medium is a factor longer than the shortest linear distance. The exact value of this increase factor is difficult to determine, in fact it cannot be distinguished from the effect of only partly accessible porosity. So in practice (and in this work) these two effects are lumped into a single factor. The geometrical factor is a fit-parameter that can be determined only based on experimental data. As the combined effect of constrictivity and tortuosity is not individually measurable in experiments, it is either measured in combination with accessible porosity (in case of anions) or in combination with retardation (cations), assuming the geometrical factor is equal 1.

In case of cations (sorbing species) the uncertainty for the transport is mainly related to the uncertainty in the sorption (spanning 1 to several orders of magnitude). The uncertainty on the pore diffusion coefficient D_{pore} will remain within the same order of magnitude. The G factor may indeed be different from one species to another but this difference will remain low compared to the impact of sorption. Therefore a G value range similar to Boom Clay at Mol (max ~0.07 for iodide and min~0.1 for HTO) will be considered and the D_{pore} will be calculated based on the diffusion coefficient in free water (D_o) and geometrical factor G.

To estimate the ranges for other cations, they are scaled based on the difference in D_0 value. The D_0 for the bivalent cations Ba (2+) is not known, therefore for these radionuclides the value range for Sr (2+) is adopted. The D_0 values are given for a temperature of 25 °C therefore the recalculation of the D_{pore} range for a temperature of 23-24 °C corresponding to a repository situated at 500 m depth is not necessary.

Table 6-7 Calculated pore diffusion coefficients without considering surface diffusion of cations.

	D_o [m^2s^{-1}]	D_{pore}	
		min	max
Cs (+)	2.05 10^{-09} [Maes et al., 2011b, p.61]	1.44 10^{-10}	2.05 10^{-10}
K (+)	1.96 10^{-09} [Appelo et al., 2009]	1.37 10^{-10}	1.96 10^{-10}
Sr (2+)	7.94 10^{-10} [Appelo et al., 2009]	5.56 10^{-11}	7.94 10^{-11}
Ca (2+)	7.94 10^{-10} [Appelo et al., 2009]	5.56 10^{-11}	7.94 10^{-11}
Ba (2+)	-	5.56 10^{-11}	7.94 10^{-11}
Ra (2+)	7.5 10^{-10} [Van Loon, 2014, Tab.20]	5.25 10^{-11}	7.50 10^{-11}

By combining the value ranges estimated above (Table 6-6, Table 6-7), a value range for pore diffusion coefficients for cationic species can be estimated for the Boom Clay in the Dutch situation.

Table 6-8 Pore diffusion coefficients ranges for cationic species estimated for the Boom Clay in the Netherlands.

	D_o [m^2s^{-1}]	D_{pore}	
		min	max
Cs (+)	2.05 10^{-09} [Maes et al., 2011b, p.61]	1.44 10^{-10}	8.5 10^{-09}
K (+)	1.96 10^{-09} [Appelo et al., 2009]	1.37 10^{-10}	8.1 10^{-09}
Sr (2+)	7.94 10^{-10} [Appelo et al., 2009]	5.56 10^{-11}	3.3 10^{-10}
Ca (2+)	7.94 10^{-10} [Appelo et al., 2009]	5.56 10^{-11}	3.3 10^{-10}
Ba (2+)	-	5.56 10^{-11}	3.3 10^{-10}
Ra (2+)	7.5 10^{-10} [Van Loon, 2014, Tab.20]	5.25 10^{-11}	3.3 10^{-10}

Dissolved organic matter and organic matter associated nuclides

From this study and the knowledge acquired in previous studies it can be concluded that an increase of ionic strength of the Boom Clay pore water up to seawater composition could significantly decrease the concentration of dissolved organic matter (DOM) leaving only small organic molecules in solution. The consequent reduction of mobile DOM concentration and molecular weight would limit the colloid-facilitated transport of radionuclides through the Boom Clay layer. However, it is clear that the behaviour of DOM in Boom Clay under variable ionic strength is extremely complex and cannot be predicted precisely by any existing model. A full assessment of the DOM impact on radionuclides at other locations of Boom Clay requires therefore a detailed knowledge of the Boom Clay, the pore water and the DOM present.

Migration parameters for DOM as estimated in the Belgian research are: D_{eff} ranging from $4.0\ 10^{-12}$ to $1.0\ 10^{-10}$ m^2/s, available porosity from 0.05 to 0.4, R of 20-60 (See Section 3.4.2). The combined effect of retardation and slow diffusion results in D_{eff} ranging from $6.5\ 10^{-14}$ to $3.0\ 10^{-11}$ m^2/s. which is 60 to 30.000 times slower than diffusion rates of mobile aqueous ions (no retardation) with an average D_0 of ca. $2.0\ 10^{-9}$.

For nuclides that strongly interact with organic matter, migration rates will become equal to that of DOM. So the migration parameters (D_0, R) for DOM are representative for those nuclides as well. Assuming that there is organic matter present in dissolved as well as in sorbed form, a retardation factor also implies a distribution of organic matter over dissolved and solid phase. In reality this will be more complex, as the average composition and chemical behaviour of dissolved and adsorbed organic matter may very well be different. For nuclides that strongly associate with colloidal organic matter, their effective migration rates will be maximal the same as the migration rates of colloidal particles (DOM).

6.4. Database of migration parameters

The database presented in Table 6-9 summarizes the migration parameters values deduced for the Boom Clay for conditions as expected for the OPERA reference disposal concept. These values are based on the parameter ranges estimated by SCK·CEN for the Boom Clay in the Mol region. This data were adapted for conditions as expected for the future Dutch disposal facility and address uncertainties caused by the lack of geochemical characteristics of the Boom Clay in the Netherlands. The estimation of the parameters ranges was carried out in line with the recommendations given by SCK·CEN (see Section 3.5 and TNO (Section 4.6). The diffusion properties listed in Table **6-9** are valid for salinities and in situ effective stress ranging from the Belgian conditions (low salinity and in situ effective stress 2.4 MPa) and the highest expected salt level and in situ effective stress for a Dutch situation (sea water ±0.6 M, in situ effective stress 6.9 MPa).

The used methods, data and assumptions are documented in Chapters 3 to 5 of the present report. Together with the K_d values resulting from task 6.1.2 these will provide an estimation of overall apparent diffusion coefficient for the PA calculations within WP7**.**

Table 6-9 Estimated minimum, maximum and average values for the pore diffusion coefficient D_{pore}, diffusion accessible porosity η and tortuosity for Boom clay for conditions as expected for the future Dutch disposal facility.

Element	**Group**	**Diffusion accessible porosity η [-]**		**Pore diffusion coefficient D_{pore} [m^2s^{-1}]**	
		min	max	min	Max
HTO, Kr, Ar, Si	Neutral	0.14	0.40	$2.0\ 10^{-10}$	$2.6\ 10^{-10}$
I	Anion	0.05	0.40	$1.0\ 10^{-10}$	$1.6\ 10^{-10}$
Cl	Anion	0.05	0.40	$1.0\ 10^{-10}$	$1.6\ 10^{-10}$
Se (I)	Anion	0.05	0.40	$8.4\ 10^{-11}$	$1.3\ 10^{-10}$
Nb	Anion	0.05	0.40	$6.7\ 10^{-11}$	$1.1\ 10^{-10}$
C	Anion	0.05	0.40	$1.5\ 10^{-11}$	$1.0\ 10^{-10}$
Se (II)	Anion	0.05	0.40	$5.0\ 10^{-11}$	$8.0\ 10^{-11}$
Mo	Anion	0.05	0.40	$5.0\ 10^{-11}$	$8.0\ 10^{-11}$
Cs	Cation	0.14	0.40	$1.4\ 10^{-10}$	$8.5\ 10^{-09}$

Element	Group	Diffusion accessible porosity η [-]		Pore diffusion coefficient D_{pore} [m^2s^{-1}]	
		min	max	min	Max
K	Cation	0.14	0.40	1.4 10^{-10}	8.1 10^{-09}
Sr	Cation	0.14	0.40	1.9 10^{-10}	3.3 10^{-10}
Ba	Cation	0.14	0.40	1.9 10^{-10}	3.3 10^{-10}
Ca	Cation	0.14	0.40	1.9 10^{-10}	3.3 10^{-10}
Ra	Cation	0.14	0.40	1.8 10^{-10}	3.1 10^{-10}
DOM	DOM	0.07	0.17	5.7 10^{-12}	5.7 10^{-11}
Tc Ag Be Ni Pd Zr Sn Ti Pb Cd	Transition metal + DOM	0.07	0.17	5.7 10^{-12}	5.7 10^{-11}
Am Ac Cm Sm Pu Eu Ho Cf Pm	Trivalent Ln/Ac + DOM	0.07	0.17	5.7 10^{-12}	5.7 10^{-11}
U Th Np Pa	Tetravalent Ln/Ac + DOM	0.07	0.17	5.7 10^{-12}	5.7 10^{-11}

There are no thermodynamic and chemical data on Bi, Po and Re in the standard databases so it is difficult to estimate the form in which they occur. For these radionuclides the most conservative migration parameters will be assumed (see Section 5.4 for more detail).

7. Conclusions

In this report the current developments/approaches in modelling migration of radionuclides in clay were evaluated with regards to their relevance for the overall migration behaviour of radionuclides in Boom Clay in the Netherlands.

The diffusion of charged ions in a clay matrix such as Boom Clay is strongly affected by interactions of ions and water with the charged surfaces of the clay particles. This effect is enhanced by the large surface area to pore volume ratio, which makes that most of the pore solution is under the influence of the charged solid matrix. As a result diffusion of ions in clay pores is very different from diffusion of ions in free water. Due to interactions of the water with the large, charged surface areas of the Boom Clay, a significant fraction of water in the clay matrix will be present as either surface bound molecules, that behave more like a solid, or in the form of charged “double layer” in which the chemical condition differs significantly from the remaining, “free” water. Because the surface charge influences the mobility of ions in the clay pores, the mobility of radionuclides is strongly dependent on the charge density as well as the pore diameter. As a result diffusion of ions in clay pore water is dominated by processes such as anion exclusion, cation surface diffusion, and intra-particle diffusion. These processes not only affect diffusion fluxes but also the diffusion path length (tortuosity).

The overall migration behaviour of radionuclides is an intricate mixture of chemical and physical processes. The present work however focuses on the physical part of the migration processes and required model parameters. The accompanying Task 6.1.2 focuses on the chemical interaction (sorption) processes and Task 6.1.4 on the effects of the presence and mobility of colloidal material.

As part of this work a mathematical model for the migration and decay of radionuclides through the Boom Clay was developed and implemented. This model uses nuclide specific linear R/K_d factors, pore diffusion coefficients and diffusion accessible porosities. The actual R/K_d values are determined by chemical sorption processes that are studied within WP6.1.2.

An important source of relevant information for these parameters are the results of the Belgian research programme as part of which radionuclide behaviour in Boom Clay has been studied for over 30 years. However, because the Boom Clay conditions in the Netherlands regarding e.g. pressure, temperature, salt concentrations, are different from the Belgian situation, an assessment was carried out of the transferability data obtained on “Mol” samples for predicting/describing radionuclide transport in the Netherlands. The effect of changes in chemical conditions on the expected diffusion rates was estimated by translating the diffusion data from the Belgian research programme to the Dutch situation.

The results show that the effects of higher salt levels may increase diffusion rates of anions by decreasing the extent of the double layers and so increase accessible porosity. Higher temperatures are likely to increase molecular diffusion coefficients. Higher pressures affect compaction and tortuosities and slow down diffusion. The impact of the changes on migration parameters values is limited and low compared to the impact on the sorption.

The resulting estimated set of transport parameters for the Dutch situation was summarized into a database that together with the set of R values resulting from Task 6.1.2 forms the complete set input data for modelling migration of radio nuclides through the Boom Clay.

The necessarily theoretical approach followed in this work leads to relatively large ranges of uncertainty in the set of transport parameters. If the OPERA PA calculations indicate that it would be useful to reduce these uncertainty ranges, additional experimental work on selected radionuclides in Dutch Boom Clay material would be required to achieve this.

8. References

[Aertsens et al., 2004] Aertsens M., Wemaere I. and Wouters L., *Spatial variability of transport parameters in the Boom Clay*, Applied Clay Science 26, 2004, 37-45.

[Aertsens et al., 2008a] Aertsens M., De Cannière P., Lemmens K., Maes N. and Moors H., *Overview and consistency of migration experiments in clay*, Physics and Chemistry of the Earth 33, 2008, 1019-1025.

[Aertsens et al., 2008b] Aertsens M., Van Gompel M., De Canniere P., Maes N., and Dierckx A., *Vertical distribution of (HCO3-)-C-14 transport parameters in Boom Clay in the Mol-1 borehole (Mol, Belgium)*, Physics and Chemistry of the Earth **33**, 2008, S61-S66.

[Aertsens et al., 2009] Aertsens M., De Cannière P., Moors H., Van Gompel M., *Effect of ionic strength on the transport parameters of tritiated water, iodide and $H^{14}CO_3^-$ in Boom Clay*, in: Burakov, B.E., Aloy, A.S. (Eds.), Scientific Basis for Nuclear Waste Management XXXIII, MRS Materials Research Society, Warrendale, Pennsylvania, USA, St. Petersburg, Russia, 2009, pp. 497-504.

[Aertsens et al., 2013] Aertsens M., Maes N., Labat S., Van Gompel M. and Maes T., *Vertical distribution of HTO and $^{125}I^-$ transport parameters in Boom Clay in the Essen-1 borehole (Mol, Belgium)*, Physics and Chemistry of the Earth 65, 2013, 90-97.

[Altmann et al., 2012] Altmann S., Tournassat C., Goutelard F., Parneix J. C., Gimmi T., and Maes N., *Diffusion-driven transport in clayrock formations*, Applied Geochemistry **27**, 2012, 463-478.

[Altmann et al., 2014] Altmann S., Aertsens M., Appelo T., Bruggeman C., Gaboreau S., Glaus M., Jacquier P., Kupcik T., Maes N., Montoya V., Rabung T., Robinet J.-C., Savoye S., Schaefer T., Tournassat C., Van Laer L., Van Loon L., *Processes of cation migration in clayrocks (CATCLAY)*, Final Scientific Report D1.6 EC project CATCLAY grant agreement N°249624, 2014.

[Appelo & Postma, 2005] Appelo C.A.J. and Postma D., Geochemistry, *Groundwater and Pollution* (Second Edition), A.A. Balkema Publ., Leiden, The Netherlands, 2005, 649 pp.

[Appelo & Wersin, 2007] Appelo C.A.J., Wersin P., *Multicomponent diffusion modeling in clay systems with application to the diffusion of tritium, iodide and sodium in Opalinus Clay*, Env. Sci. Technol., 41, 2007, p. 5002-5007.

[Appelo et al., 2010] Appelo C.A.J., Van Loon L., Wersin P., *Multicomponent diffusion in a suite of tracers (HTO, Cl, Br, I, Na, Sr, Cs) in a single sample of Opalinus Clay, Geochimica et Cosmochimica Acta* **74**, 2010, 1201-1219.

[Arnold et al., 2014] Arnold P., Vardon P. J., Hicks M.A., Fokkens J., Fokker P., *A numerical and reliability-based investigation into the technical feasibility of a Dutch radioactive waste repository in Boom Clay*, OPERA-PU-TUD311, February 2014, 1-317.

[Behernd et al., 2015] Behrends T., van der Veen I., Hoving A., Griffoen J., *Geochemical characterization of Rupel (Boom) clay material: pore water composition, reactive minerals and cation exchange capacity*, OPERA report OPERA-PU-UTR521, May 2015, 1-47.

[Bleyen et al., 2014] Bleyen N., Mariën A., and Valcke E., *The geochemical perturbation of Boom Clay due to the $NaNO_3$ plume released from Eurobitum bituminised radioactive waste*, status April 2012, SCK·CEN-ER-221, April, 2014.

[Bourg & Sposito, 2011] Bourg I. C. and Sposito G., *Molecular dynamics simulations of the electrical double layer on smectite surfaces contacting concentrated mixed electrolyte (NaCl-CaCl2) solutions*, Journal of colloid and interface science, 360 (2), 2011, 701–15.

[Bruggeman et al., 2010a] Bruggeman C., Aertsens M., Maes N. and Salah S., *Iodine retention and migration behaviour in Boom Clay*, External Report SCK·CEN-ER-119, 10/CBr/P-44, 2010.

[Bruggeman et al., 2010c] Bruggeman C., Liu D.J. and Maes N., *Influence of Boom Clay organic matter on the adsorption of Eu(3+) by illite - geochemical modelling using the component additivity approach*, *Radiochimica Acta* **98**, 2010, 597-605.

[Bruggeman et al., 2010d] Bruggeman C., Maes N., Aertsens M., Govaerts J., Martens E., Jacops E., Van Gompel M., and Van Ravestyn L., *Technetium retention and migration behaviour in Boom Clay* - Topical Report, First Full draft, SCK report ER-101, SCK·CEN, Mol, Belgium, 2010.

[Bruggeman & Craen, 2012a] Bruggeman C., De Craen M., *Boom Clay natural organic matter*, Status report 2011, SCK·CEN-ER-206, SCK·CEN, Mol, Belgium, 2012.

[Bruggeman et al., 2012b] Bruggeman C., Salah S., Maes N., *Americium retention and migration behaviour in Boom Clay*, Topical Report, first full draft, SCK·CEN-ER-201, SCK·CEN, Mol, Belgium, 2012b.

[Bruggeman et al., 2013] Bruggeman C., Maes N., Aertsens M., De Cannière P., *Tritiated water retention and migration behaviour in Boom Clay*, SFC1 level 5 report, first full draft status 2009, SCK·CEN-ER-248, SCK·CEN, Mol, Belgium, 2013.

[Canniere et al., 2010] De Canniere P., Maes A., Williams S. J., Bruggeman C., Beauwens T., Maes N., and Cowper M. M., *Behaviour of Selenium in Boom Clay*, State-of-the-art report, SCK·CEN-ER-120, SCK·CEN, Mol, Belgium, 2010.

[Craen et al., 2006] De Craen M., Wemaere I., Labat S. and Van Geet M., *Geochemical analyses of Boom Clay pore water and underlying aquifers in the Essen-1 borehole*, External report, SCK·CEN-ER-19, SCK·CEN, Mol, Belgium, November, 2006.

[Cygan et al., 2004] Cygan R.T., Liang J.-J., Kalinichev A.G., *Molecular Models of Hydroxide, Oxyhydroxide, and Clay Phases and the Development of a General Force Field*, The Journal of Physical Chemistry B, 108 (4), 2004, 1255–1266.

[De Preter et al., 1992] De Preter P. M., Put M., De Canniere P., Moors H., *Migration of radionuclides in Boom Clay*, State-of-the-art report June 1992, NIROND 92-07, ONDRAF/NIRAS, Brussels, Belgium, 1992.

[Dijkstra et al., 2009] Dijkstra J. J., Meeussen J. C. L., Comans R. N. J., *Evaluation of a generic multisurface sorption model for inorganic soil contaminants*, Environ. Sci. Technol. 2009, vol. 43, no 16, p. 6196-6201.

[Durce et al., 2016] Durce D., Salah S., Maes N., *Presence and mobility of colloidal particles*, OPERA-PU-SCK614, 2016.

[Dzombak, 1990] Dzombak D. A., Morel F. M. M., *Surface complexation modeling: hydrous ferric oxide*, John Wiley & Sons, Inc.: New York, 1990.

[Galan & Ferrel, 2013] Galán E. and Ferrell R.E., *Genesis of clay minerals*, Developments in Clay Science, Vol. 5A, Edited by F. Bergaya and G. Lagaly, ISBN: 978-0-08-098259-5, 2013.

[Garcia-Gutierez et al., 2004] Garcia-Gutierrez M., Cormenzana J. L., Missana T., Mingarro M., *Diffusion coefficients and accessible porosity for HTO and* ^{36}*Cl in compacted FEBERX bentonite*, Applied Clay Science 26, 2004, 65-73.

[Gimmi&Kosakowski, 2011] Gimmi T., Kosakowski G., *How Mobile Are Sorbed Cations in Clays and Clay Rocks?*, Environ. Sci. Technol., 2011, 45(4), p. 1443-1449.

[Glaus et al., 2007] Glaus M.A., Baeyens B., Bradbury M.H., Jakob A., Van Loon L.R., Yaroshchuk A., *Diffusion of Na and Sr in montmorillonite: Evidence of interlayer diffusion being the dominant pathway at high compaction*, Environmental Science & Technology 41, 2007, 478-485.

[Glaus et al., 2010] Glaus M. A., Frick S., Rosse R., and Van Loon L. R., *Comparative study of tracer diffusion of HTO, Na-22(+) and Cl-36(-) in compacted kaolinite, illite and montmorillonite*, Geochimica Et Cosmochimica Acta **74**, 1999-2010.

[Greathouse & Cygan, 2005] Greathouse J.A. and Cygan R.T., *Molecular dynamics simulation of uranyl(VI) adsorption equilibria onto an external montmorillonite surface*, Physical chemistry chemical physics 7 (20), 2005, 3580–3586.

[Griffioen, 2015] Griffioen J., *The composition of deep groundwater in the Netherlands in relation to disposal of radioactive waste*, OPERA report OPERA-PU-TNO521-2, April 2015, 1 51.

[Grupa et al., 2015] Grupa J.B., Meeussen J.C.L., Rosca-Bocancea E., Buhmann D., Laggiard E., Wildenborg A. F. B., *Report on migration model in Boom Clay*, OPERA-PU-NRG7212 1st draft, 30-st of June 2015.

[Hart, 2014A] Hart J., *Reference list of waste inventory, Part A: Radionuclides*, OPERA-PU-NRG1111A, October 2014.

[Hart, 2014B] Hart J., *Determination of the inventory, Part A: Radionuclides*, OPERA-PU-NRG1112A, 16 December 2014, 1-60.

[Hemes et al., 2013] Hemes S., Desbois G., Urai J.L., De Craen M. and Honty M., *Variations in the morphology of porosity in the Boom Clay Formation: insights from 2D high resolution BIB-SEM imaging and Mercury injection Porosimetry*, Netherlands Journal of Geosciences 92 (4), 2013, 275-300.

[Henrion et al., 1991] Henrion P. N., Put M. J., Vangompel M.,*The influence of compaction on the diffusion of non-sorbed species in Boom Clay*, Radioactive waste Management and Environmental Restoration, 16 (1), 1991, 1-14.

[Hiemstra et al., 1996] Hiemstra T., van Riemsdijk W.H., *A surface structural approach to ion adsorption: The charge distribution (CD) model*, J. Colloid Interface Sci. 1996, 179, p.488-508.

[Horseman et al., 1996] Horseman S. T., Higgo J., Alexander J., and Harrington J. F., *Water, gas and solute movement through argillaceous media*, NEA report CC-96/1, NEA/OECD, Paris,1996.

[Houben et al., 2014] Houben M.E., Desbois G. and Urai J.L., *A comparative study of representative 2D microstructures in shaly and sandy facies of Opalinus Clay (Mont Terri, Switzerland) inferred from BIB-SEM and MIP methods*, Marine and Petroleum Geology 49, 2014,143-161.

[Kinniburgh et al., 1999] Kinniburgh D.G., van Riemsdijk W.H., Koopal L.K., Borkovec M., Benedetti M.F., Avena M.J., *Ion binding to natural organic matter: competition, heterogeneity, stoichiometry and thermodynamic consistency*, Colloids Surf. A, 1999, 151, p.147-166.

[Koenen & Griffioen, 2014] Koenen M., Griffioen J., *Mineralogical and geochemical characterization of the Boom Clay in the Netherlands*, OPERA report OPERA-PU-TNO521-1, November 2014, 1-106.

[Koneshan et al., 1998] Koneshan S., Rasaiah J.C., Lynden-Bell R.M. and Lee S.H., *Solvent Structure*, Dynamics, and Ion Mobility in Aqueous Solutions at 25 °C, The Journal of Physical Chemistry B, 102 (21), 1998, 4193–4204.

[Kozaki et al., 1998] Kozaki T., Saito N., Fujishima A., Sato S., and Ohashi H., *Activation energy for diffusion of chloride ions in compacted sodium montmorillonite*, Journal of Contaminant Hydrology **35**, 1998, 67-75.

[Kozaki et al., 2001] Kozaki T., Inada K., Sato S., and Ohashi H., *Diffusion mechanism of chloride ions in sodium montmorillonite*, Journal of Contaminant Hydrology **47**, 2001, 159-170.

[Laird, 2006] Laird D.A., *Influence of layer charge on swelling of smectites*, Applied Clay Science 34, 2006, 74-87.

[Lee, 2013] Lee S.H., *Temperature Dependence on Structure and Self-Diffusion of Water: A Molecular Dynamics Simulation Study using SPC/E Model*, Bulletin of the Korean Chemical Society 34 (12), 2013, 3800-3804.

[Leroy et al., 2007] Leroy P., Revil A., Altmann S. and Tournassat C., *Modeling the composition of the pore water in a clay-rock geological formation (Callovo-Oxfordian, France)*, Geochimica et Cosmochimica Acta 71, 2007, 1087-1097.

[Li & Gregory, 1974] Li Y. H. and Gregory S., *Diffusion of ions in sea-water and in deep-sea sediments*, Geochimica Et Cosmochimica Acta **38**, 1974, 703-714.

[Lindsay, 1999] Lindsay W.L., *Equilibria in Soils*, John Wiley & Sons, New York, 1979.

[Liu et al., 2004] Liu P., Harder E. and Berne B.J., *On the calculation of diffusion coefficients in confined fluids and interfaces with an application to the liquid-vapor interface of water*, Journal of Physical Chemistry B 108, 2004, 6595-6602.

[Liu et al., 2007] Liu X., Lu X., Wang R., Zhou H. and Xu S., *Interlayer Structure and Dynamics of Alkylammonium-intercalated Smectites with and without Water: A Molecular Dynamics Study*, Clays and Clay Minerals, 55 (6), 2007, 554–564.

[Maes et al., 1979] Maes A., Stul M.S. and Cremers A., *Layer charge-cation-exchange capacity relationships in montmorillonite*, Clays and Clay Minerals 27 (5), 1979, 387–392.

[Maes et al., 2003] Maes A., Bruggeman C., Geraedts K., and Vancluysen J., *Quantification of the interaction of Tc with dissolved boom clay humic substances*, Environmental Science & Technology **37**, 2003, 747-753.

[Maes et al., 2006] Maes N., Wang L., Hicks T., Bennett D., Warwick P., Hall T., Walker G., and Dierckx A., *The role of natural organic matter in the migration behaviour of americium in the Boom Clay - Part I: Migration experiments*, Physics and Chemistry of the Earth 31, 2006, 541-547.

[Maes et al., 2008] Maes N., Salah S., Jacques D., Aertsens M., Van Gompel M., De Canniere P., and Velitchkova N., *Retention of Cs in Boom Clay: Comparison of data from batch sorption tests and diffusion experiments on intact clay cores*, Physics and Chemistry of the Earth **33**, 2008, S149-S155.

[Maes et al., 2009] Maes N., Aertsens M., Salah S., Jacques D., and Van Gompel M., *Cs, Sr and Am retention on argillaceous host rocks: comparison of data from batch sorption tests and diffusion experiments*, Updated version of the PID1.2.18 delivered to the FUNMIG project, External Report SCK·CEN-ER-98, SCK·CEN, Mol, Belgium, 2009.

[Maes et al., 2011a] Maes N., Bruggeman C., Govaerts J., Martens E., Salah S., and Van Gompel M., *A consistent phenomenological model for natural organic matter linked migration of Tc(IV), Cm(III), Np(IV), Pu(III/IV) and Pa(V) in the Boom Clay*, Physics and Chemistry of the Earth **36**, 2011,1590-1599.

[Maes et al., 2011b] Maes N., Salah S., Bruggeman C., Aertsens M., and Martens E., *Caesium retention and migration behaviour in Boom Clay*, Topical report - first full draft, External report SCK·CEN-ER-153, SCK·CEN, Mol, Belgium, 2011.

[Maes et al., 2012] Maes N., Salah S., Bruggeman C., Aertsens M., Martens E., Van Laer L., *Strontium retention and migration behaviour in Boom Clay*, Topical report first full draft, SCK·CEN-ER-197, SCK·CEN, Mol, Belgium, 2012.

[Martens et al., 2010] Martens E., Maes N., Weetjens E., Van Gompel M., and Van Ravestyn L., *Modelling of a large-scale in-situ migration experiment with C-14-labelled natural organic matter in Boom Clay*, Radiochimica Acta **98**, 2010, 695-701.

[Matsunaga et al., 2004] Matsunaga T., Nagao S., Ueno T., Takeda S., Amano H. and Tkachenko Y., *Association of dissolved radionuclides released by the Chernobyl accident with colloidal materials in surface water*, Applied Geochemistry **19**, 2004, 1581-1599.

[Meeussen, 2003] Meeussen J. C. L., *ORCHESTRA: An object-oriented framework for implementing chemical equilibrium models*, Environ. Sci. Technol. 2003, 37, (6), 1175-1182.

[Melkior et al., 2005] Melkior T., Yahiaoui S., Motellier S., Thoby D., and Tevissen E., *Cesium sorption and diffusion in Bure mudrock samples*, Applied Clay Science **29**, 2005, 172-186.

[Melkior et al., 2007] Melkior T., Yahiaoui S., Thoby D., Motellier S., and Barthes V., *Diffusion coefficients of alkaline cations in Bure mudrock*, Physics and Chemistry of the Earth **32**, 2007, 453-462.

[Milne et al., 2003] Milne C. J., Kinniburgh D. G., Van Riemsdijk W. H., Tipping E., *Generic NICA-Donnan model parameters for metal-ion binding by humic substances*, Environ. Sci. Technol., 2003, 37,958–971.

[Molera & Eriksen, 2002] Molera M., Eriksen T., *Diffusion of* $^{22}Na^{+}$, $^{85}Sr^{2+}$, $^{134}Cs^{+}$ *and* $^{57}Co^{2+}$ *in bentonite clay compacted to different densities: experiments and modelling*, Radiochimica Acta 90, 2002, 753-760.

[Molera, 2002] Molera M., *On the sorption and diffusion of radionuclides in Bentonite clay*, PhD thesis at the Swedish royal institute of Technology TRITA-KKE-0201, KTH Stockholm, Sweden, 2002.

[Moors, 2005] Moors H., *Topical report on the effect of the ionic strength on the diffusion accessible porosity of Boom Clay*, External Report SCK·CEN-ER-02, 05/HMo/P-53, Waste & Disposal Department, SCK·CEN, Mol, Belgium, 2005.

[Muurinen, 1994] Muurinen A., *Diffusion of anions and cations in compacted sodium bentonite*, Publication No. 168, VTT, Espoo, Finland, 1994.

[Nakashima, 1995] Nakashima S., *Diffusivity of ions in pore water as a quantitative basis for rock deformation rate estimates*, Tectonophysics 245, 1995, 185-203.

[NEA/OECD, 1996] Horseman S.T., Higgo J.J.W., Alexander J., Harrington J.F., *Water, Gas and Solute Movement Trough Argillaceous Media*, Nuclear Energy Agency Report CC-96/1, 1996, 1-306.

[Oscarson et al., 1992] Oscarson D.W., Hume N.G., Sawatsky N.G., Cheung S.C.H., *Diffusion of iodide in compacted bentonite*, Soil Science of America Journal, 56 (5), 1992, 1400-1406.

[Pathria & Beale, 2011] Pathria R.K. and Beale P.D., *Statistical Mechanics*, Third Edition. Elsevier Ltd. ISBN 978-0-12-382188-1, 2011, 722p.

[Plimpton & Thompson, 2012] Plimpton S.J. and Thompson A.P., *Computational Aspects of Many-body Potentials*, MRS Bulletin 37, 2012, 513-521.

[Pusch et al., 1990] Pusch R., Karnland O., and Hökmark H., *GMM — A general microstructural model for qualitative and quantitative studies of smectite clays*, SKB Technical Report TR90-43, Svensk Kärnbränslehantering AB, Stockholm, Sweden,1990.

[Robinet et al., 2011] Robinet J.C., Coelho D. and Altmann S., *State of the art on cation diffusion in clay mineral systems*, CatClay Deliverable D-N°:1-1, 2011.

[Salah & Wang, 2012] Salah S., Wang L., *Speciation and solubility calculations for waste relevant radionuclides in Boom Clay,* First Full Draft, SCK·CEN-ER-198, SCK·CEN, Mol, Belgium, 2012.

[Salah et al., 2015] Salah S., Bruggeman C., Maes N., *Uranium retention and migration behaviour in Boom Clay*, Topical report status 2004, SCK·CEN-ER-305, SCK·CEN, Mol, Belgium , 2015.

[Schröder et al., 2016a] Schröder T.J., Meeussen J.C.L., Dijkstra J.J., Bruggeman C., Maes N., *Report on model representation of radionuclide sorption in Boom Clay*, OPERA report OPERA-PU-NRG6121, 2016.

[Schröder et al., 2016b] Schröder T.J., Meeussen J.C.L., *Final report on radionuclide sorption in Boom Clay*, OPERA report OPERA-PU-NRG6123, 2016.

[Shackelford & Moore, 2013] Shackelford C. D., Moore S. M., *Fickian diffusion of radionuclides for engineered containment barriers: Diffusion coefficients, porosities, and complicating issues*, Engineering Geology 152, 2013, 133-147.

[Tipping, 1998] Tipping, E., *Humic ion-binding model VI: An improved description of the interactions of protons and metal ions with humic substances*, Aquatic Geochemistry 4, 1998, 3-48.

[Tournassat et al., 2009] Tournassat C., Chapron Y., Leroy P., Bizi M., and Boulahya F., *Comparison of molecular dynamics simulations with triple layer and modified Gouy-Chapman models in a 0.1M NaCl-montmorillonite system*, Journal of colloid and interface science, 339 (2), 2009, 533–41.

[Tournassat & Appelo, 2011] Tournassat C., Appelo C. A. J., *Modelling approaches for anion-exclusion in compacted Na-bentonite*, Geochimica et Cosmochimica Acta 75, 13 2011, p. 3698-3710.

[Van Loon et al., 2003a] Van Loon L.R., Soler J.M., Bradbury M.H., *Diffusion of HTO, 36Cl- and 125I- in Opalinus Clay samples from Mont Terri. Effect of confining pressure*, Journal of Contaminant Hydrology 61, 2003, 75-83.

[Van Loon et al., 2003b] Van Loon L.R., Soler J.M., Jakob A., Bradbury M.H., *Effect of confining pressure on the diffusion of HTO, 36Cl- and 125I- in a layered argillaceous rock (Opalinus Clay): diffusion perpendicular to the fabric*, Applied Geochemistry 18, 2003, 1653-1662.

[Van Loon et al., 2004] Van Loon L. R., Wersin P., Soler J. M., Eikenberg J., Gimmi T., Hernan P., Dewonck S., and Savoye S., *In-situ diffusion of HTO, Na-22(+), Cs+ and I- in Opalinus Clay at the Mont Terri underground rock laboratory*, Radiochimica Acta **92**, 2004, 757-763.

[Van Loon et al., 2005] Van Loon L. R., Baeyens B., and Bradbury M. H., *Diffusion and retention of sodium and strontium in Opalinus clay: Comparison of sorption data from diffusion and batch sorption measurements, and geochemical calculations*, Applied Geochemistry **20**, 2005, 2351-2363.

[Van Loon et al., 2007] Van Loon L.R., Glaus M.A. and Müller W., *Anion exclusion effects in compacted bentonites: Towards a better understanding of anion diffusion*, Applied Geochemistry 22, 2007, 2536-2552.

[Van Loon et al., 2009] Van Loon L. R., Baeyens B., and Bradbury M. H., *The sorption behaviour of caesium on Opalinus Clay: A comparison between intact and crushed material*, Applied Geochemistry **24**, 2009, 999-1004.

[Van Loon, 2014] Van Loon L.R., *Effective Diffusion Coefficients and Porosity Values for Argillaceous Rocks and Bentonite: Measured and Estimated Values for the Provisional Safety Analyses for SGT-E2*, Technical Report 12-03, Nagra, November 2014.

[Verhoef et al., 2016] Verhoef E.V., Neeft E.A.C., Deissmann G., Filby A., Wiegers R.B., Kers D.A., *Waste families in OPERA*, OPERA report OPERA-PG-COV023, March 2016, 1-18.

[Wang et al., 2011] Wang L., Salah S., and De Soete H., *MOLDATA: A Thermochemical Data Base for phenomenological and safety assessment studies for disposal of radioactive waste in Belgium - Data compilation strategy*, SCK·CEN, Mol, Belgium, 2011.

[Weetjens et al., 2014] Weetjens E., Maes N., Van Ravestyn L., *Model validation based on in situ radionuclide migration tests in Boom clay: status of a large-scale migration experiment, 24 years after injection*, Geological society, London, Special publications 2014, v400, 613-623.

[Weng et al., 2006] Weng L., Van Riemsdijk W.H., Koopal L.K. and Hiemstra T., *Ligand and Charge Distribution (LCD) model for the description of fulvic acid adsorption to goethite*, Journal of Colloid and Interface Science **302**, 2006, 442-457.

[Weng et al., 2008a] Weng L., Van Riemsdijk W.H. and Hiemstra T., *Cu2+ and Ca2+adsorption to goethite in the presence of fulvic acids*, Geochimica et Cosmochimica Acta **72**, 2008, 5857-5870.

[Weng et al, 2008b] Weng L., Van Riemsdijk W.H. and Hiemstra T., *Humic Nanoparticles at the Oxide-Water Interface: Interactions with Phosphate Ion Adsorption*, Environmental Science & Technology 42, 2008, 8747-8752.

[Weng et al., 2009] Weng L., Van Riemsdijk W.H. and Hiemstra T., *Effects of Fulvic and Humic Acids on Arsenate Adsorption to Goethite: Experiments and Modeling*, Environmental Science & Technology **43**, 2009, 7198-7204.

[Wisseal at al., 2016] Wisseal A., Graham C., Zihms S., Haarington J., Cuss R., Gregory S., Shaw R., *Properties and behaviour of the Boom Clay formation within a Dutch Repository Concept*, draft report OPERA-PU-XXXNNN, December 2015, 1-134.

[Vis &Verweij] Vis G.-J., Verweij J.M., *Geological and geohydrological characterization of the Boom Clay and its overburden*, OPERA-PU-TNO411, March 2014, 1-91.

[Zang et al., 1997] Zhang Y.J., Bryan N.D., Livens F.R. and Jones M.N., *Selectivity in the complexation of actinides by humic substances*, Environmental Pollution **96**, 1997, 361-367.

[Zhao et al., 2011] Zhao P., Zavarin M., Leif R. N., Powell B. A., Singleton M.J., Lindvall R. E., Kersting A. B., *Mobilization of actinides by dissolved organic compounds at the Nevada Test Site*, Applied Geochemistry 26, 2011, 308-118.

[Zheng et al., 2011] Zheng L., Liu H.H., Birkholzer J., *Diffusion Modelling in Clay Repository*, Fuel Cycle Research and development, FCRD-LBNL-2011-SLM, July 2011, p. 1-25.

[Zhou et al., 1996] Zhou Z., Gunter W.D., Kadatz B. and Cameron S., *Effect of clay swelling on reservoir quality*, Petrolum Society of Canada, Doi:10.2118/96-07-02, 1996.

[Zhou et al., 1997] Zhou Z., Cameron S., Kadatz B. and Gunter W.D., *Clay swelling diagrams: Their applications in formation damage control*, Society of Petroleum Engineers, 1997.

Disclaimer

This report has been prepared at the request and for the sole use of the Client and for the intended purposes as stated in the agreement between the Client and Contractors under which this work was completed.

Contractors have exercised due and customary care in preparing this report, but have not, save as specifically stated, independently verified all information provided by the Client and others. No warranty, expressed or implied is made in relation to the preparation of the report or the contents of this report. Therefore, Contractors are not liable for any damages and/or losses resulting from errors, omissions or misrepresentations of the report.

Any recommendations, opinions and/or findings stated in this report are based on circumstances and facts as received from the Client before the performance of the work by Contractors and/or as they existed at the time Contractors performed the work. Any changes in such circumstances and facts upon which this report is based may adversely affect any recommendations, opinions or findings contained in this report. Contractors have not sought to update the information contained in this report from the time Contractors performed the work.

The Client can only rely on or rights can be derived from the final version of the report; a draft of the report does not bind or obligate Contractors in any way. A third party cannot derive rights from this report and Contractors shall in no event be liable for any use of (the information stated in) this report by third parties.

OPERA

Meer informatie:

Postadres
Postbus 202
4380 AE Vlissingen

T 0113-616 666
F 0113-616 650
E info@covra.nl

www.covra.nl